

2004

Thermomechanical property evaluation of molybdenum alloys

Ashok Varadarajan
West Virginia University

Follow this and additional works at: <https://researchrepository.wvu.edu/etd>

Recommended Citation

Varadarajan, Ashok, "Thermomechanical property evaluation of molybdenum alloys" (2004). *Graduate Theses, Dissertations, and Problem Reports*. 1469.
<https://researchrepository.wvu.edu/etd/1469>

This Thesis is protected by copyright and/or related rights. It has been brought to you by the The Research Repository @ WVU with permission from the rights-holder(s). You are free to use this Thesis in any way that is permitted by the copyright and related rights legislation that applies to your use. For other uses you must obtain permission from the rights-holder(s) directly, unless additional rights are indicated by a Creative Commons license in the record and/ or on the work itself. This Thesis has been accepted for inclusion in WVU Graduate Theses, Dissertations, and Problem Reports collection by an authorized administrator of The Research Repository @ WVU. For more information, please contact researchrepository@mail.wvu.edu.

**THERMOMECHANICAL PROPERTY EVALUATION OF
MOLYBDENUM ALLOYS**

Ashok Varadarajan

Thesis submitted to the College of Engineering and Mineral Resources
at West Virginia University in partial fulfillment of the
requirements for the degree of

Master of Science
in
Mechanical Engineering

Bruce S. Kang, Ph.D., Chair
Charles Stanley, Ph.D.
Nithi Sivaneri, Ph.D.

Mechanical and Aerospace Engineering Department, West Virginia University

Morgantown, West Virginia
2004

Keywords: Molybdenum base Alloys, Coefficient of thermal expansion, Thermo cycling.

Abstract

The ultra high temperature structural intermetallic molybdenum and its alloys were studied for their thermal properties and correlated to the material microstructure. Thermal expansion tests were carried out using thermo-mechanical analyzer (TMA). Thermo cycling tests were conducted around 650°C for spinel dispersed molybdenum alloys with 3% wt of spinel or 6% wt of spinel (MgAl_2O_4) particles. Results show that the coefficient of thermal expansion (CTE) value decreases with the addition of spinel and silicide particles. Furthermore, pure molybdenum alloys with different processing method also affect the CTE values. Thermo cycling tests show that molybdenum alloy with 6% wt of spinel (MgAl_2O_4) develops microcracks which are related to the number of cycles. The microcracks are caused by the thermal expansion mismatch between the spinel particles and molybdenum matrix, as well as the processing conditions. After the tests, the specimen was polished suitable to examine them using Scanning Electron Microscope (SEM) and Energy Dispersive Spectroscopy (EDS) and the micro cracks were detected, which were developed due to the thermal stresses.

Acknowledgements

First and foremost, I wish to place on record my heartfelt gratitude to my research advisor Dr. Bruce. S. Kang who was at all times on my side and gave me excellent suggestions. There were many instances when I ran into complications and without his understanding and guidance this research would not have seen the light of the day. I also thank him for the light he showed me in the field of material science

I would also like to thank my committee members Dr. Charles Stanley and Dr. Nithi Sivaneri for giving me timely advice and invaluable suggestions, which paved the way for the successful completion of this work. This research work is supported by a Department of Energy project (Grant/Contract No.: DE-FG02-01ER45899, Project Title: Understanding and Improving High Temperature Structural Properties of Metal-Silicide Intermetallics).

It will be a bad part on me if I forget to thank Ms. Diane. S. Berry, research biologist PPRB Lab NIOSH Morgantown WV., who gave her valuable time and technical expertise in using the Scanning Electron Microscope, without whom the research work will be barely finished and I would haven't learnt more about the electron microscope.

Special thanks to Dongxiang Sun, who worked with me in this project. I also thank my other fellow research students in the group for their support. Finally, I would like to thank my parents, for the support and confidence in me at critical stages of this research.

Table of Contents

Abstract	ii
Acknowledgements	iii
Table of Contents	iv
List of Figures	vi
List of Tables	ix
Chapter 1 INTRODUCTION	1
1.1 Background	1
1.2 Research objectives	3
1.3 Organization	4
Chapter 2 LITERATURE SURVEY	5
2.1 Introduction	5
2.2 Intermetallic	5
2.3 Metal Silicides	7
2.4 Molybdenum Base Alloys	8
2.4.1 Strength	9
2.4.2 Oxidation Resistance	10
2.4.3 Fracture Toughness	10
2.4.4 Microstructure	10
2.5 Spinel and its Properties	11
2.6 Applications of Molybdenum and its Alloys	11
2.6.1 Carburizing Steel	12
2.6.2 High Strength Low Alloy (HSLA) Steels	12
2.6.3 Oil Industries	12
2.6.4 Heating Elements	13
2.6.5 Gas Turbines	13
2.6.6 Diesel Engines	13
2.6.7 Industrial Gas Burners	14
Chapter 3 EXPERIMENTAL PROGRAM	15
3.1 Molybdenum Base Alloys	15
3.2 Tests and Testing Equipment	16
3.3 Coefficient of Thermal Expansion (CTE)	16
3.4 The Thermo-Mechanical Analyzer (TMA 2940)	16
3.4.1 Introduction	16
3.4.2 Theory of Operation	17

3.4.3 Working Procedure	18
3.5 The Differential Thermal Analyzer (DTA 1600)	19
3.5.1 Introduction	19
3.5.2 Theory of Operation	20
3.5.3 Working Procedure	20
3.6 Scanning Electron Microscope	21
3.7 Thermo-Cycling Test	21
3.7.1 Testing Conditions	22
Chapter 4 RESULTS AND DISCUSSIONS	23
4.1 Introduction	23
4.2 Coefficient of Thermal Expansion Using TMA 2940	23
4.2.1 Thermal expansion test: Molybdenum (ref. # 648)	23
4.2.2 Thermal expansion test: Molybdenum silicide (ref. # 649)	26
4.2.3 Thermal expansion test: Molybdenum (ref. # 677)	29
4.2.4 Thermal expansion test: Molybdenum- Spinel (ref. # 678)	31
4.2.5 Thermal expansion test: Molybdenum- Spinel (ref. # 697)	34
4.3 Thermo-Cycling Tests	36
4.4 Discussions	36
4.4.1 Coefficient of Thermal Expansion (CTE).	36
4.4.1.1 Explanation of the result for pure molybdenum #648	36
4.4.1.2 Explanation of the result for molybdenum silicide #649	37
4.4.1.2 Explanation of the result for pure molybdenum #677	37
4.4.1.3 Explanation of the result for molybdenum- spinel #678	37
4.4.1.3 Explanation of the result for molybdenum- spinel #697	38
4.4.2.1 Thermo-cycling tests on molybdenum-spinel (#678)	39
4.4.2.2 Thermo-cycling tests on molybdenum-spinel (#697)	40
4.4.3 Comparison of Alloy #678 and #697	40
Chapter 5 CONCLUSIONS AND RECOMMENDATIONS	61
5.1 Conclusions	61
5.1.1 Coefficient of Thermal Expansion Test	61
5.1.2 Thermo-cycling Test.	62
5.2 Recommendations	63
APPENDIX A	64
APPENDIX B	70
REFERENCES	73

List of Figures

Figure 1.1 Energy separation curve for two atoms, materials that display a steep curve with a deep trough have low linear coefficients of the expansion [1].	3
Figure 2.1 Crystal structure of silicon and MoSi ₂	7
Figure 2.2 Fracture modes on intermetallic compounds	8
Figure 3.1 Schematic Layout of the TMA 2940	17
Figure 3.2 (a) The figure shows the schematic diagram of the DTA furnace and thermocouple assembly. (b) The figure shows the positioning of the thermocouples under the specimen and the reference material.	19
Figure 3.3 Schematic Diagram showing Typical results From Differential Temperature Analyzer.	20
Figure 3.4 Graph showing the thermo-cycle process.	22
Figure 4.1 Coefficient of thermal expansion of molybdenum #648. Test 1	25
Figure 4.2 Coefficient of thermal expansion of molybdenum #648 Test 2	25
Figure 4.3 Coefficient of thermal expansion of molybdenum #648 Test 3	26
Figure 4.4 Coefficient of thermal expansion of molybdenum silicide #649 Test 1	27
Figure 4.5 Coefficient of thermal expansion of molybdenum silicide #649 Test 2	28
Figure 4.6 Coefficient of thermal expansion of molybdenum silicide #649 Test 3	28
Figure 4.7 Coefficient of thermal expansion of molybdenum #677 Test 1	30
Figure 4.8 Coefficient of thermal expansion of molybdenum #677 Test 2	30
Figure 4.11 Coefficient of thermal expansion of molybdenum-spinel #678 Test 2	33
Figure 4.12 Coefficient of thermal expansion of molybdenum-spinel #678 Test 3	33
Figure 4.13 Coefficient of thermal expansion of molybdenum-spinel #697	34
Figure 4.14 Comparison of coefficient of thermal expansion between #678 and #697	39
Figure 4.15 The micrograph of pure molybdenum #648 showing some defects due to casting	41
Figure 4.16 The SEM picture at X230 magnification, shows the broader picture of the MoSi alloy after test which has the oxide formation at high temperature after the TMA test	42
Figure 4.17 The SEM picture of MoSi after the TMA test shows the silicon oxide between the grain boundaries X1200 magnification	43
Figure 4.18 The grain boundary between the molybdenum and silicon are seen with the oxides of silicon formed at high temperature	43
Figure 4.19 The SEM picture at 3300 magnification, gives a clear picture of the molybdenum silicon oxygen interaction clearly	44
Figure 4.20 In the BS Image, the lighter particles is shown in high contrast, whereas the heavier particle has less contrast. (Mo is heavy when compared to Si)	44
Figure 4.21 The EDS map shows that the darker areas are Silicon and the lighter areas are Molybdenum with some oxygen content after the test	45
Figure 4.22 Showing the distribution of the MgAl ₂ O ₄ at 20 times magnification	45
Figure 4.23 Shows the MgAl ₂ O ₄ are not even in size and distribution as it is clearly seen at 330 times magnification	46

Figure 4.24 Microstructure of Mo-MgAl ₂ O ₄ #678, the darker region being MgAl ₂ O ₄ at lesser magnification (X 90) which shows the distribution of the MgAl ₂ O ₄ . The size of the MgAl ₂ O ₄ is not even as clearly seen from the picture.....	46
Figure 4.25 Microstructure of Mo-MgAl ₂ O ₄ #678, the darker region being MgAl ₂ O ₄	47
Figure 4.26 EDS map showing the composition distribution of Mo-MgAl ₂ O ₄ #678 before tests	47
Figure 4.27 The SEM picture of Mo-Spinel alloy #678 after the TMA test shows the distribution and the size of the Spinel particle is not uniform	48
Figure 4.28 The EDS map, which has to show the presence oxygen element only in the areas where both Mg and Al are present which forms Spinel with them, whereas in this the oxygen is seen all over the matrix which proves the formation of molybdenum oxides	48
Figure 4.29 showing the fracture surface of the Mo-MgAl ₂ O ₄ under the EDS mapping.	49
Figure 4.30 The SEM picture showing the gaps created after 1 thermo-cycle in Mo-MgAl ₂ O ₄ between the Molybdenum and the Spinel particle.....	49
Figure 4.31 The SEM picture at magnification 1800 times, showing the gaps created after 1 thermo-cycle in Mo- MgAl ₂ O ₄ between the Molybdenum and the Spinel.....	50
Figure 4.32 The BSI picture at magnification 1800 times, showing the gaps created after 1 thermo-cycle in Mo- MgAl ₂ O ₄ between the Molybdenum and the Spinel particle.....	50
Figure 4.33 EDS map showing the Mo- MgAl ₂ O ₄ after one thermo-cycle test. The Mo area (blue area) in the figure has a black gap between the molybdenum particles which is seen clearly in the BS Image	51
Figure 4.34 The picture shows the gap formation between the Molybdenum and Spinel particle after 1 cycle of thermo-cycling	51
Figure 4.35 The BS Image of the Spinel alloy #678 shows that the cracks propagate along on the grain boundary of the molybdenum matrix from the Spinel particle after 10 cycles of thermo-cycling.....	52
Figure 4.36 The composition of the Mo-MgAl ₂ O ₄ Alloy #678 and the gap formation are clearly visible after 1 cycle of testing in the EDS image.....	52
Figure 4.37 The SEM picture showing the crack nucleation point after 10 cycles of thermo-cycling at a magnification of 3700	53
Figure 4.38 The EDS map showing the oxygen content all over the surface of the specimen after 10 cycles proving the formation of oxide after the thermo-cycling .	53
Figure 4.39 The SEM picture clearly showing the cracks propagating from the MgAl ₂ O ₄ towards the Mo particle	54
Figure 4.40 The EDS map clearly showing that the cracks start from dark region which are the spinel particle (MgAl ₂ O ₄)	54
Figure 4.41 In the SEM picture, the big darker spinel particle cause lots of stress concentration points in the Mo matrix which causes more cracks to develop in the nearby matrix, which proves that bigger the spinel particle concentration causes more micro-cracks in the matrix	55
Figure 4.42 The EDS map, which shows the cracks triangular shaped region are cracks which are devoid of any material.....	55
Figure 4.43 Another area of the Spinel #678 clearly shows that the bigger spinel particle causes some micro cracks in the Mo matrix	56

Figure 4.44 The EDS map shows the triangular regions are devoid of any material, which proves that they are cracks in the molybdenum matrix	56
Figure 4.45 Clear view of the triangular cracks in the molybdenum matrix at a magnification of 2700	57
Figure 4.46 The EDS map shows the composition of the alloy #678 with cracks after 20 cycles of thermo-cycling.....	57
Figure 4.47 At a magnification of 6000, the triangular cracks which are formed in the matrix are clearly visible.....	58
Figure 4.48 The micrograph of #697 before any tests	58
Figure 4.49 Micrograph of #697 after 1 thermo cycling showing no significant change.	59
Figure 4.50 Micrograph of #697 after 10 cycles showing no significant changes	59
Figure 4.51 Micrograph after 20 cycles in which the cracks can be clearly seen.....	60
Figure A1 Probe Calibration Step 1	64
Figure A2 Probe Calibration Step 2.....	64
Figure A3 Probe Calibration Step 3.....	65
Figure A4 Probe Calibration Step 4.....	65
Figure A5 Force Calibration Step 1	66
Figure A6 Force Calibration Step 2.....	66
Figure A7 Force Calibration Step 3	67
Figure A8 Force Calibration Step 4.....	67
Figure A9 Force Calibration Step 5.....	68
Figure A10 Force Calibration Step 6.....	68
Figure A11 Force Calibration Step 7	69
Figure A12 Temperature and Expansion Calibration (Aluminium).....	69
Figure B1 DTA result of pure molybdenum #648.....	70
Figure B2 Comparison of CTE values between TMA and Moiré test on #648	71
Figure B3 Comparison of CTE values between TMA and Moiré test on #649	71
Figure B4 (a) Microstructure of Mo-MgAl ₂ O ₄ . (b) Particle size (µm) and number	72
Figure B5 Bending test results show that #678 is more ductile than #697.....	72

List of Tables

Table 2.1 Table of selected properties of Molybdenum at room temperature [4].	6
Table 2.2 Selected properties of Molybdenum Disilicide at room temperature [4]	9
Table 3.1 Material compositions and the heat treatment provided by Oak Ridge National Lab	15
Table 4.1 Parameters of the CTE test on Molybdenum 648.	24
Table 4.2 Parameters of the CTE test on Molybdenum Silicide 649.	26
Table 4.3 Parameters of the CTE test on Molybdenum 677.	29
Table 4.4 Parameters of the CTE test on Molybdenum-Spinel 678	31
Table 4.5 Coefficient of thermal expansion values of alloys Using TMA	35

Chapter 1 INTRODUCTION

1.1 Background

Molybdenum and its alloys are considered to be the important material for the high temperature application because of its unique characteristics. Most of the land and aircraft turbine components are exposed to severely oxidizing environments and high temperatures for reasonable time periods. Mechanical integrity under these conditions is critical. The Molybdenum-Silicon alloy offers good strength, high melting point, stiffness, oxidation resistance and excellent creep behavior as well as low mass density, which are all necessary for high temperature structural applications. The molybdenum alloys taken into study were tested for their thermal and mechanical properties to prove their compatibility for high temperature applications. The alloys considered were pure Molybdenum, Molybdenum with 2.5% of silicon and molybdenum with 3.4% (Wt) of Spinel ($MgAl_2O_4$). The materials considered previously were the steel and super alloys but when compared to them, molybdenum and its alloys have properties which are quite promising but so far no substantial results have been obtained so some tests were performed to check and evaluate the alloys of molybdenum. The main properties taken into consideration were Coefficient of Thermal Expansion (CTE), Ductile Brittle transition temperature (DBTT), high temperature tensile tests and comparison of the results with their microstructure.

Metallography is the art of studying metals and their behavior. It consists of microscopic study of the structural characteristics of a metal or an alloy. The microscopic study reveals the grain size and grain boundary orientation, by which each alloy or metal can be

distinguished. Every alloy or metal has different microstructure depending upon the method they had been processed and the heat treatment done. It helps in determining the size and shape of the crystallites, to discover the micro-defects like non-metallic inclusions, micro-cracks etc., to determine the chemical composition and to indicate the quality of heat treatment.

The coefficient of thermal expansion depends upon the increase in the dimensions of the material when the thermal energy is supplied. An atom that gains thermal energy and begins to vibrate behaves as though it has a larger atomic radius. The average distance between the atoms and the overall dimensions of the material increases. The increase in the dimensions of the material Δl per unit length is given by the *linear coefficient of thermal expansion* (α).

$$\Delta l = \alpha \Delta T$$

Where “ Δl ” is the change in dimension

“ ΔT ” is the temperature change and

“ α ” is the coefficient of thermal expansion.

The linear coefficient of thermal expansion is related to the strength of the atomic bonds. In order for the atoms to move from their equilibrium separation, energy must be introduced to the material. If a very deep energy trough caused by strong atomic bonding is characteristic of the material, the atoms separate to a lesser degree and have a low linear coefficient of thermal expansion. As shown in Figure 1.1, this relationship also indicates that materials having a high melting temperature also due to strong atomic attractions have low linear coefficients of thermal expansion.

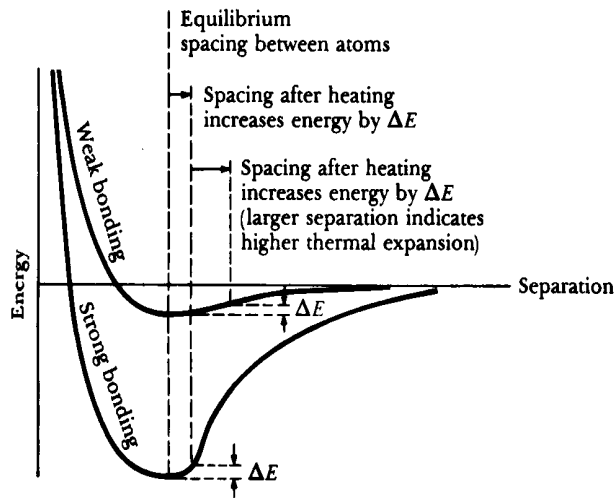


Figure 1.1 Energy separation curve for two atoms, materials that display a steep curve with a deep trough have low linear coefficients of the expansion [1].

1.2 Research objectives

The objective of this study is to develop a comprehensive understanding of the molybdenum alloys and its thermal properties at high temperature. In particular the optimal composition of the alloys, which will improve the thermo-mechanical properties at high temperature applications. The results will also determine the method and duration of the alloy processing to an extent by the results from the thermo-cycling tests conducted in this research.

The parameters which affect the properties are,

- 1) alloy composition
- 2) processing time and method
- 3) transition temperature from brittle to ductile.

In order to achieve the objective based on the above parameters a test matrix was developed and a series of tests were performed. The tests were coefficient of thermal

expansion (CTE) and thermo-cycling tests reaching a maximum temperature of 650°C. After the thermo-cyclic tests the microstructure of the tested specimen was examined using Scanning Electron Microscope (SEM) and Energy Dispersive Spectroscopy (EDX). The tests yielded the data and images which determine the coefficient of thermal expansion, and the various micrograph showing micro cracks occur in the alloys in different alloy processes.

1.3 Organization

The first chapter gives a brief introduction and objectives of this research work. Chapter 2 presents a literature review of past research done in the area of molybdenum and its alloys. The approach on the methodology of analysis is dealt with in detail in Chapter 3. Chapter 4 presents the results obtained from the analysis. The summary and conclusions of this research study are presented in Chapter 5.

Chapter 2 LITERATURE SURVEY

2.1 Introduction

The recent trend in the use of materials for the high temperature applications have made the researchers in search of new alloys which have very good high temperature material properties. After the end of World War II, there was a need for materials which has very good high temperature properties like strength, oxidation resistance and fracture toughness. An alloy was developed for the use in turbo superchargers and aircraft turbines that required very good performance at elevated temperatures. The alloy was termed as "superalloy". This increased the range of applications in different field and had expanded to many areas, which includes aircrafts, land-based gas turbines, rocket engines, chemical and petroleum plants [2]. They were well suited for those demanding applications because of their ability to retain most of their strength even after long exposure times above 650°C (1,200°F). But the 650°C temperature barrier was not enough, so the search for still higher temperature materials continued.

2.2 Intermetallic

The superalloys paved the way to the intermetallic material which has more high temperature properties better than those of superalloys. Intermetallic material is defined as a "mixture of two metallic elements in a specific proportion which forms a different periodic crystalline structure different from those of the original elements". They are often called "bulk intermetallics" [3]. They differ in a number of important ways from conventional metal alloys. Conventional alloys consist basically of a disordered solid solution of one or more metallic elements and they do not have any particular chemical formula, and are best described as consisting of a base material to which certain percentages of other elements have been added. In chemical terms, alloys are mixtures of phases. For example, a popular stainless steel has the composition Fe-18%Cr-8%Ni. An intermetallic compound, on the other hand, is a particular chemical compound based on a definite atomic formula, with a fixed or narrow range of chemical composition and the best example could be MoSi_3 and Ni_3Al .

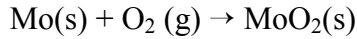
Molybdenum, which is hard silvery-white metal, belongs to the group 6 and period 5 of the periodic table (transition metals). Molybdenum has a body-centered cubic (bcc) crystal structure. It has a high melting point (2623°C) [4] with high strength at high temperature. It has a high elastic modulus which makes it in the applications which require high stiffness and low weight. It has a very good thermal conductivity and low coefficient of thermal expansion. The important properties of molybdenum at room temperature are given in Table 1.

Atomic Symbol	Mo
Density	10.22 g/cm ³
Boiling Point	4639°C
Melting Point	2636°C
Crystal Structure	BCC
Young's Modulus (E)	324 GPa
Yield Strength ^{1,2}	690 MPa
Tensile Strength ²	835 MPa
Elongation ²	12%
Hardness ²	240 HV
Coefficient of Thermal Expansion	4.9 X 10-6 /°C
Thermal Conductivity	135 W/(mK)
Specific Heat	0.27 J/kg K
Poisson's Ratio	0.321
Electrical Resistivity	0.06 μ Ωm

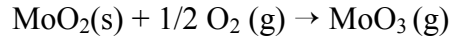
Table 2.1 Table of selected properties of Molybdenum at room temperature [4].

The property of molybdenum which makes it not suitable for high temperature structural material is its oxidation resistance at high temperature. It oxidizes readily at high temperature and forms MoO₂ in the presence of oxygen partial pressures, which is volatile in nature around 700°C [5], as the temperature raises it forms MoO₃, which

readily vaporizes at high temperature (~800°C) hence at anytime there is no steady state oxide formation in molybdenum.



As the temperature increases, it forms



Whereas, when the Molybdenum when mixed with silica it forms molybdenum disilicide (MoSi₂) which has very good oxidation resistance at high temperature, because of the formation of the thin protective and adherent silica layer in high oxygen partial pressures at high temperatures.

2.3 Metal Silicides

Silicides are considerate as an intermediate materials between ceramics and metals. For example, transition metal silicides are often classified as intermetallic compounds because of the similarities shown, nevertheless silicon is a semiconductor and not a metal. Crystal structure of silicon is shown in Figure 2.1.

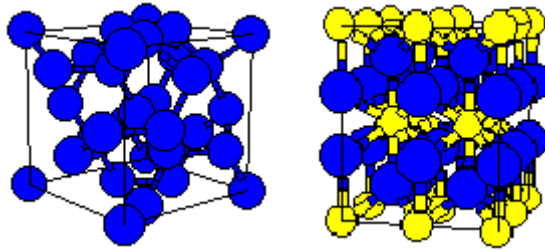


Figure 2.1 Crystal structure of silicon and MoSi₂

The particular structure of intermetallic compounds is because of the respectively larger strength of bounding between the unlike atoms than between like atoms. The result is an ordered atom distributions where atoms are preferentially surrounded by unlike atoms. This strength of bounding is the main reason of the high hardness of intermetallic compounds that can be observed by the modes of fracture. In fact, intermetallic

compounds have three different modes of fracture such as: intergranular fracture, transgranular cleavage and a mixed of these two modes, as shown in Figure.2.2.

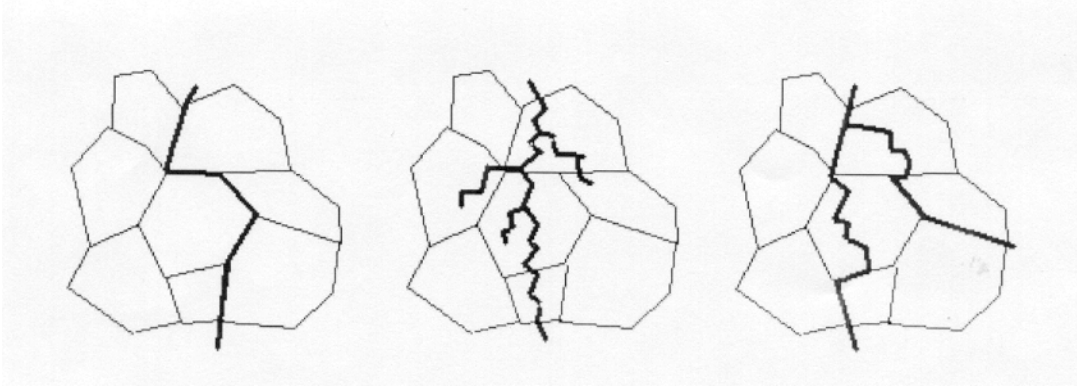


Figure 2.2 Fracture modes on intermetallic compounds

2.4 Molybdenum Base Alloys

Generally, molybdenum metal is developed by casting or by powder metallurgy techniques, in which Mo powder is hydrostatically compacted and sintered at high temperature (2100°C). Hot working is done in the 850°C-1250°C range. As discussed in the oxidation of molybdenum alloy it forms a volatile oxide when heated above 650°C, and thus limiting the use of alloys at high temperature only in oxidizing free or vacuum environment. Molybdenum silicide, are made by pressure sintering techniques. This material is generally used as heating element and its properties made it a possible candidate material for high temperature structural applications. The main aspects are moderate density, high melting point, excellent oxidation resistance and high Young's modulus at elevated temperatures. But the main drawbacks of using these alloys as structural material are low fracture toughness at less than 1000°C and poor creep resistance above 1200°C. The table below shows the general physical and mechanical properties of molybdenum disilicide.

Density (g.cm-3)	6.29
Melting Point (°C)	2230
Young's Modulus (GPa)	430
Bend Strength (MPa)	250
Fracture Toughness K1C (MPa.m0.5)	3
Hardness (GPa)	9
Resistivity (ohm.cm)	3.5 x 10-7

Table 2.2 Selected properties of Molybdenum Disilicide at room temperature [4]

2.4.1 Strength

The MoSi₂, in the polycrystalline form, exhibits a brittle-to-ductile transition in the vicinity of 1000°C. It has a high thermal conductivity which is very beneficial for increased cooling effectiveness of engine components. The room temperature mechanical strength of the MoSi₂ is low when compared to other intermetallics because the brittle-to-ductile transition temperature is around 1000°C and hence it is limited to brittle fracture, while at high temperature it is governed by plastic flow. Above the DBTT (900-1000°C) of MoSi₂, the ductility is greater when compared to other structural intermetallics and the fracture toughness will be high with a good resistance to catastrophic fracture, thus making it more dependable [6]. Depending upon the heat treatment and the composition the flexure strength varies from 300 to 600 MPa. Despite the high strength the alloys shows plasticity at temperature around 1400°C. The alloys retain a reasonably high strength at 1200°C showing their potential as high temperature structural materials.

2.4.2 Oxidation Resistance

The oxidation resistance of the MoSi_2 is significant when compared to other intermetallic compounds based on titanium, niobium and tantalum composites as well as the single crystal nickel-based superalloy [7]. The addition of the silica makes the alloy to have a high oxidation resistance because at high temperature, the silica forms a thin layer which acts as a barrier and reduces the oxygen permeation rate. The addition of boron to the MoSi_2 increases the oxidation resistance as it forms a glassy layer of borosilicate [6].

2.4.3 Fracture Toughness

The fracture toughness of the MoSi_2 decreases while the temperature increases, this was overcome by adding 2 wt% C which increases the fracture toughness [8]. The fracture mode also changes from intergranular to transgranular due to the addition of the C and the removal of the silica grain boundary phase reaction with carbon.

2.4.4 Microstructure

Depending upon the composition and heat treatment, a wide range of microstructure can be obtained. After grinding and polishing and viewing the microstructure of the specimens using SEM. Annealing causes a much more uniform microstructure of Mo_3Si particles. Finer grain alloys generally have Grain Boundary Sliding (GBS), which is their principal deformation mode. The compounds, which are rich in Mo. like Mo_3Si , Mo_5Si_3 , Mo_5SiB_2 , MoB, Mo_2B are brittle at ambient temperature. The Mo_5SiB_2 creates a number of ternary phase fields, which allows controlling the mechanical properties by micro structural manipulations.

2.5 Spinel and its Properties

Spinel is Magnesium Aluminum Oxide ($MgAl_2O_4$) or known as magnesia spinel. Due to various impurities, the color of the spinel ranges from blood red to blue, green, brown, and colorless. Spinel is found in basic igneous rocks, granite pegmatites, and contact metamorphic limestone deposits. Synthetic spinel has been manufactured since the early 20th century for use as imitation gemstones. Spinel may also refer more broadly to any of various mineral oxides of magnesium, iron, zinc, or manganese in combination with aluminum, chromium, or iron. It has a hardness value of 8 in Moh's scale. The specific gravity is about 3.58 to 3.61. The cleavage of the spinel particle is imperfect and the fracture type is either conchoidal or uneven. The crystallographic arrangement of spinel is isometric. Spinel and Ruby have the same chemical properties, where spinel is magnesium aluminum oxide and ruby is aluminum oxide. Spinel and ruby although have the same refractive index, the ruby is harder than spinel [9].

2.6 Applications of Molybdenum and its Alloys

Molybdenum and its alloys have been applied in various industrial applications, due to the alloy's good high temperature mechanical properties and electrical conductivity [4]. Some of the applications are nuclear reactor control rod production, rocket skirts, cones and heat shields, missile components heat shields in high temperature vacuum furnaces. Molybdenum was primarily used as an alloying additive in both low and high carbon steel. By addition of molybdenum to steel, it improves certain mechanical properties. The molybdenum atom is large relative to the other alloying elements in steel, due to that it increases the creep strength up to 600°C and yield strength [4].

2.6.1 Carburizing Steel

Molybdenum is used to carburizing steels (0.15-0.3%) to increase, simultaneously the hardenability of the low carbon steel and toughen the high carbon steel. In low carbon it increases the hardenability whereas it increases toughness of the alloy. It minimized surface cracking and spalling. Because of the oxidizing resistance during the process, and thus acting as a hardening agent, molybdenum avoids the hydrogen diffusion and minimizing hydrogen induced surface cracking. Because of these property enhancements, high temperature carbon steel alloys with 0.5% Mo had been used worldwide in oil refineries, power plants and petrochemical plants [4].

2.6.2 High Strength Low Alloy (HSLA) Steels

Molybdenum plays a important role in the development of low carbon steel. Addition of 0.1 -0.3%of molybdenum, increases yield strength without extensive heat treatment. It gives a fine grain structure and enhances precipitation hardness effects alloying with other elements.

2.6.3 Oil Industries

Oil industries uses AISI 4100 Cr-Mo steels which contains 0.15 – 0.2% of Mo. As the depth increases in exploring deep reservoirs, the corrosive hydrogen disulphide, carbon dioxide and high chloride brines, environmental attacks are reduced by using higher molybdenum content stainless steels. Molybdenum increases the pitting and crevice corrosion resistance in stainless steel.

2.6.4 Heating Elements

The molybdenum alloys have been employed as a heating element for air furnaces for a long time since they have a very high melting point. The problem of these elements is that the elements have brittle fracture, which makes them difficult to handle and also the high temperature creep. Improvements in the properties will enhance the use of these alloys which will have greater life and creep resistance

2.6.5 Gas Turbines

High temperature materials are required for a Blade Outer Air Seal (BOAS) hot section component of the high temperature gas turbines. In the engine, the BOAS is a stationary part, which is located directly opposite the rotating hot section turbine blades. The main purpose of the BOAS is to maintain a small gap of stable dimensions between itself and the turbine blade. If the gap widens during the operation of the turbine, it directly affects the turbine efficiency. Although stationary, the BOAS is exposed to high turbine gas temperatures and thus incurred significant thermal stresses. A material which has low thermal coefficient and high temperature impact strength is ideal for BOAS application. The MoSi_2 which posses these significant properties have been tested for use of the gas turbine blades [6]. Molybdenum is also used in nickel- and cobalt- base high performance superalloys for turbine engine components.

2.6.6 Diesel Engines

The Toyota Central R&D facility in Japan has recently developed molybdenum silicide composite diesel engine glow plugs [6]. The material contains 30-40% MoSi_2 phase in a

Si₃N₄ matrix. The glow plugs had two main advantages when compared to the conventional metal glow plugs. First, they are highly resistant to the diesel fuel combustion environment and thus have a long lifetime. Second, they can be heated at higher heating rates with the result that the diesel engine can be started faster.

2.6.7 Industrial Gas Burners

The industrial gas burners are used for oxygen-natural gas mixtures to reduce NO_x environmental emissions. Because of the presence of oxygen environment the gas burners must operate at higher temperatures, so there is a need to develop a new material which can withstand the oxygen-natural gas combustion environment. Studies have shown that the MoSi₂ has a good resistance to the oxygen-natural gas combustion process [6].

The other applications due to the properties of molybdenum base alloys are

- High temperature heating elements, radiation shield, extrusion forging dies etc.
- Rotating X-ray anodes used in clinical diagnostics
- Glass melting furnace electrodes and components that are resistant to molten glass
- Sprayed coatings on automotive piston rings and machine components to reduce friction and improve wear.

Chapter 3 EXPERIMENTAL PROGRAM

3.1 Molybdenum Base Alloys

The base alloys in this study were pure molybdenum, molybdenum with 0.745 weight percent silicon, molybdenum with 3.4 weight percent of Spinel ($MgAl_2O_4$) and molybdenum with 6% weight percentage of spinel ($MgAl_2O_4$). The specimens were processed at Oak Ridge National Lab, Tennessee. Table 3.1 shows the material composition and the processing method of the alloys under investigation. The heat treatment was done on the specimens as shown in the table. The test specimens were polished using SiC papers from 240 to 600, step by step.

Ref. #	SPECIMEN	MATERIAL COMPOSITION	HEAT TREATMENT/PROCESS
648	PURE MOLYBDENUM	100% Molybdenum	Annealed 24hr/1600 ⁰ C/Vaccum
649	MOLYSILICIDE	99.255% Wt. Molybdenum 0.745% Wt. Silicon	Annealed 24hr/1600 ⁰ C/Vaccum
677	PURE MOLYBDENUM	100% Molybdenum	Hot pressed from 2-8 μ m Mo. Powder. 4hr/1800 ⁰ C/3Ksi/Vaccum
678	MOLYBDENUM-SPINEL Mo-MgAl ₂ O ₄	3.4% Wt. MgAl ₂ O ₄ Rest Molybdenum	Hot pressed from 2-8 μ m Mo. Powder and 1-5 μ m MgAl ₂ O ₄ Powder fused. 4hr/1800 ⁰ C/3Ksi/Vaccum
697	MOLYBDENUM-SPINEL Mo-MgAl ₂ O ₄	6% Wt. MgAl ₂ O ₄ Rest Molybdenum	Hot pressed from 2-8 μ m Mo. Powder and 5 μ m MgAl ₂ O ₄ Powder fused 1hr/1800 ⁰ C/3Ksi/Vaccum

Table 3.1 Material compositions and the heat treatment provided by Oak Ridge National Lab

3.2 Tests and Testing Equipment

The specimens stated above were mainly subjected to thermal tests to evaluate their thermal properties and to compare the composition and processing method. The following tests were conducted.

- Coefficient of thermal expansion test using a *Thermo-Mechanical Analyzer*.
- Thermo cycling test.
- Test for determining the energy transformation pattern using a *Differential Temperature Analyzer*.
- Scanning Electron Microscope (SEM), Energy Dispersive Spectroscopy (EDS) for examining the specimens after the tests.

3.3 Coefficient of Thermal Expansion (CTE)

When thermal energy is added to a material, a change in its dimensions occurs. This phenomenon is known as thermal expansion and the property of a material responsible for this is known as *coefficient of thermal expansion*. The coefficient of thermal expansion is the amount of expansion in a unit length of a solid material as a result of a temperature rise of 1 degree (1°).

Coefficient of thermal expansion, $\alpha = 1/l \cdot dl/dT = d\epsilon/dT$

Where, l is the length, and dl/dT is the strain (dl/l)

Coefficient of thermal expansion, though it may be assumed to be a constant, for most materials, it increases slightly with temperature and changes with any phase change in the material.

3.4 The Thermo-Mechanical Analyzer (TMA 2940)

3.4.1 Introduction

The TMA 2940 is an analytical instrument used to test the physical properties of many different materials. It has two major parts, the TMA module cabinet and TMA assembly.

The TMA assembly has various parts which covers the hardware *viz.*, the balance enclosure, the probe assembly, stage, which is interchangeable and supports the sample during measurement, the furnace assembly which surrounds the stage. The furnace also encapsulates the thermocouple. The weight tray, located behind the weight tray door, holds the weights to exert known force on the sample. The module cabinet contains the electronics and software needed to control the module, perform and store experiments and results.

3.4.2 Theory of Operation

Thermo-mechanical analyzer 2940 is capable of heating or cooling the samples while applying the predetermined force on the material. The specimen is placed on the stage and the quartz probe is placed in contact with the sample, any linear or volumetric changes in dimension are determined at the selected temperature and force.

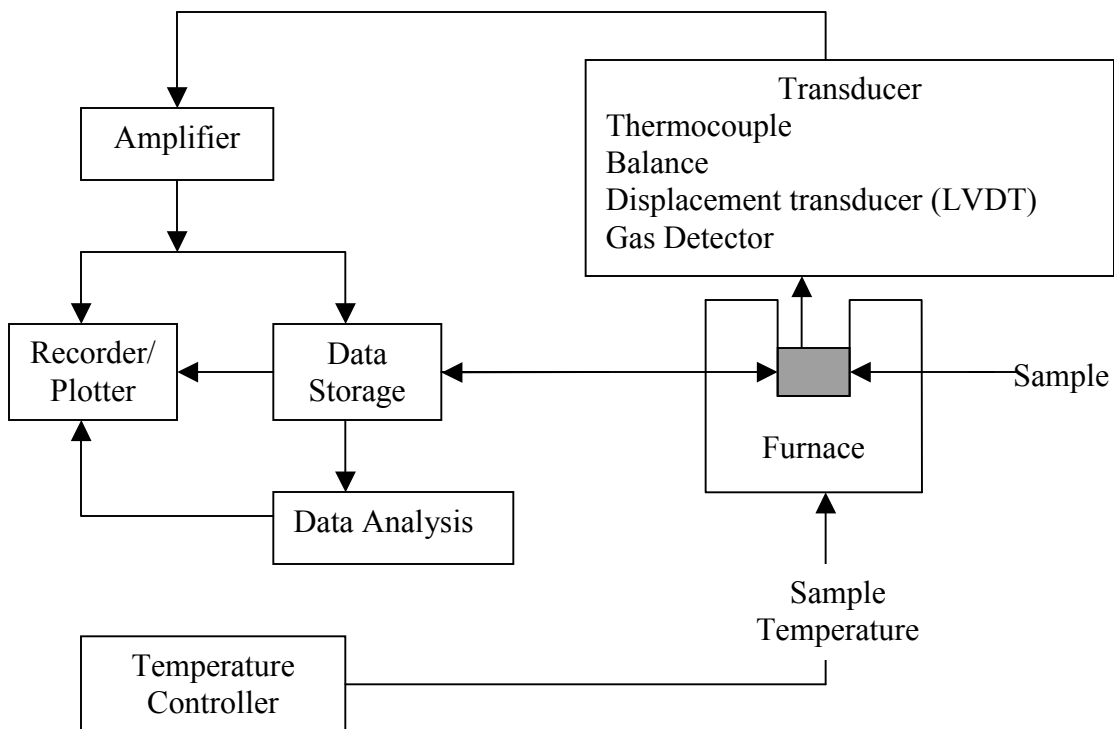


Figure 3.1 Schematic Layout of the TMA 2940

3.4.3 Working Procedure

The sample according to the ASTM E831 is to be prepared and polished, so that at least two parallel sides are optically flat. The specimen's flat surface must be placed on the stage and the probe should touch the other side of the specimen. Before placing the specimen the probe must be made to read zero at the start of the test the probe. Once the sample is placed and the probe is made to touch it, the sample's dimension will be measured, this can be done by pressing the "measure" button on the display panel. The initial parameters are automatically fed to the module controller which stores the data in the GPIB. The program must be keyed in according to the requirements for the test. The program will be saved in the GPIB. The thermocouple, which measures the temperature is placed close to the sample. The furnace must be brought back to the initial place and an inert gas is allowed to pass through the chamber, to ensure an environment, where the process of oxidation is prevented. The experiment is started and the thermocouple reads the furnace temperature and the change in dimensions is sensed by the probe, which is connected to a LVDT. The data will be stored in the GPIB memory for analysis. The controller plots a real time graph and the data's can be analyzed using Universal Analysis® software in the TMA 2940.

3.5 The Differential Thermal Analyzer (DTA 1600)

3.5.1 Introduction

The Differential Scanning Calorimeter (DSC) is a thermal analysis technique, used to measure the temperature and heat flow associated in materials when there is a phase transition. This analyzer provides qualitative and quantitative information about the materials as a function of time and temperature. Differential Thermal Analyzer (DTA1600) which is mounted on the DSC, measures the difference in temperature between the sample and a thermally inert material as the temperature is increased.

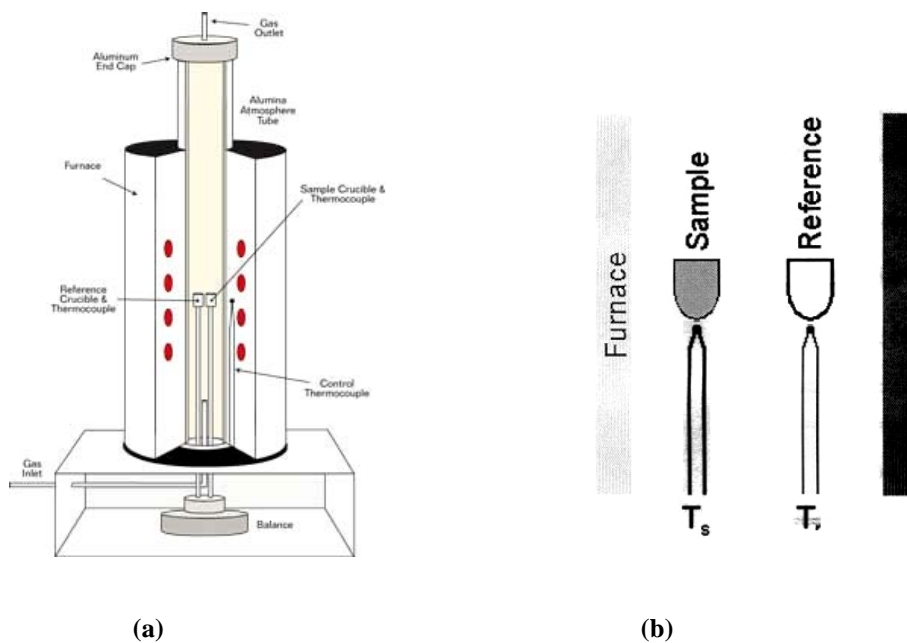


Figure 3.2 (a) The figure shows the schematic diagram of the DTA furnace and thermocouple assembly. (b) The figure shows the positioning of the thermocouples under the specimen and the reference material.

3.5.2 Theory of Operation

The DTA has two thermocouples (T/Cs) for measuring the temperature. On the left T/C sits a sample containing cup. On the right is an empty cup. The furnace heats up both cups at the same rate and so $T_s - T_r$ is approximately zero until endothermic (exothermic) transition is reached. At this point energy (heat) is absorbed (released) by the sample and the sample thermometer becomes cooler (warmer). After the sample has completed the transition, T_r and T_s once again become equal. A plot of $T_s - T_r$ versus T_r will show a negative (positive) peak at the temperature transition. The peak height corresponds to the amount of energy absorbed (released) by the sample and the peak width corresponds to the temperature range over which the transition occurred.

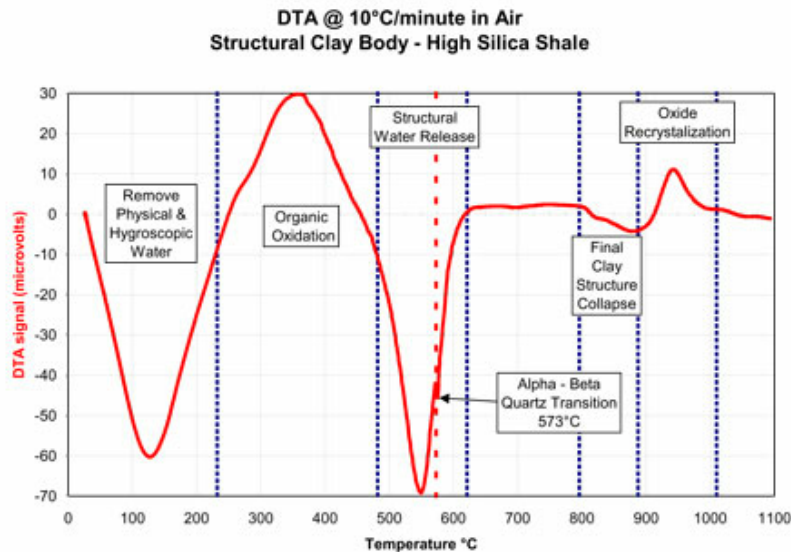


Figure 3.3 Schematic Diagram showing Typical results From Differential Temperature Analyzer.

3.5.3 Working Procedure

The specimen is to be prepared according to ASTM E 473. The specimen is weighed using a balance and it is placed in the reference cup inside the furnace on the right side. The furnace must be closed and the inert gas must be supplied through the furnace tube to

maintain a oxidation free environment. The furnace is turned on by using the controller in which the program must be stored in the GPIB, which controls the analyzer. The thermocouple senses the temperature change between the sample and the reference material and the values are stored in the GPIB for the analysis. A real time plot is shown in the display. The data can be analyzed using the Universal Analyzer provided along with the instrument.

3.6 Scanning Electron Microscope

The JEOL scanning electron microscope was used for the post-mortem of the specimens after the tests to examine the cross-section to study the arrangement of crystals and to check the grain boundaries for any micro-cracks after thermo-cycling tests and to check for any oxides present after the tests. The phase identification in the alloys tested was difficult because of the presence of both light elements and heavy elements. The light elements having low atomic number like silicon, aluminum, oxygen and magnesium, whereas the heavy element having high atomic number like molybdenum. The X-ray diffraction method was used to identify the phases present in the specimen, for example Mo-MgAl₂O₄, once the phases are identified, backscattered electron detector was used to detect the phases present. Backscattering electron detector detects the element by its contrast from the atomic number differences. For example, in this case the material molybdenum- spinel, molybdenum being heavy appears light and the spinel particle being lighter one appears dark. The oxygen, which forms the spinel by mixing with aluminum and magnesium, is not only found in the spinel region but also seen in the molybdenum matrix, which proves the presence of Molybdenum oxide formation at high temperature.

3.7 Thermo-Cycling Test

The alloys #678 and #697, Molybdenum with spinel (3.4% and 6% of MgAl₂O₄), in which the size of the molybdenum particle is 2-8 μ m and MgAl₂O₄ particle is 1-5 μ m,

which are subjected to thermo cycling tests to evaluate the cracking pattern due to thermal stresses and expansion at high temperature.

3.7.1 Testing Conditions

The specimens were placed in a furnace, where the temperature reaches a maximum of 650°C. The heating rate was 200°C/min as shown in figure 3.4. The specimens were maintained at isothermal once it reached 650°C for 5 minutes [10]. The specimens were air-cooled after that. 3 different specimens were used for 1 cycle, 10 cycles and 20 cycles. After the tests, the specimen's surface was polished using diamond polish suspension till 0.5 micron. Once the test were done and polished, post-mortem of the samples was done using the Scanning Electron Microscope (SEM).

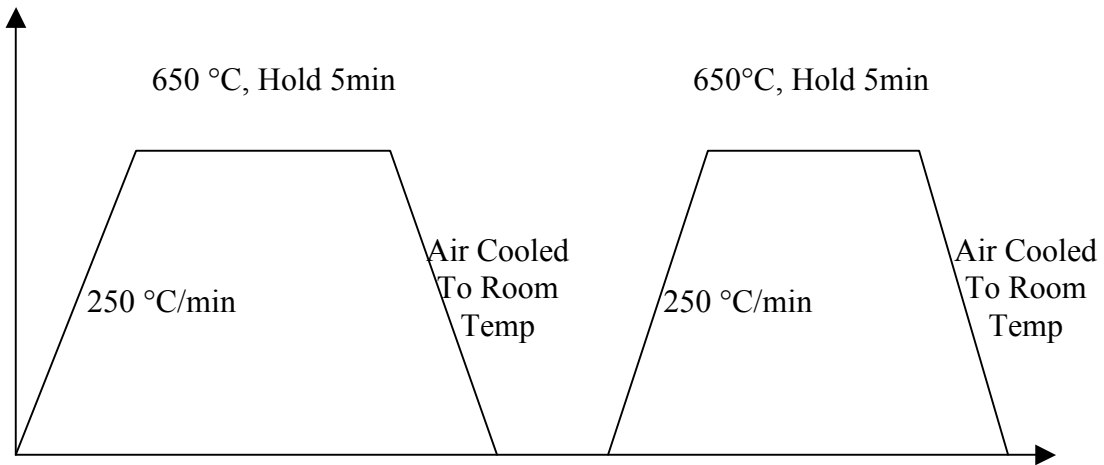


Figure 3.4 Graph showing the thermo-cycle process.

Chapter 4 RESULTS AND DISCUSSIONS

4.1 Introduction

In this chapter the results from the tests performed on the molybdenum base alloys are discussed. The molybdenum base alloys which were subjected to coefficient of thermal expansion test and thermo-cycling tests were polished to study the metallographic changes after the tests, by which a suitable alloy can be developed which has good thermo-mechanical properties and long work life in the use of high temperature applications.

4.2 Coefficient of Thermal Expansion Using TMA 2940

The coefficient of thermal expansion (CTE) is one of the most important thermal property of the material, which is used in high temperature application, as the material must have low value of thermal expansion, because as the temperature increases the material must not expand on a large scale as it will hinder the long term usage of the material, where the dimensions of the material are important. The molybdenum base alloys were tested for the coefficient of thermal expansion (CTE). The working conditions and results are discussed. For the use of TMA in measuring the CTE value, the test specimen should be between 2 and 10 mm in length and shall not exceed 10 mm in lateral dimension and the specimen must be flat on both ends. The specimens were prepared using Electrical Discharge Machining (EDM) CNC-10A, as the alloys have metallic nature of bonding. After the machining was done the specimens were cleaned in acetone and then air dried before conducting the tests. After the tests [11], the specimens were polished again for post mortem microstructure analysis.

4.2.1 Thermal expansion test: Molybdenum (ref. # 648)

Due to the constraint in availability of this material only three tests were carried out, thus forming a standard test pattern to maintain consistency for all the other alloys.

	TEST 1*	TEST 2	TEST 3
SAMPLE	MO	MO	MO
SIZE	2.7862	3.3185	2.9220
CELL CONSTANT	1.0000	1.0000	1.0000
METHOD	MOTEST	MOTEST	MOTEST

* Flow rate of argon was 100cc/min.

Table 4.1 Parameters of the CTE test on Molybdenum 648

The method file is given below and it was maintained the same in order to maintain the consistency.

Universal Analysis

File: D:\TA\ASH.001 Run

Program: Universal V1.8M Run Number: 1, 2 and 3

TA Instruments Thermal Analysis -- TMA Standard

Force 0.050 N

Equilibrate at 30.00 °C

Ramp 10.00 °C/min to 250.00 °C

Ramp 10.00 °C/min to 500.00 °C

Ramp 10.00 °C/min to 750.00 °C

Ramp 10.00 °C/min to 1000.00 °C

End of method

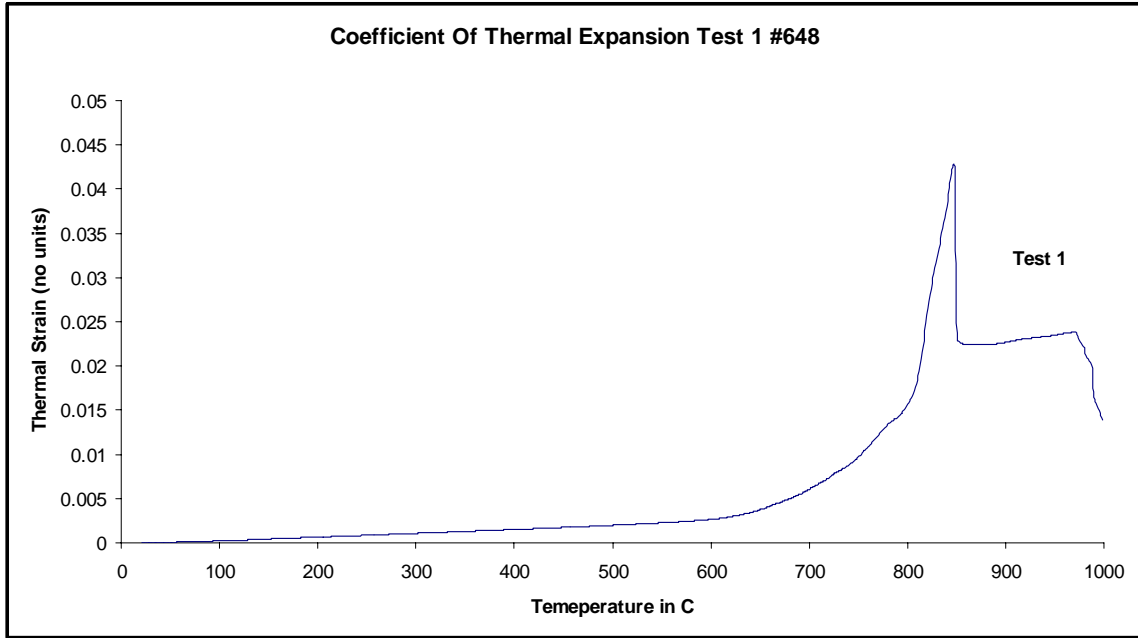


Figure 4.1 Coefficient of thermal expansion of molybdenum #648. Test 1

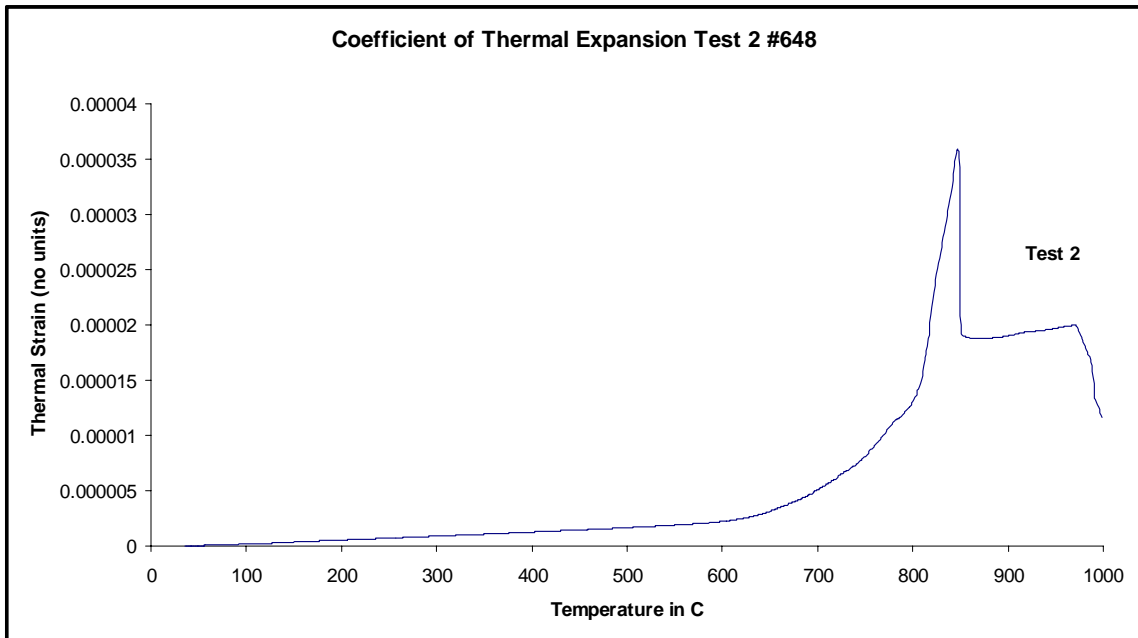


Figure 4.2 Coefficient of thermal expansion of molybdenum #648 Test 2

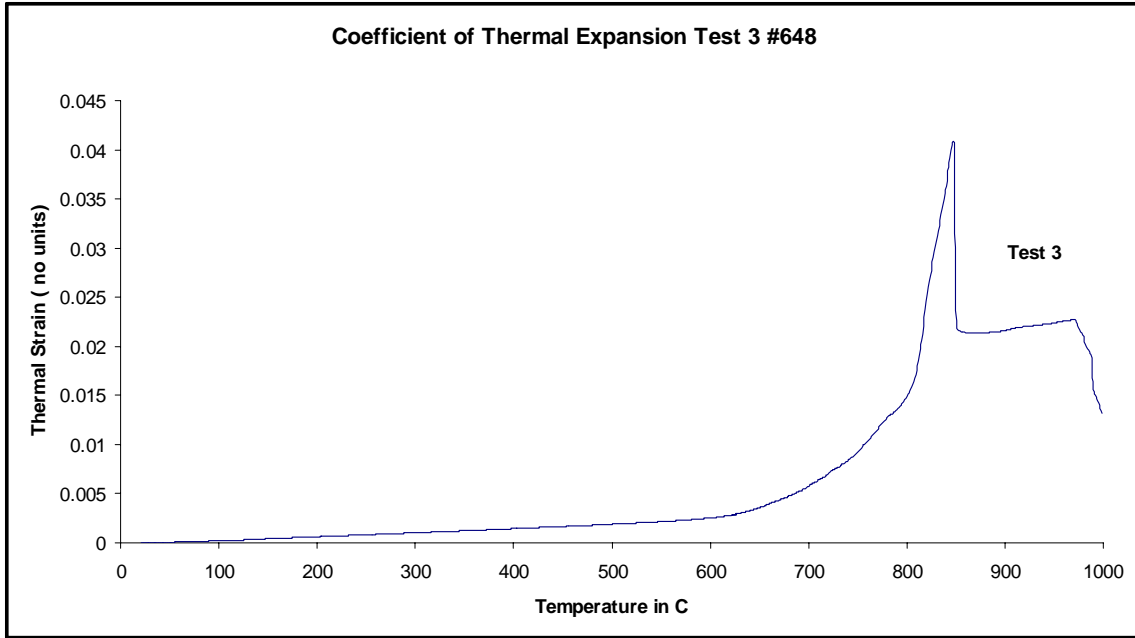


Figure 4.3 Coefficient of thermal expansion of molybdenum #648 Test 3

4.2.2 Thermal expansion test: Molybdenum silicide (ref. # 649)

	TEST 1	TEST 2	TEST 3
SAMPLE	MOSI	MOSI	MOSI
SIZE	4.1036	3.6092	4.7702
CELL CONSTANT	1.0000	1.0000	1.0000
METHOD	MOSITEST	MOSITEST	MOSITEST

Table 4.2 Parameters of the CTE test on Molybdenum Silicide 649

The method file is given below and it was maintained the same in order to maintain the consistency.

Universal Analysis

File: D:\TA\ASH.001 Run
Program: Universal V1.8M Run Number: 4, 5 and 6

TA Instruments Thermal Analysis -- TMA Standard

Force 0.050 N
Equilibrate at 30.00 °C
Ramp 10.00 °C/min to 250.00 °C
Ramp 10.00 °C/min to 500.00 °C
Ramp 10.00 °C/min to 750.00 °C
Ramp 10.00 °C/min to 1000.00 °C
End of method

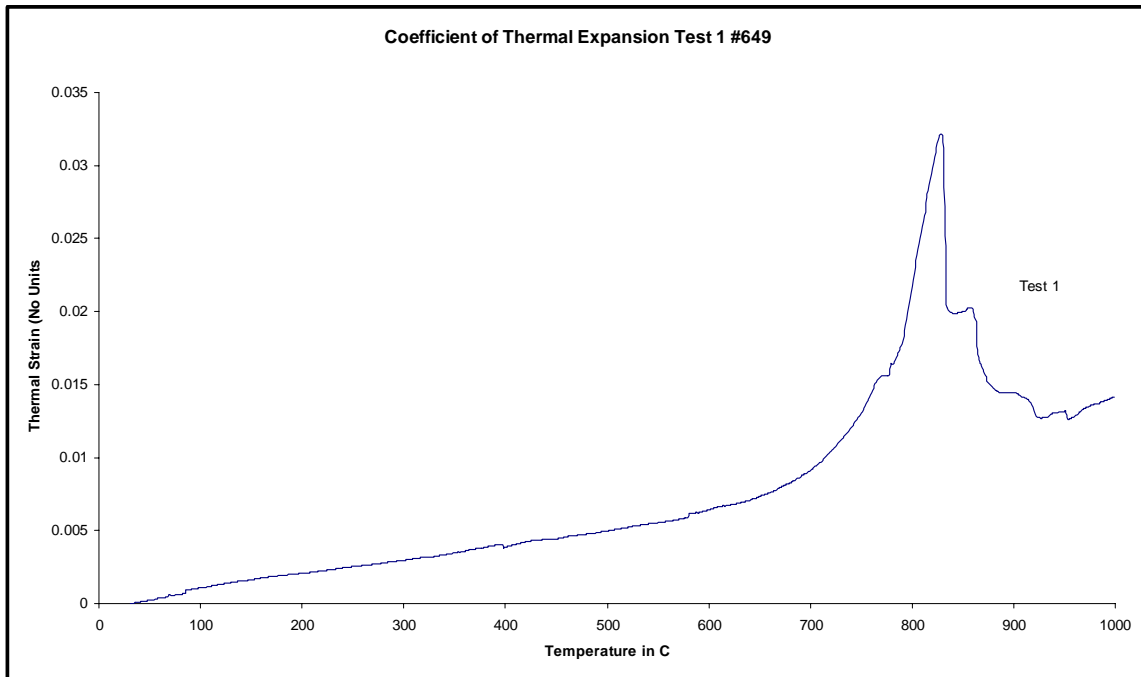


Figure 4.4 Coefficient of thermal expansion of molybdenum silicide #649 Test 1

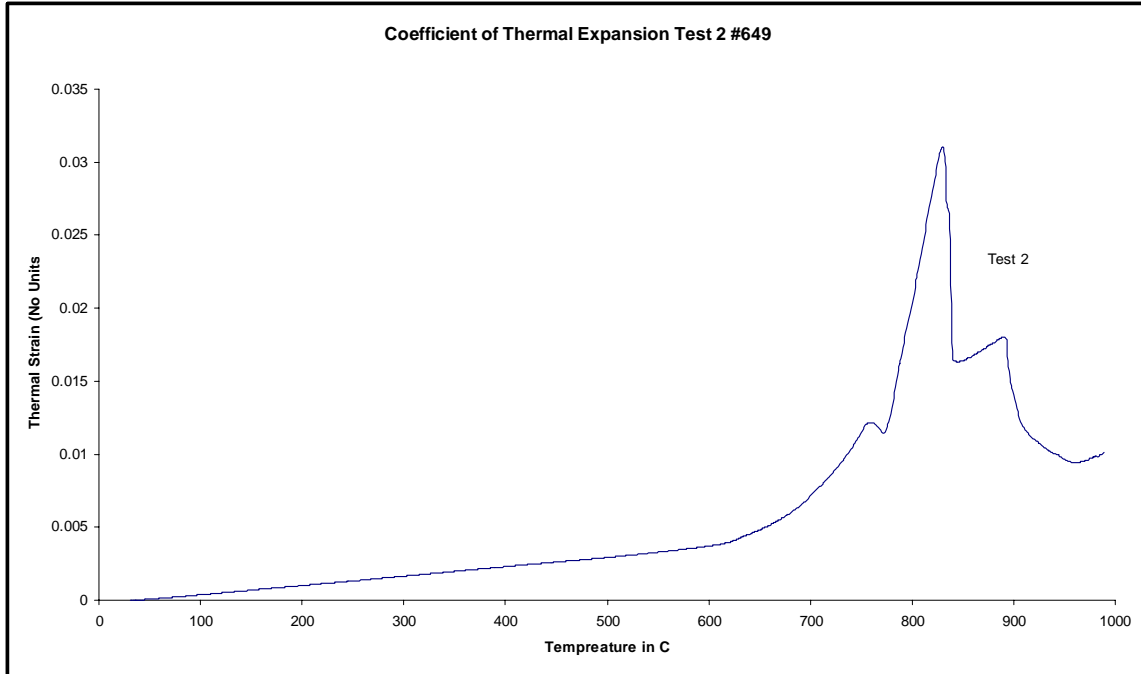


Figure 4.5 Coefficient of thermal expansion of molybdenum silicide #649 Test 2

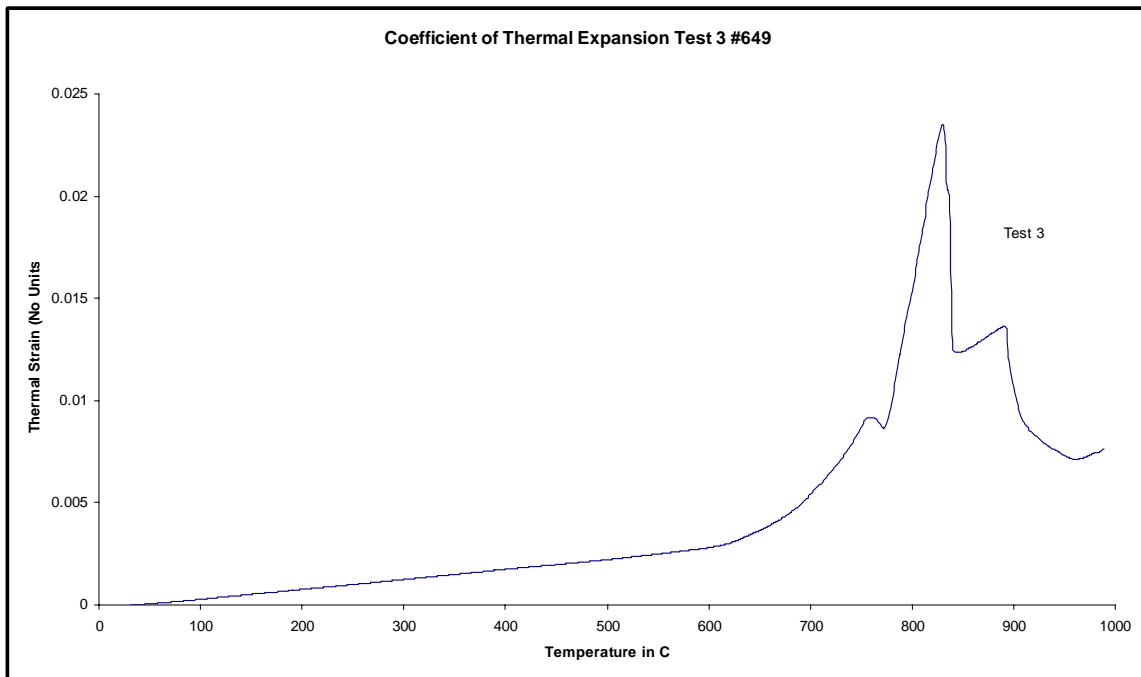


Figure 4.6 Coefficient of thermal expansion of molybdenum silicide #649 Test 3

4.2.3 Thermal expansion test: Molybdenum (ref. # 677)

	TEST 1	TEST 2	TEST 3
SAMPLE	MO	MO	MO
SIZE	3.5742	2.9840	3.5210
CELL CONSTANT	1.0000	1.0000	1.0000
METHOD	MOTEST	MOTEST	MOTEST

Table 4.3 Parameters of the CTE test on Molybdenum 677

The method file is given below and it was kept the same in order to maintain the consistency.

Universal Analysis

File: D:\TA\ASH.001 Run

Program: Universal V1.8M Run Number: 7, 8 and 9

TA Instruments Thermal Analysis -- TMA Standard

Force 0.050 N

Equilibrate at 30.00 °C

Ramp 10.00 °C/min to 250.00 °C

Ramp 10.00 °C/min to 500.00 °C

Ramp 10.00 °C/min to 750.00 °C

Ramp 10.00 °C/min to 1000.00 °C

End of method

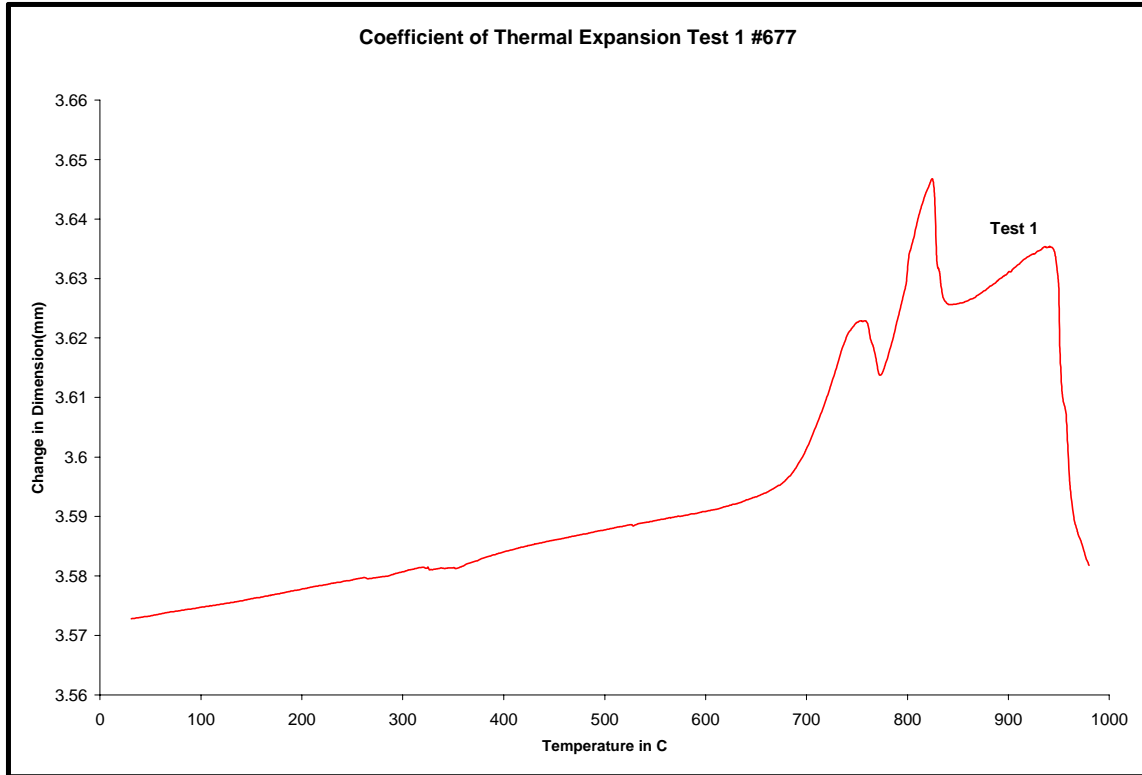


Figure 4.7 Coefficient of thermal expansion of molybdenum #677 Test 1

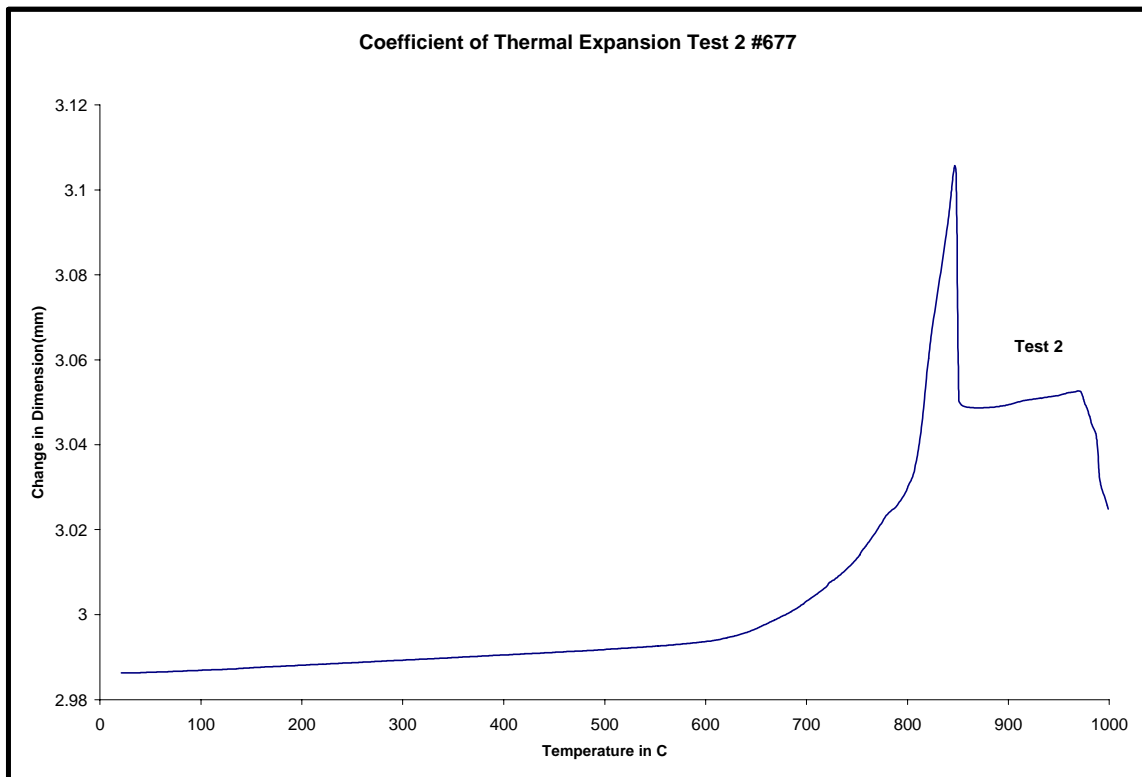


Figure 4.8 Coefficient of thermal expansion of molybdenum #677 Test 2

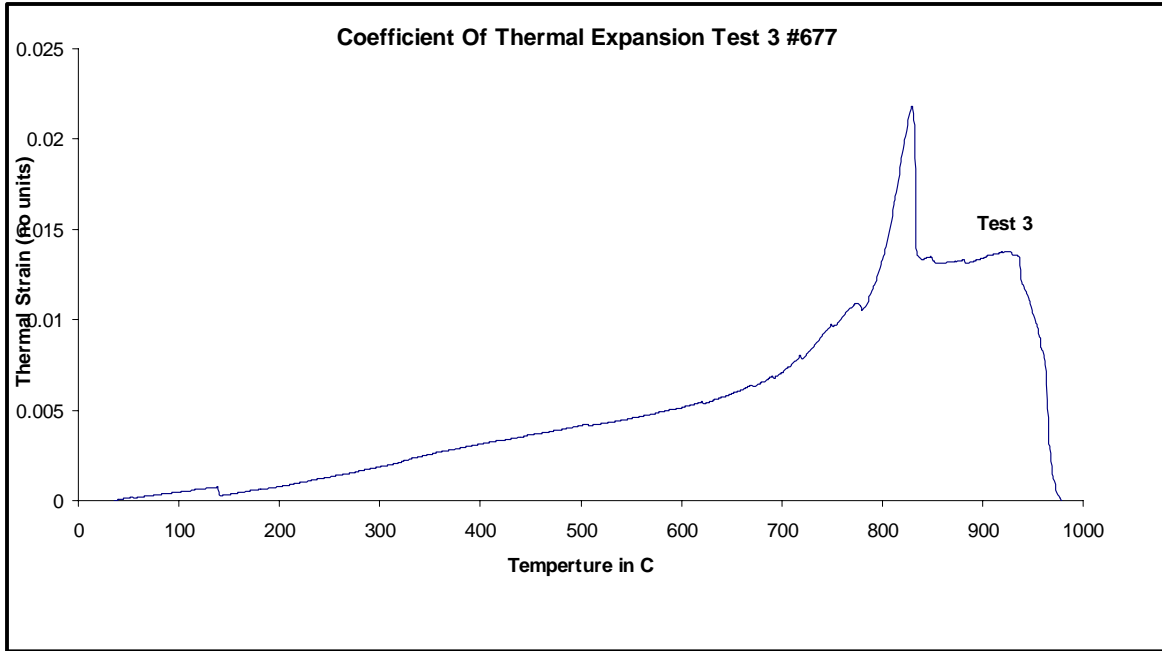


Figure 4.9 Coefficient of thermal expansion of molybdenum #677 Test 3

4.2.4 Thermal expansion test: Molybdenum- Spinel (ref. # 678)

	TEST 1	TEST 2	TEST 3
SAMPLE	MO-MgAl₂O₄	MO-MgAl₂O₄	MO-MgAl₂O₄
SIZE	3.8366	2.8429	4.0121
CELL CONSTANT	1.0000	1.0000	1.0000
METHOD	MoSpinel	MoSpinel	MoSpinel

Table 4.4 Parameters of the CTE test on Molybdenum-Spinel 678

The method file is given below and it was maintained the same in order to maintain the consistency.

Universal Analysis

File: D:\TA\ASH.001 Run

Program: Universal V1.8M Run Number: 10, 11 and 12

TA Instruments Thermal Analysis -- TMA Standard

Force 0.050 N

Equilibrate at 30.00 °C

Ramp 10.00 °C/min to 250.00 °C

Ramp 10.00 °C/min to 500.00 °C

Ramp 10.00 °C/min to 750.00 °C

Ramp 10.00 °C/min to 1000.00 °C

End of method.

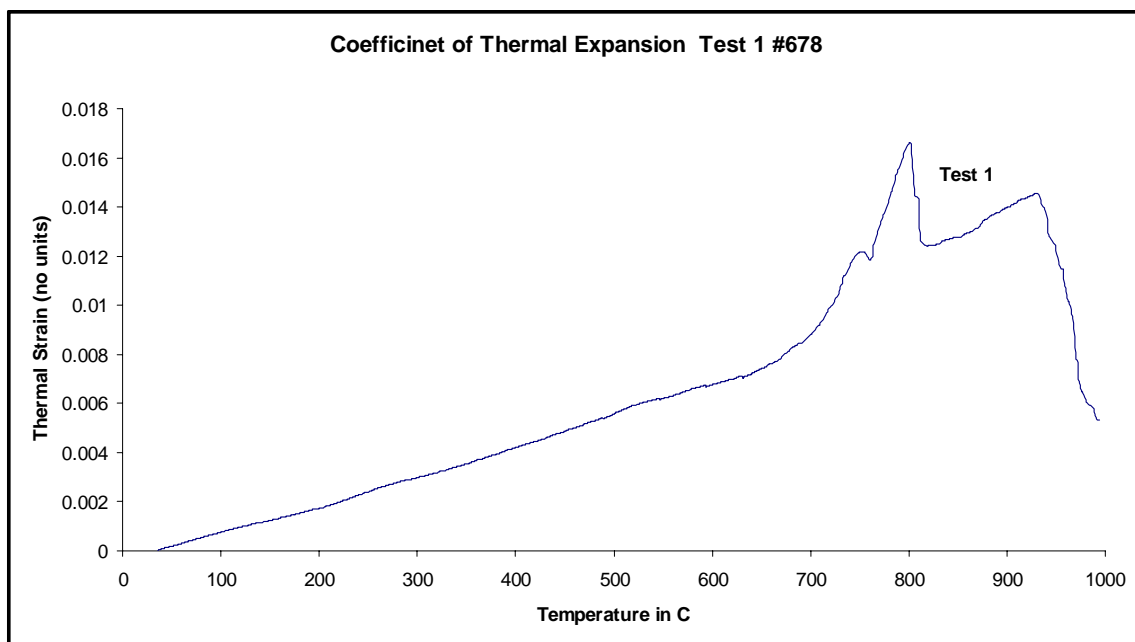


Figure 4.10 Coefficient of thermal expansion of molybdenum-spinel #678 Test 1

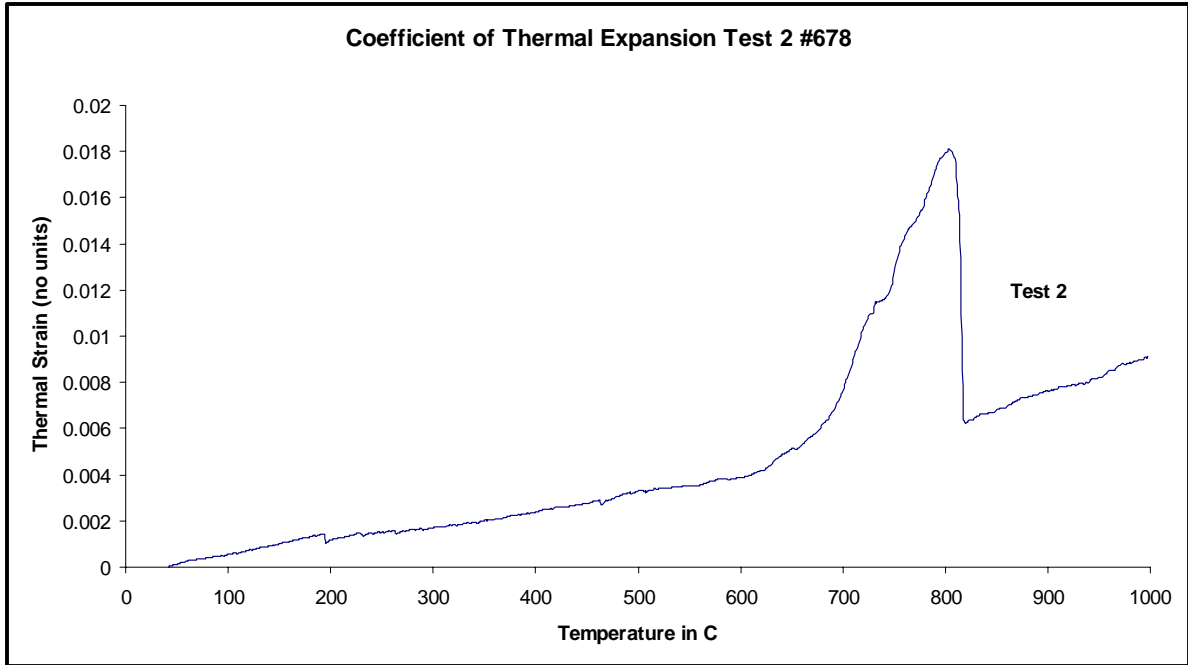


Figure 4.11 Coefficient of thermal expansion of molybdenum-spinel #678 Test 2

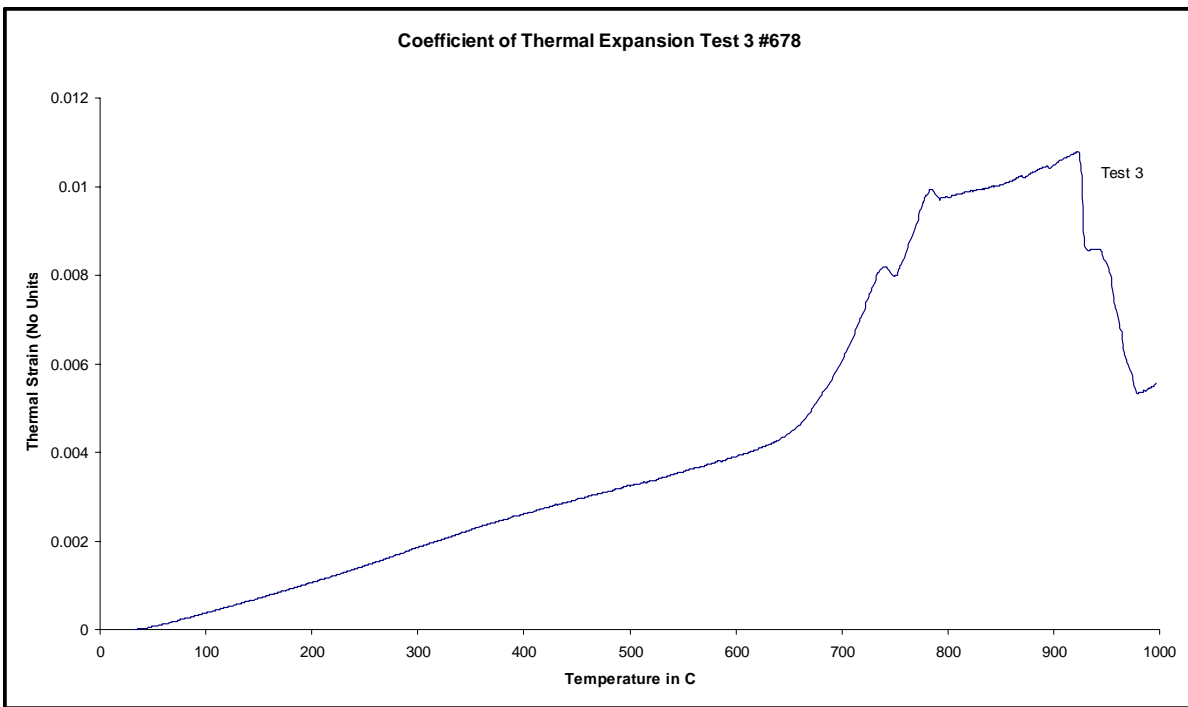


Figure 4.12 Coefficient of thermal expansion of molybdenum-spinel #678 Test 3

4.2.5 Thermal expansion test: Molybdenum- Spinel (ref. # 697)

Parameters of the tests conducted

Test #1.

Sample: Spinel
Size: 3.8366 mm
Cell Constant: 1.0000
Operator: Ashok
Method: MoSpinel

Universal Analysis

File: D:\TA\697.001 Run

Program: Universal V1.8M Run Number: 13.

TA Instruments Thermal Analysis -- TMA Standard

Equilibrate at 30.00 °C

Ramp 10.00 °C /min to 250.00 °C

Ramp 10.00 °C /min to 500.00 °C

Ramp 10.00 °C /min to 750.00 °C

Ramp 10.00 °C /min to 1000.00 °C

End of method

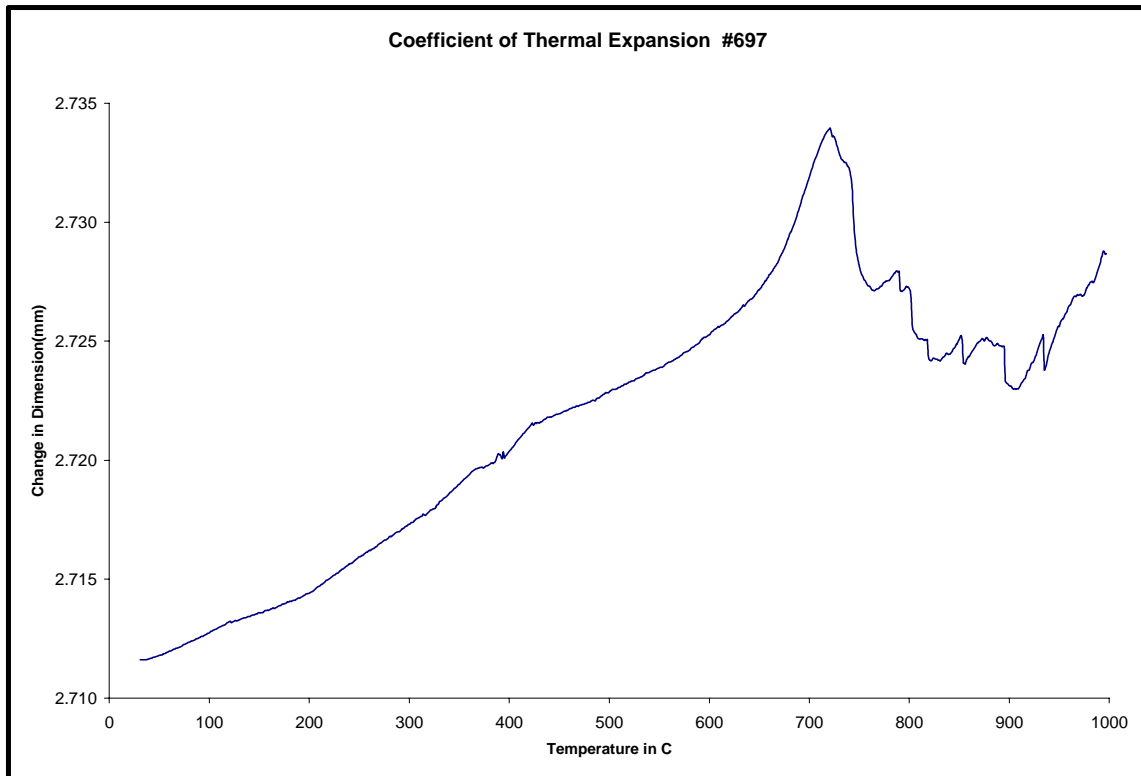


Figure 4.13 Coefficient of thermal expansion of molybdenum-spinel #697

Condition (Temperature)	COEFFICIENT OF THERMAL EXPANSION ($\mu\text{m}/\text{m}^\circ\text{C}$)				
	Molybdenum #648	Moly Silicide #649	Molybdenum #677	Molybdenum- Spinel #678	Molybdenum- Spinel #697
50	4.93	3.16	4.55	4.88	5.78
100	5.56	6.23	4.83	6.55	8.25
150	7.98	6.24	6.41	6.94	5.08
200	6.683	6.28	6.541	7.22	9.19
250	6.65	6.34	6.58	7.77	10.9
300	6.63	6.63	6.2	7.97	10.9
350	7.04	6.66	6.69	8.17	14.5
400	6.60	6.41	6.7	6.42	13.8
450	7.10	6.02	6.875	6.81	6.16
500	9.88	6.58	9.54	5.64	7.83
550	9.49	7.56	9.65	7.24	7.84
600	9.82	8.82	10.0	7.11	12.3
650	14.5*	28.9*	18.5*	17.2*	20.0*
700	35.78*	60.1*	104.0*	47.8*	46.5*
750	49.26*	106.0*	35.8*	10.5*	-95.5**
800	178.3*	359*	262.0*	4.51*	-52.2**
850	248.5*	-892.0**	9.36*	6.71*	-6.08**
900	79.73*	-242.1**	37.5*	10.3*	-36.3**
950	-349.82**	-38.2**	-613.0**	-77.3**	34.3**
1000		2.03*	-166.0**	15.9*	30.3**

* Due to the formation of molybdenum oxide (MoO_2) which accumulates over the specimen surface thereby increasing the CTE value drastically [5].

** Around a temperature range of 750-850°C formation of molybdenum oxide (MoO_3) which is very volatile in nature reduces the specimen thickness thus we have negative CTE value [5].

Table 4.5 Coefficient of thermal expansion values of alloys Using TMA

4.3 Thermo-Cycling Tests

The thermo cycling tests were conducted to determine if failure by thermal stresses may occur. Three specimens of each molybdenum-spinel material differing in processing procedure were considered to check and differentiate the alloy, which has good resistance to thermo-cycling. Each specimen was cut using the EDM CNC 10-A. for each thermal cycle, the specimen was heated in a furnace up to 650°C, maintained at 650°C for 5 minutes, and then allowed to air cooled. For each alloy, three specimens were used to conduct 1, 10 and 20 cycles [10]. After the tests, the specimens were ground using SiC papers and polished till 0.5 microns using diamond suspension polishing agent. Post mortem microstructural analyses were done on the tested specimens. The specimens were investigated using Scanning Electron Microscope (SEM) and Energy Dispersive Spectroscopy (EDS) and the micrographs were obtained and the results are discussed in the next section.

4.4 Discussions

4.4.1 Coefficient of Thermal Expansion (CTE).

4.4.1.1 Explanation of the result for pure molybdenum #648

Using the TMA 2940 tests, the CTE values of all the alloys under consideration were determined. The first and the foremost question which arises is that, the coefficient of thermal expansion appeared to be nonlinear, i.e. the data and graphs obtained from the tests doesn't resemble any linearity after certain temperature. The nonlinearity may be due to the oxidation process of Molybdenum, silicon and spinel materials [5]. The molybdenum, around 700-800°C oxidizes to form molybdenum oxide (MoO_2), which is stable and accumulates over the parent material at around 700-800°C, hence the sudden peak i.e., the sudden increase of the TMA data as shown in Figures 4.1 to 4.13. Furthermore, as the temperature crosses 850°C the molybdenum oxide (MoO_2) oxidizes changed to MoO_3 [5], which is volatile in nature and thus it evaporates and leaves the substrate molybdenum surface exposed to the environment, this causes the sudden drop in the curve i.e., the dimension of the specimen decreases abruptly. Now, another layer of molybdenum oxide (first MoO_2 and then quickly changed to MoO_3) is gradually

building up as temperature continued to increase and hence the second peak observed. It should be noted that although Argon gas was supplied through the furnace to maintain an oxidizing-free atmosphere during the TMA test. The flow, which was maintained around 100 cc/min for the first test, may not be able to prevent the presence of residual oxygen in the test chamber. The maximum flow of 150 cc/min, which can be provided with the equipment, was tried out and similar results were obtained.

4.4.1.2 Explanation of the result for molybdenum silicide #649

The CTE graph of molybdenum silicide shows the similar pattern as that of the molybdenum around the same temperature range, but small peak was observed, which is caused by the oxidization of the silicon particle present in the alloy. First the silicon particle gets oxidized to form silicon oxide (SiO) subsequently forming SiO₂. The oxide which is formed is gaseous in nature thus forming a non-protective smoke rather than a continuous and protective SiO₂ film. The subsequent temperature increase temperature starts the oxidizing of molybdenum substrate. Thus the formation of silicon oxide reduces the thermal expansion coefficient of the alloy.

4.4.1.2 Explanation of the result for pure molybdenum #677

The Thermal expansion coefficient value of the pure molybdenum #677 has the same peak around 700-800°C was because of the oxidation of molybdenum forming molybdenum oxide. But the value of thermal expansion coefficient between them differs because of the method of processing the material. The #648 was cast whereas the #677 was hot pressed from the molybdenum powder and followed by heat treatment. The casting has some voids and porosity as shown in the Figure 4.15, causes the change in the CTE value.

4.4.1.3 Explanation of the result for molybdenum- spinel #678

The thermal expansion of the molybdenum spinel follows the same pattern like other alloys considered, whereas many small peaks were observed. This can be well explained by considering the alloying agent in this material like molybdenum as the base with aluminum, magnesium and oxygen as the alloying agent. The spinel (MgAl₂O₄) particle

which has a high thermal coefficient expands depending upon the particle size since they are distributed in the same volume fraction and size. Temperature reaching around 700-800°C, the molybdenum starts oxidizing. The importance of adding the spinel particle can be seen when the temperature is around 400°C as they tend to decrease the value of the expansion coefficient of the material because of the utilization of increase in temperature by them.

4.4.1.3 Explanation of the result for molybdenum- spinel #697

Due to problems in machining of this material, the test was concluded with only one successful completion. In this particular material, lots of peaks was observed after 750°C because the material while processing by hot pressing process was maintained at 1800°C for only 1 hour, thus leaving only very less time for tight bonding between the alloying agents, hence the temperature increases the reaction between the alloying agents starts especially between the bigger spinel particle and the base material.

Comparing the two molybdenum-spinel alloys (#678 and #697) for their thermal expansion values. The figure 4.14 shows that #678 has higher CTE value than the #697, which may because of two reasons (i) the composition of spinel (MgAl_2O_4) particle is more in #697 than #678 and (ii) the processing time for them is also different.

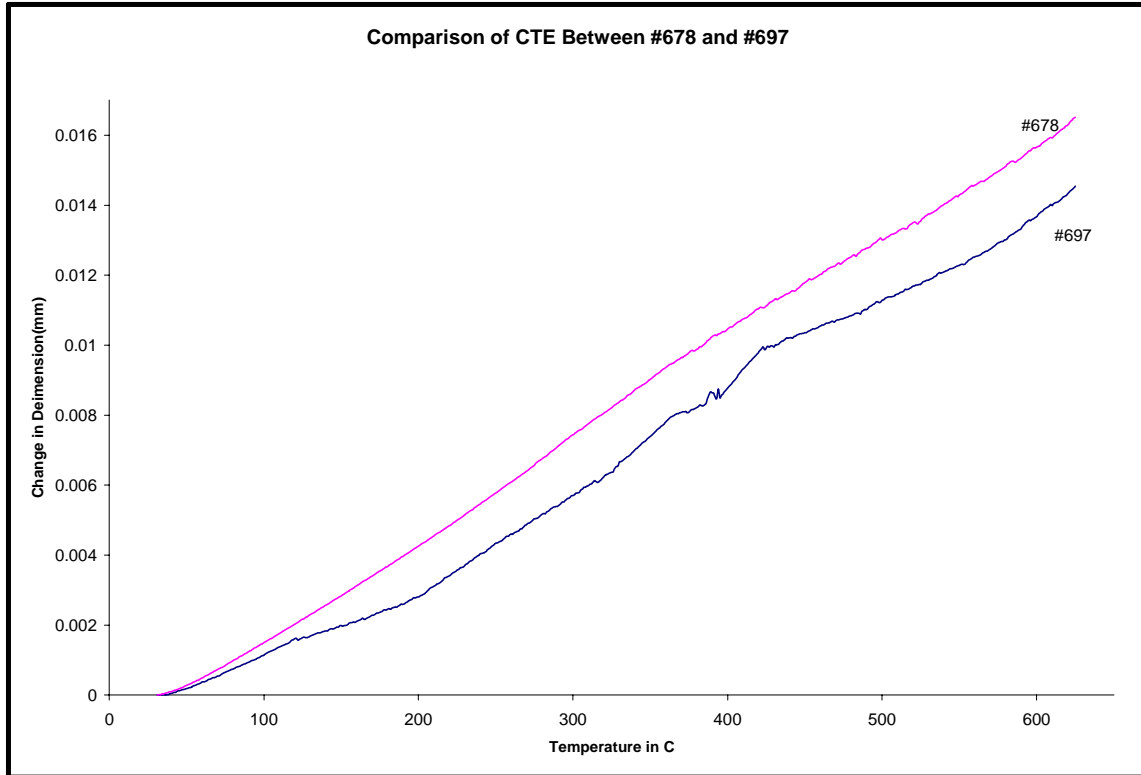


Figure 4.14 Comparison of coefficient of thermal expansion between #678 and #697

4.4.2 Thermo-cycling Test

The thermo-cycling tests were carried out in order to evaluate the microcracks which formed due to the thermal stresses on the material. After the tests specimens were polished and post mortem microstructural analyses were carried out using SEM and EDX. The specimens considered for the thermo-cycling tests were molybdenum-spinel alloys (#678 and #697).

4.4.2.1 Thermo-cycling tests on molybdenum-spinel (#678)

After the end of the thermo-cycling cycling tests the molybdenum-spinel (#678) showed some characteristics, which are explained with the help of the SEM micrographs shown below. At the end of the first cycle, due to the energy supplied, spinel particles in the molybdenum matrix were expanded and then contracted and thus may form a small interfacial gap between the spinel and molybdenum matrix as shown in Figure 4.30. Figures 4.31, 4.32 and 4.33, which were taken at higher magnification, clearly show the

gap formation between the molybdenum matrix and spinel particles. Figures 4.34, 4.35 and 4.36 shows the gap formation at different locations at higher magnification.

After ten thermal cycles, the spinel particles, which were expanded and contracted repeatedly at each cycle, may generate microcracks originated from the interfacial gap as shown in Figures 4.39 and 4.40. These microcracks are generally seen near the larger spinel particles.

After twenty thermal cycles, the spinel particles induced more stress on the molybdenum matrix and due to the mismatch of coefficient of thermal expansion between the molybdenum matrix and the spinel particles they may caused further interfacial microcracks, however, the opposite was observed, i.e. the interfacial microcracks were gone. This phenomenon may be attributed to the repeated thermo cycles such that the molybdenum matrix also expanded and thus closed these interfacial microcracks, as shown in Figures 4.41 to 4.47.

4.4.2.2 Thermo-cycling tests on molybdenum-spinel (#697)

After the first cycle as well as ten cycles, there was not much significant changes seen in the microstructure, whereas after twenty thermal cycles, substantial microcracks were seen starting from the spinel particles, propagating through the molybdenum matrix grain boundaries, and linking one spinel to its neighboring spinel particles. The cracks can be seen very clearly using an optical microscope.

4.4.3 Comparison of Alloy #678 and #697

Comparing #678 and #697, the #678 showed more resistant to thermo-cycling than #697.

This is because the spinel particle distribution in #678 is more even when compared to that of #697 and also the hot pressing time of the #678 was maintained at the 1800°C high temperature for four hours while #697 was maintained at 1800°C for only one hour.

In summary, processing method and the uniform dispersing of the spinel particle distribution are important factors that correspond to the thermo-mechanical property evaluation.

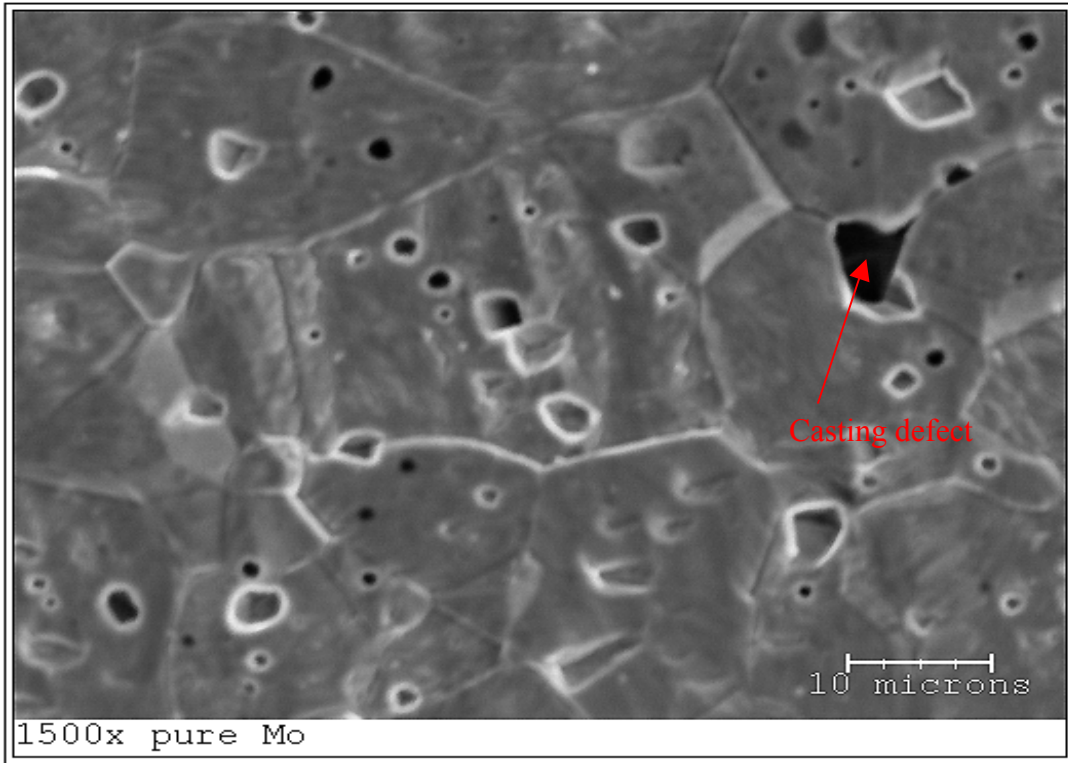


Figure 4.15 The micrograph of pure molybdenum #648 showing some defects due to casting

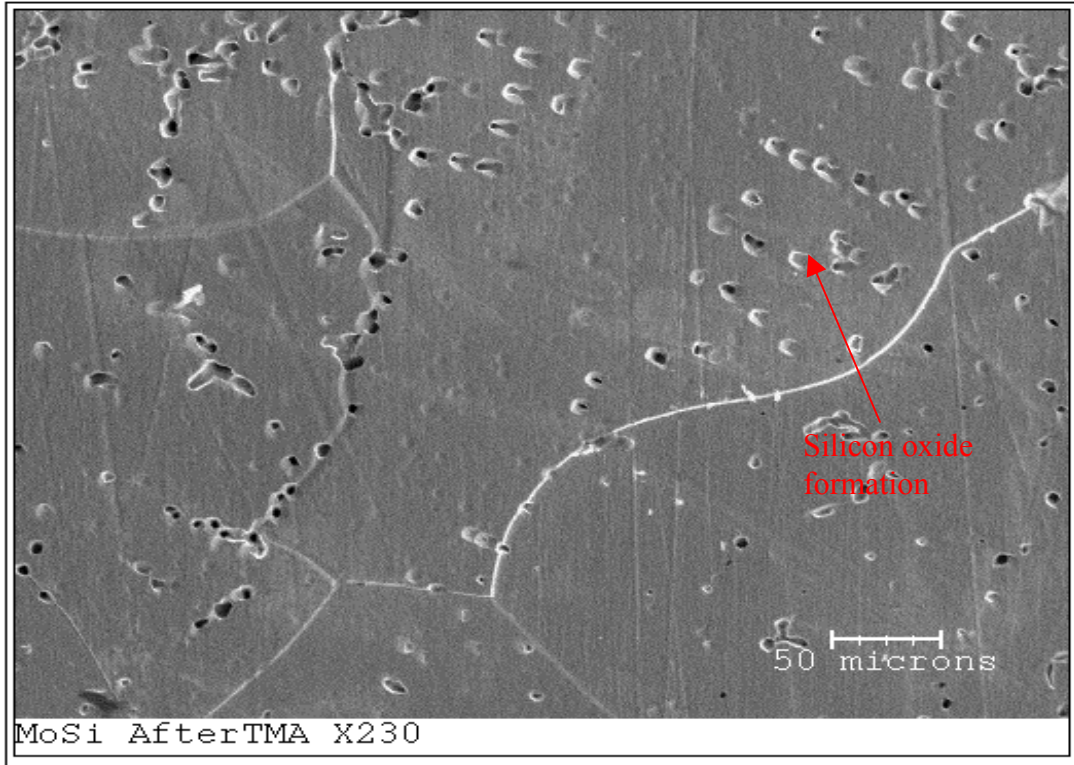


Figure 4.16 The SEM picture at X230 magnification, shows the broader picture of the MoSi alloy after test which has the oxide formation at high temperature after the TMA test

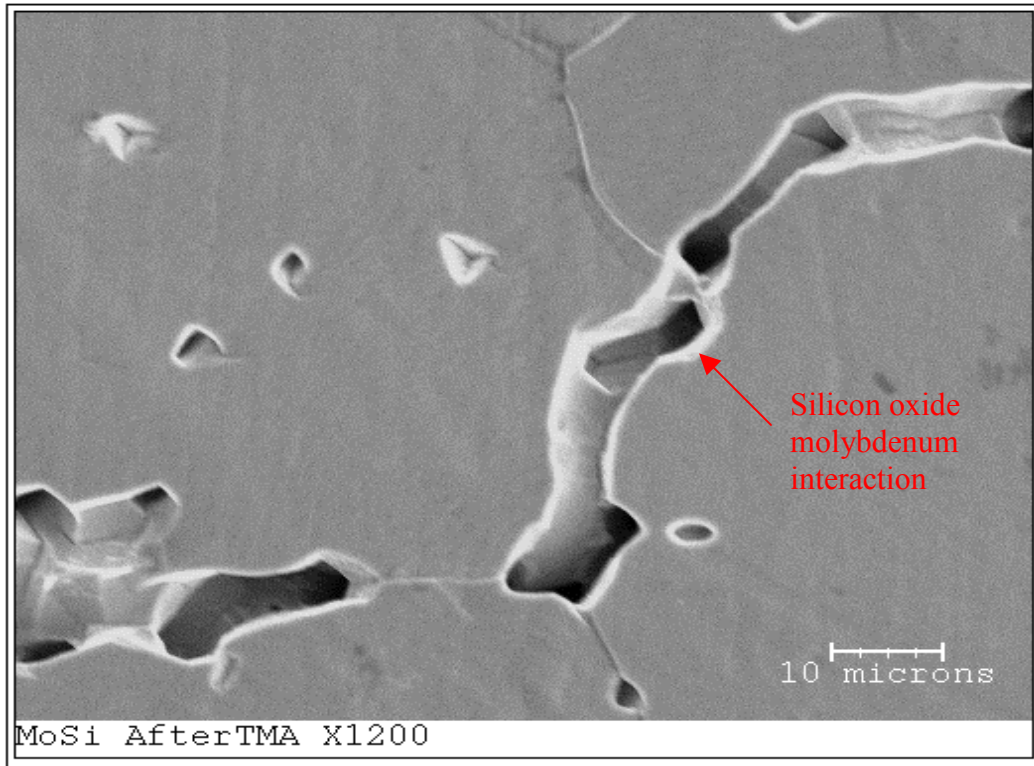


Figure 4.17 The SEM picture of MoSi after the TMA test shows the silicon oxide between the grain boundaries X1200 magnification

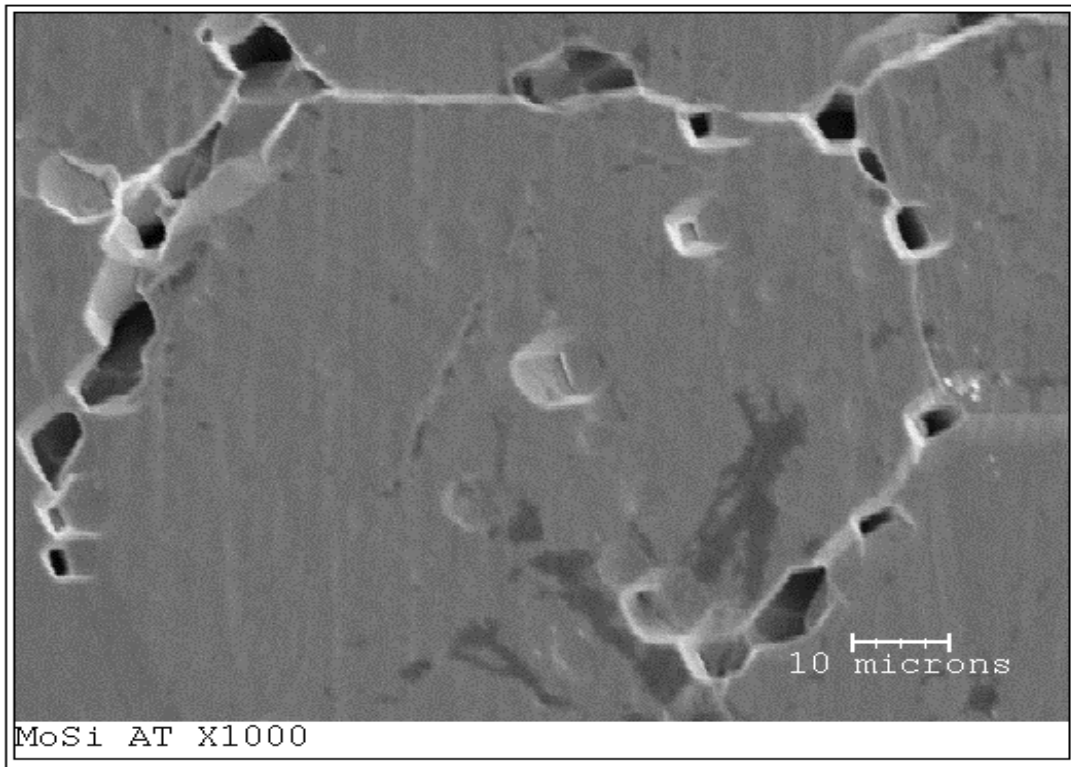


Figure 4.18 The grain boundary between the molybdenum and silicon are seen with the oxides of silicon formed at high temperature

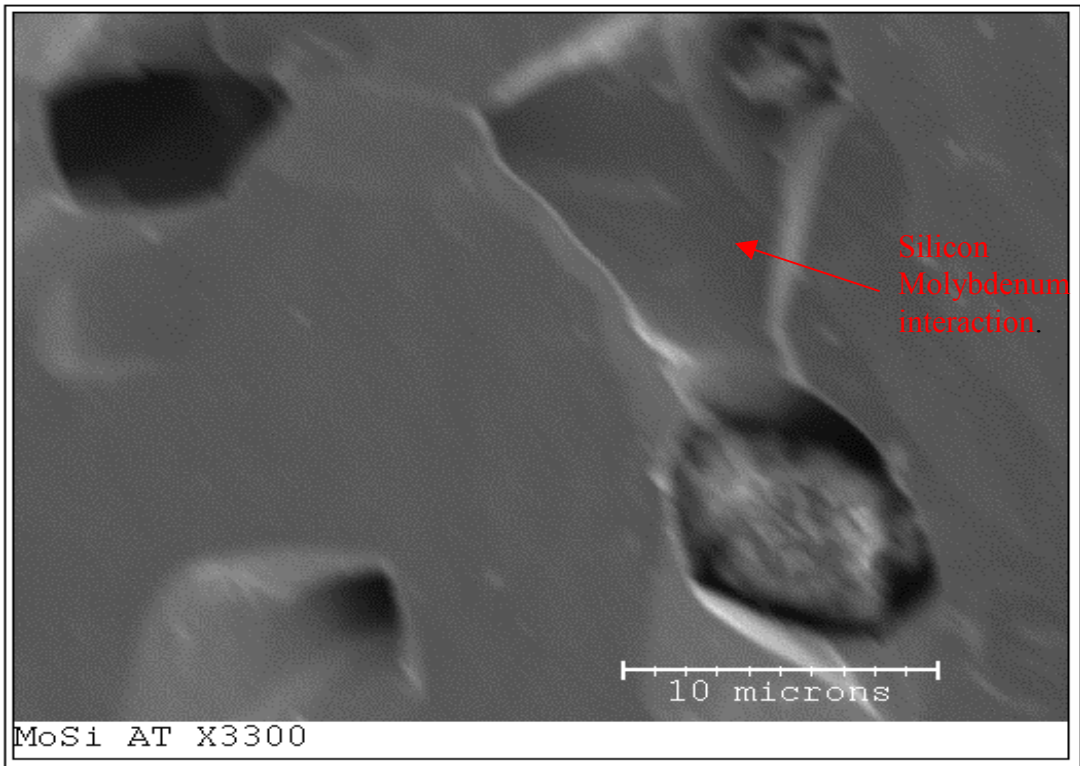


Figure 4.19 The SEM picture at 3300 magnification, gives a clear picture of the molybdenum silicon oxygen interaction clearly

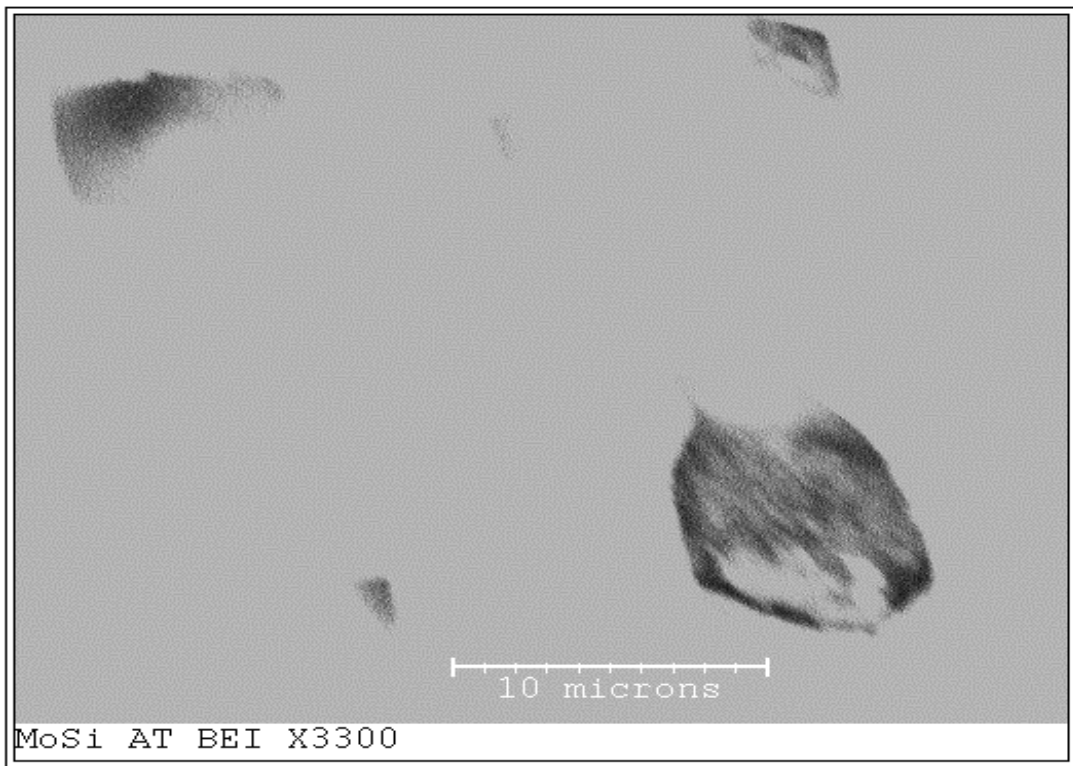


Figure 4.20 In the BS Image, the lighter particles is shown in high contrast, whereas the heavier particle has less contrast. (Mo is heavy when compared to Si)

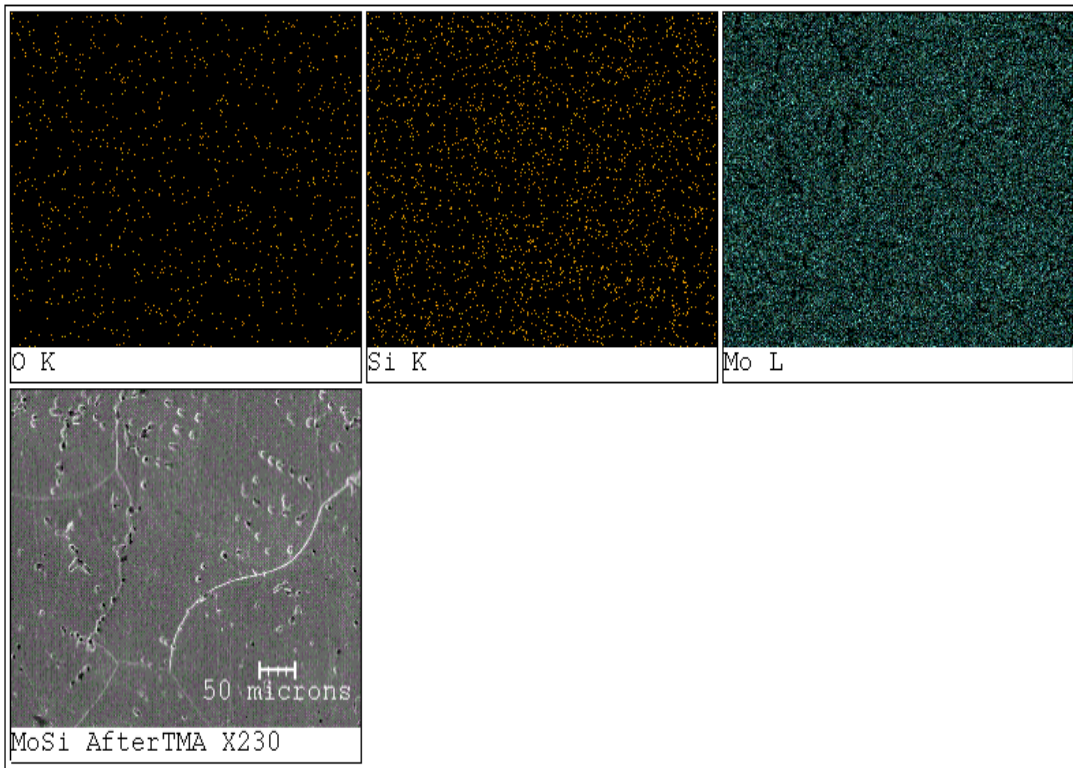


Figure 4.21 The EDS map shows that the darker areas are Silicon and the lighter areas are Molybdenum with some oxygen content after the test

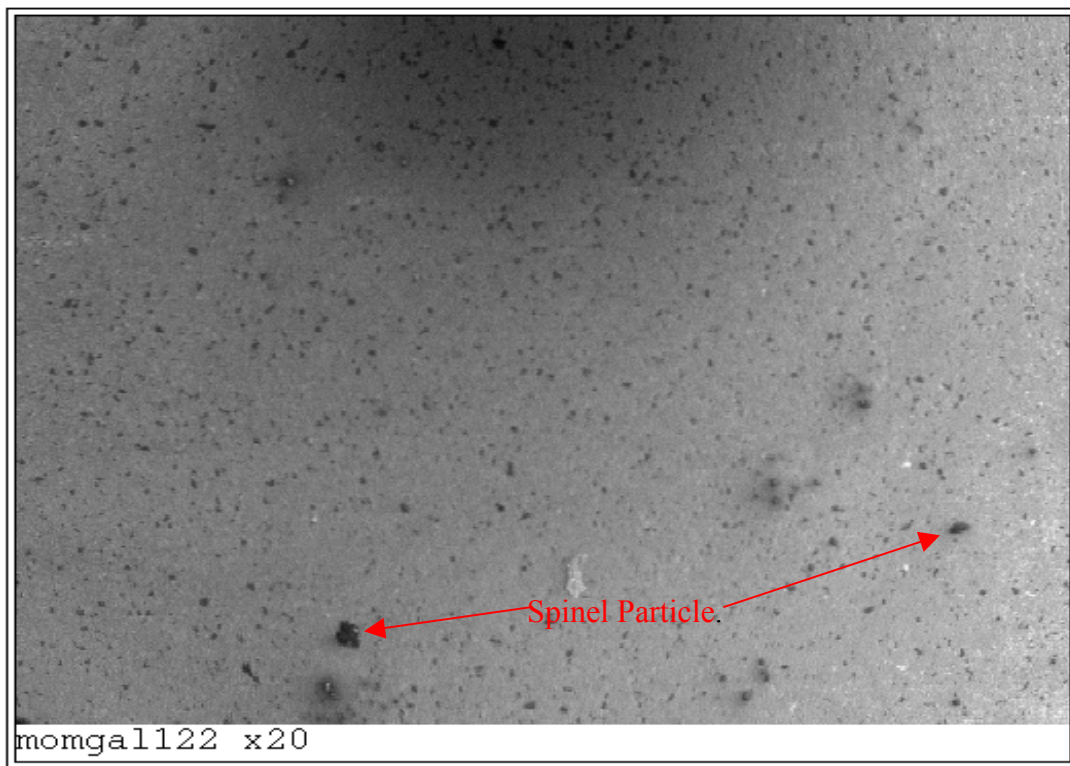


Figure 4.22 Showing the distribution of the $MgAl_2O_4$ at 20 times magnification

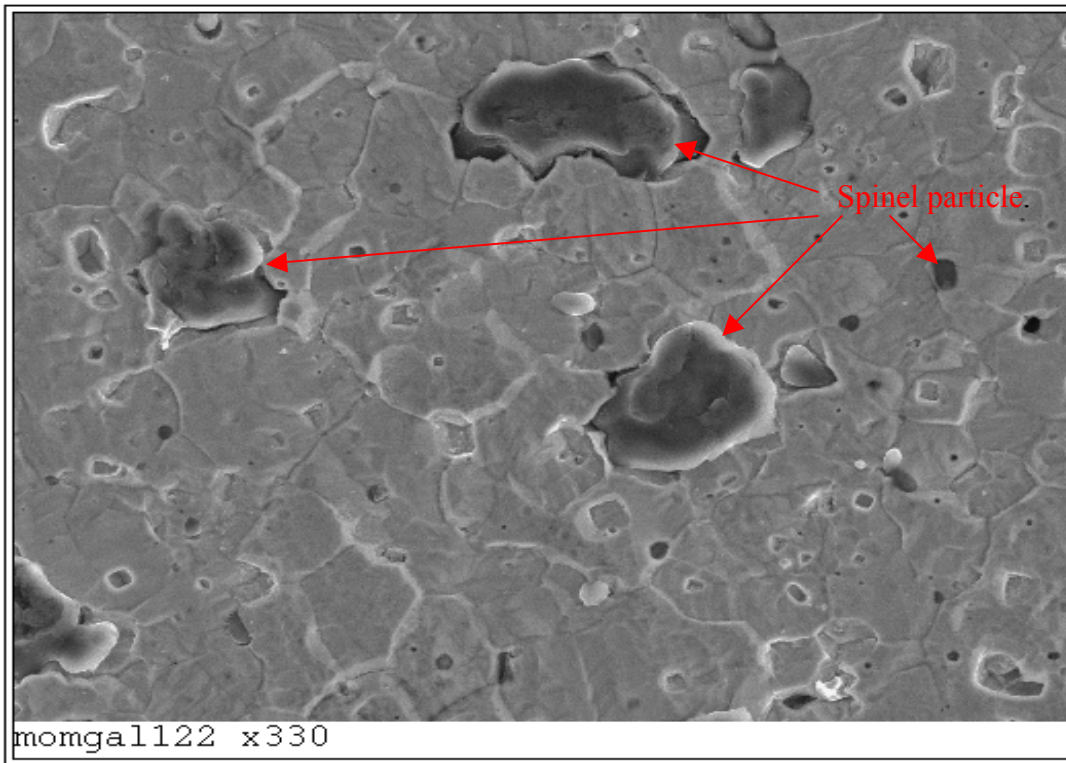


Figure 4.23 Shows the MgAl₂O₄ are not even in size and distribution as it is clearly seen at 330 times magnification

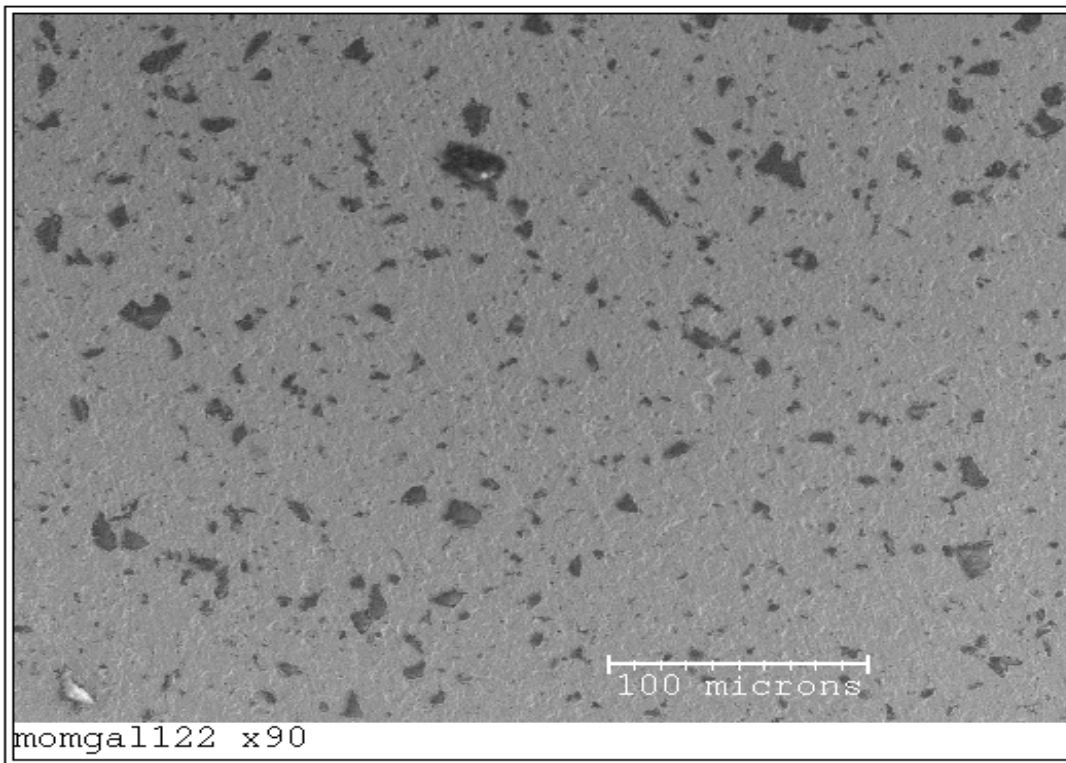


Figure 4.24 Microstructure of Mo-MgAl₂O₄ #678, the darker region being MgAl₂O₄ at lesser magnification (X 90) which shows the distribution of the MgAl₂O₄. The size of the MgAl₂O₄ is not even as clearly seen from the picture

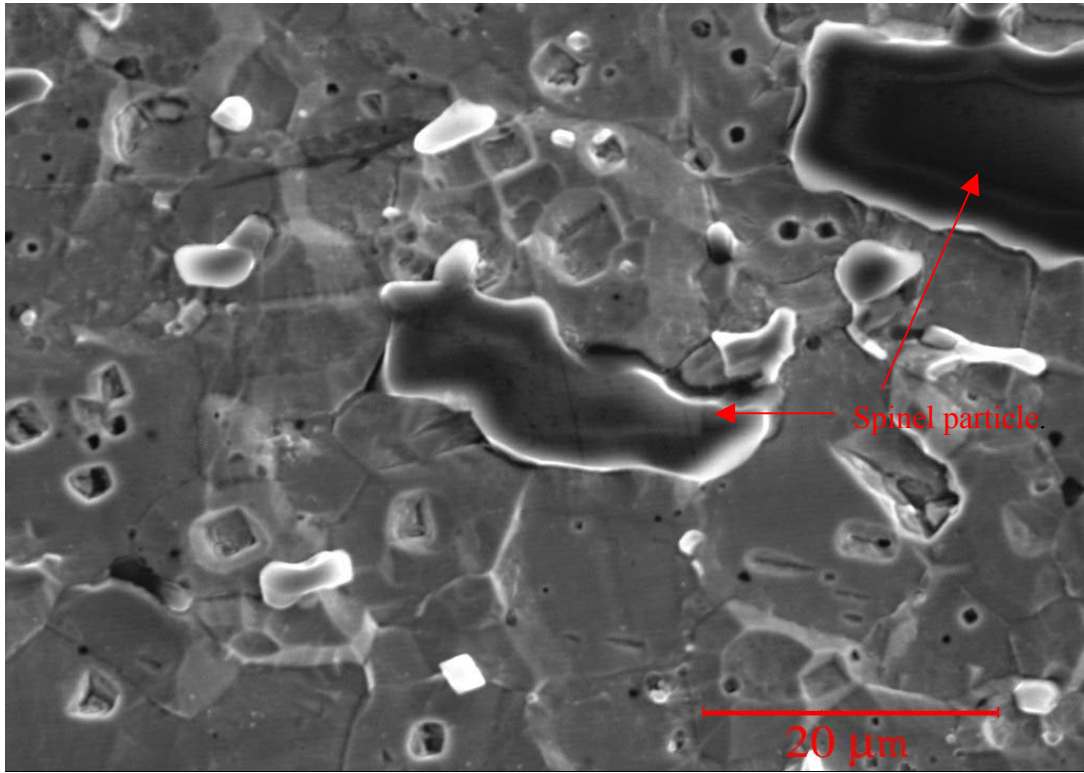


Figure 4.25 Microstructure of Mo-MgAl₂O₄ #678, the darker region being MgAl₂O₄

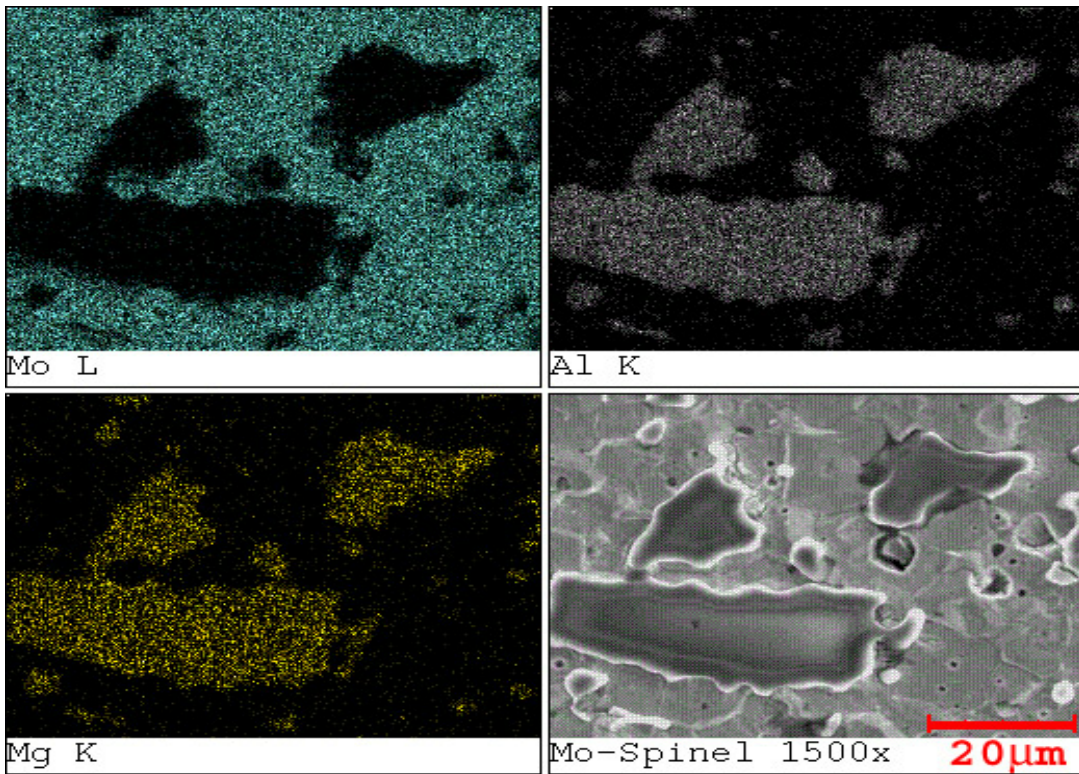


Figure 4.26 EDS map showing the composition distribution of Mo-MgAl₂O₄ #678 before tests

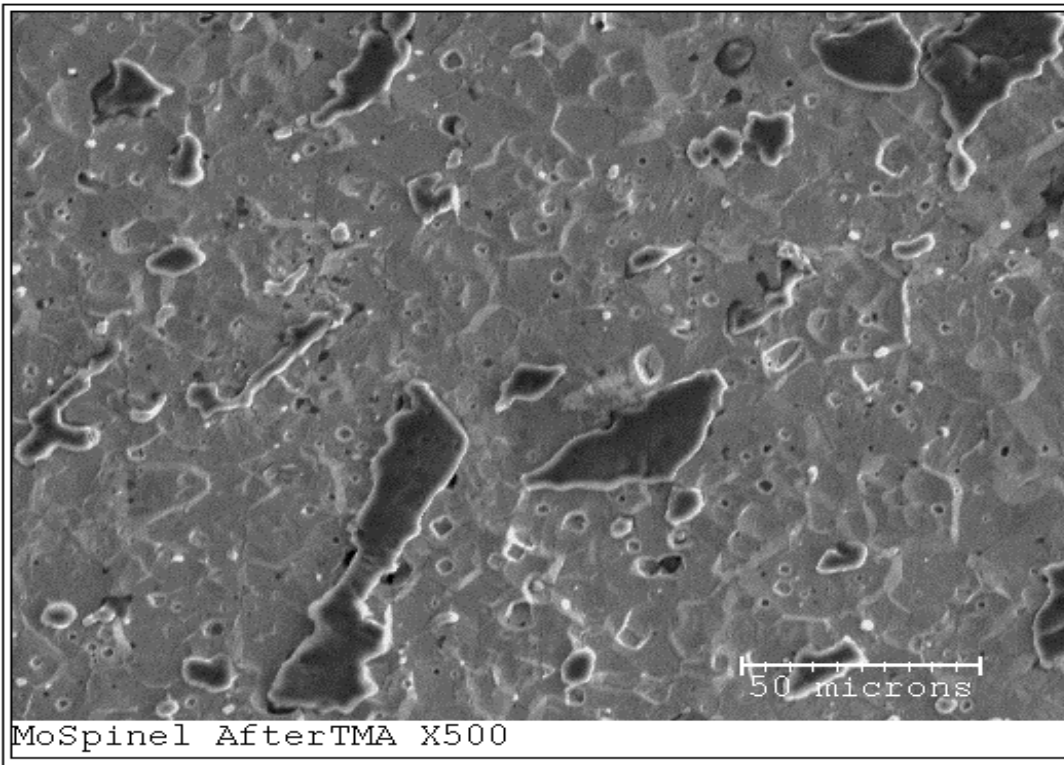


Figure 4.27 The SEM picture of Mo-Spinel alloy #678 after the TMA test shows the distribution and the size of the Spinel particle is not uniform

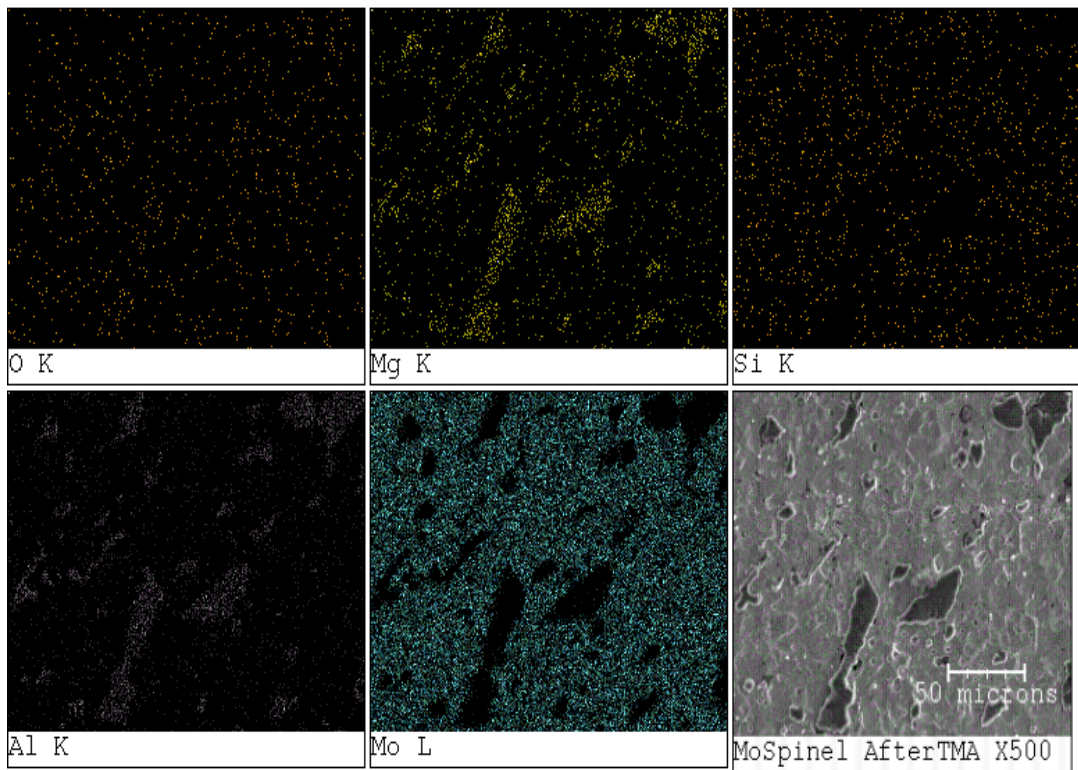


Figure 4.28 The EDS map, which has to show the presence oxygen element only in the areas where both Mg and Al are present which forms Spinel with them, whereas in this the oxygen is seen all over the matrix which proves the formation of molybdenum oxides

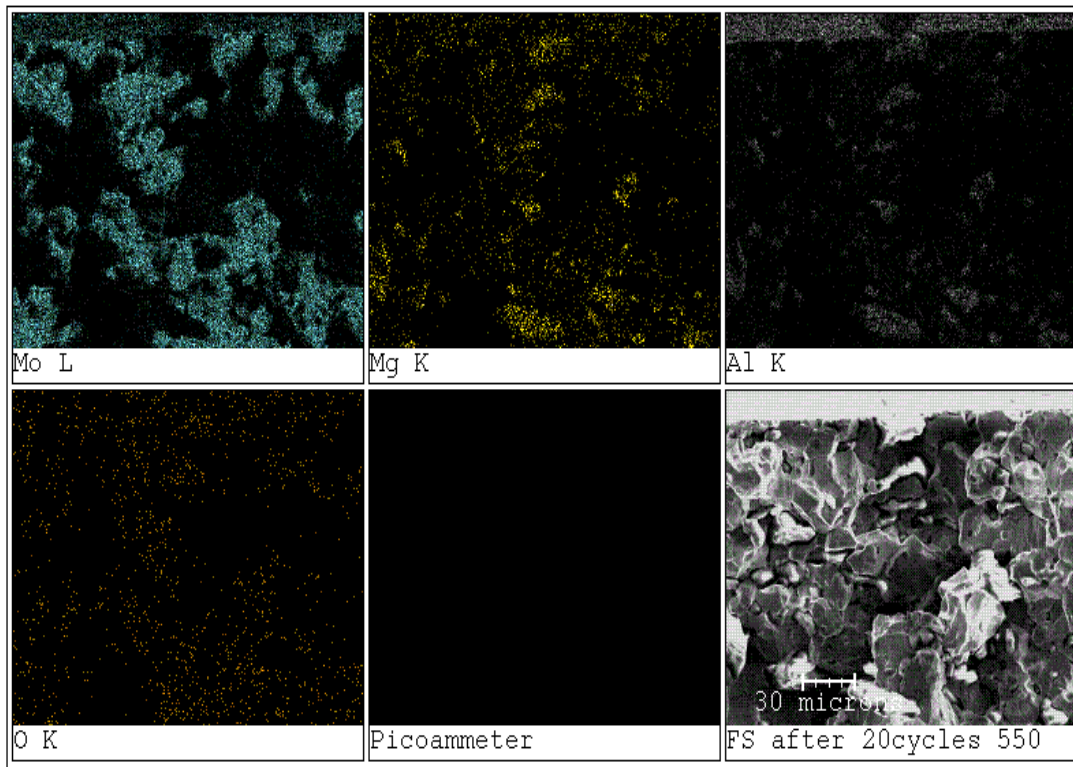


Figure 4.29 showing the fracture surface of the Mo-MgAl₂O₄ under the EDS mapping

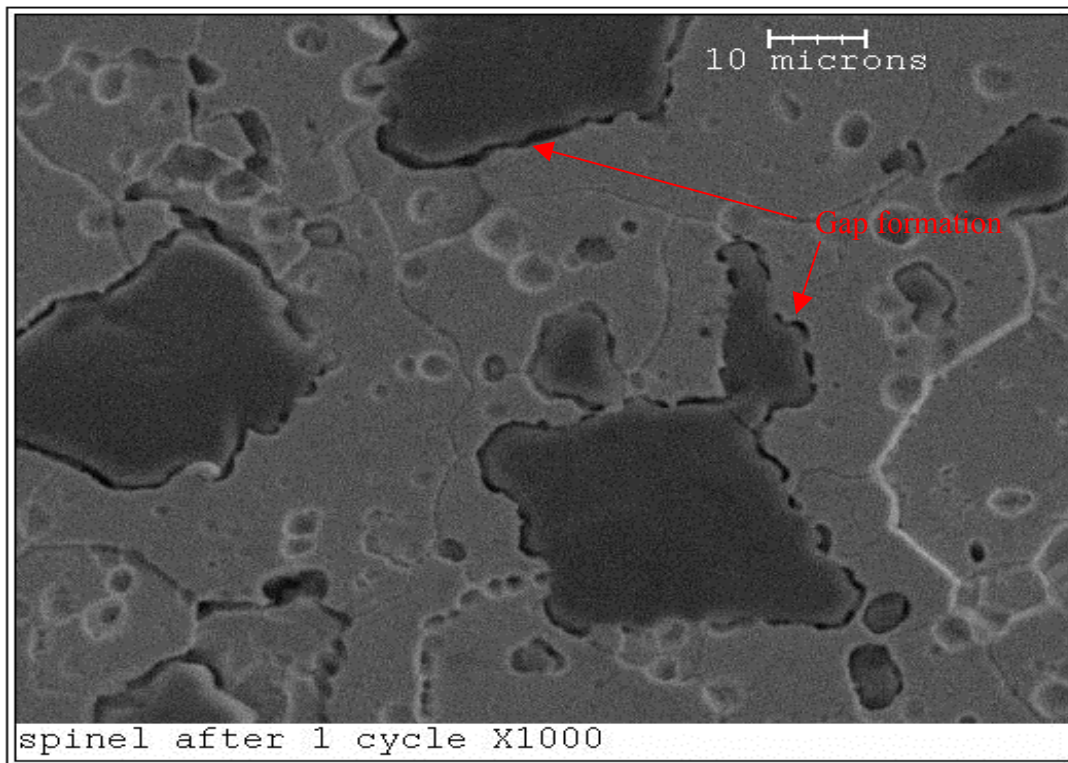


Figure 4.30 The SEM picture showing the gaps created after 1 thermo-cycle in Mo-MgAl₂O₄ between the Molybdenum and the Spinel particle

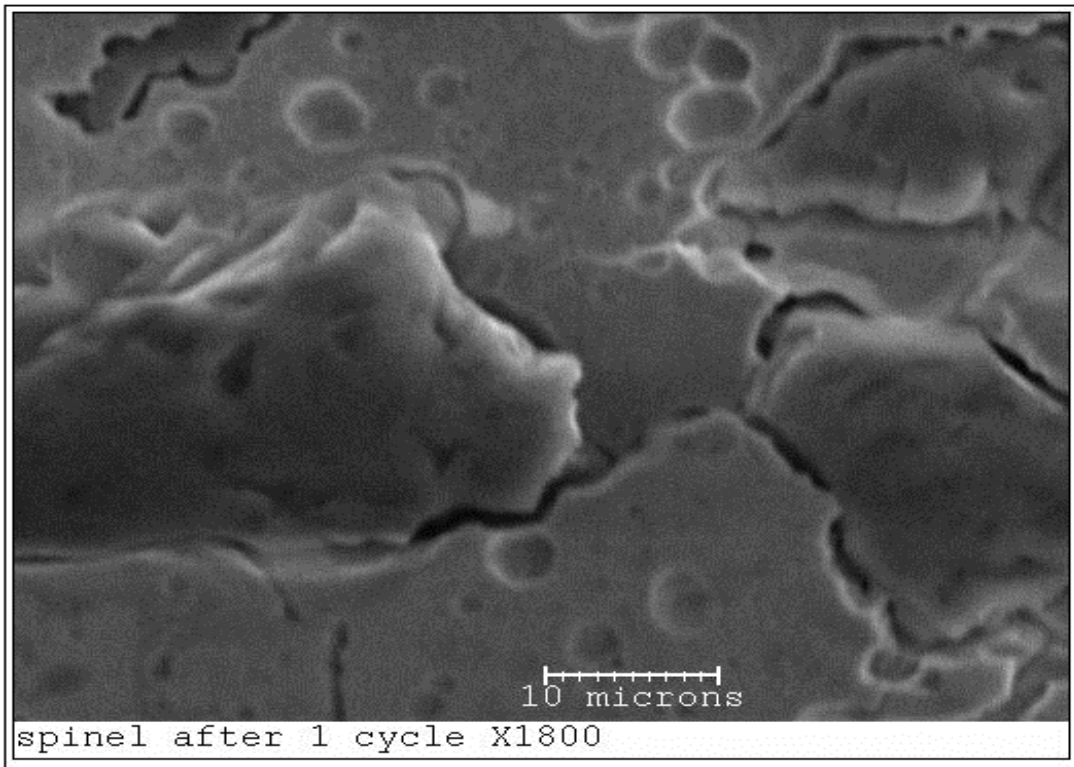


Figure 4.31 The SEM picture at magnification 1800 times, showing the gaps created after 1 thermo-cycle in Mo- MgAl_2O_4 between the Molybdenum and the Spinel

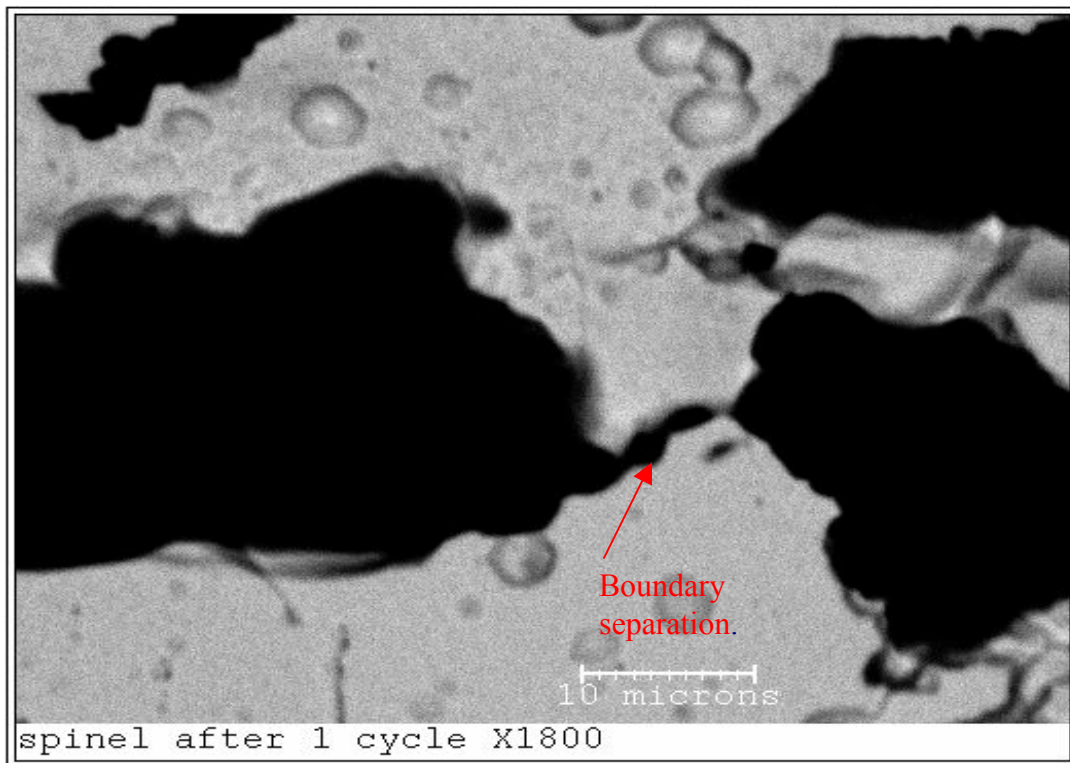


Figure 4.32 The BSI picture at magnification 1800 times, showing the gaps created after 1 thermo-cycle in Mo- MgAl_2O_4 between the Molybdenum and the Spinel particle

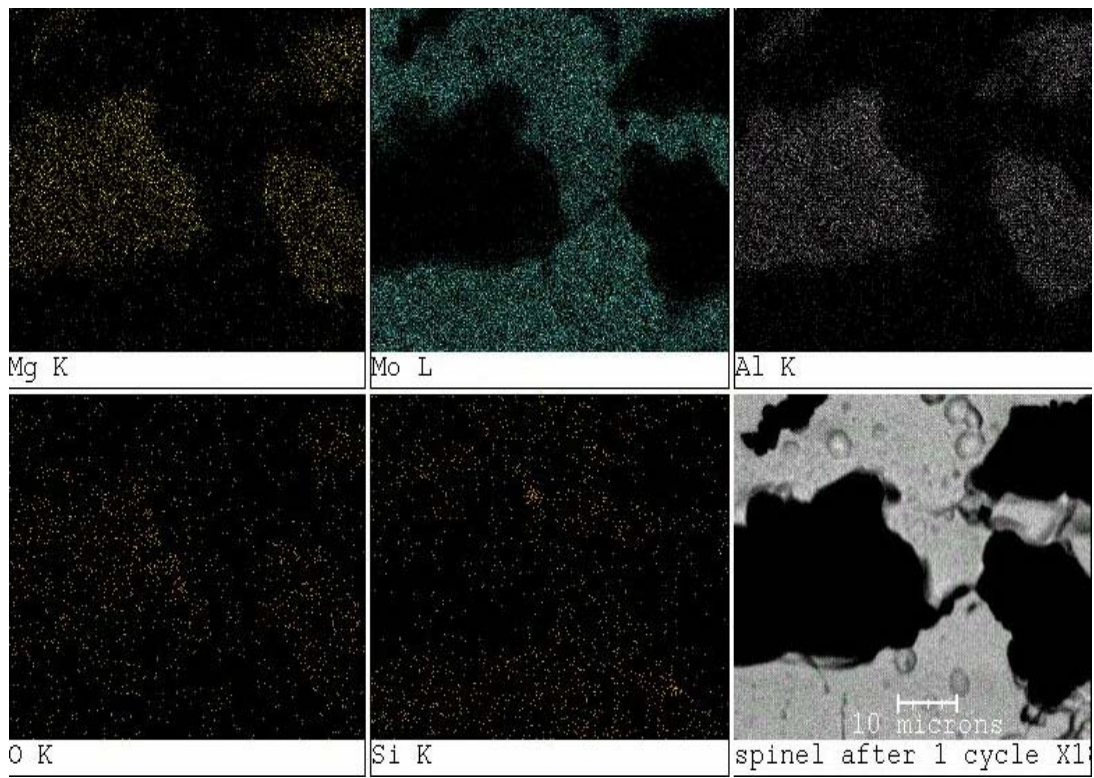


Figure 4.33 EDS map showing the Mo- $MgAl_2O_4$ after one thermo-cycle test. The Mo area (blue area) in the figure has a black gap between the molybdenum particles which is seen clearly in the BS Image

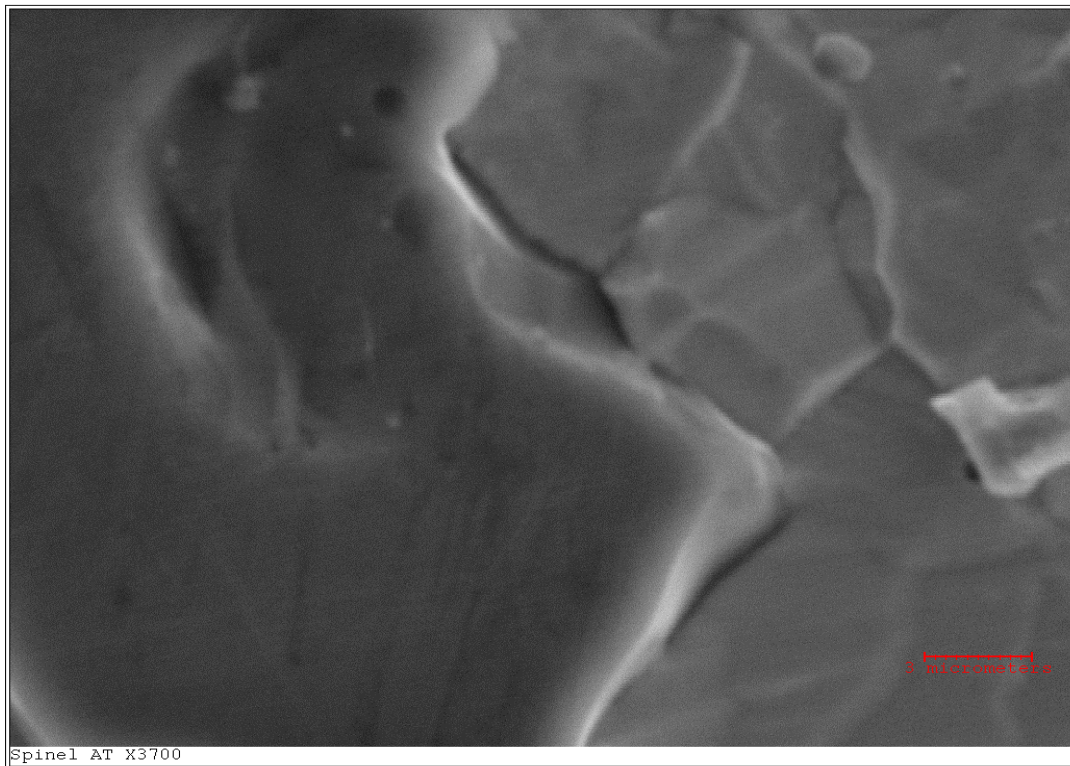


Figure 4.34 The picture shows the gap formation between the Molybdenum and Spinel particle after 1 cycle of thermo-cycling

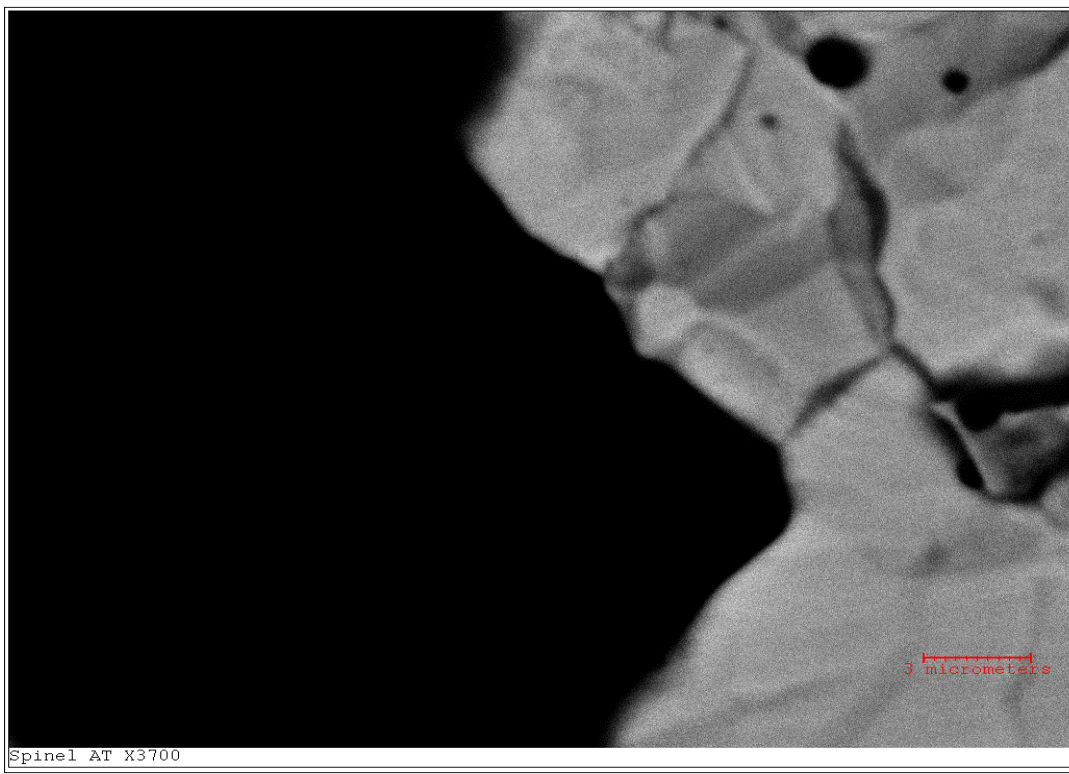


Figure 4.35 The BS Image of the Spinel alloy #678 shows that the cracks propagate along on the grain boundary of the molybdenum matrix from the Spinel particle after 10 cycles of thermo-cycling

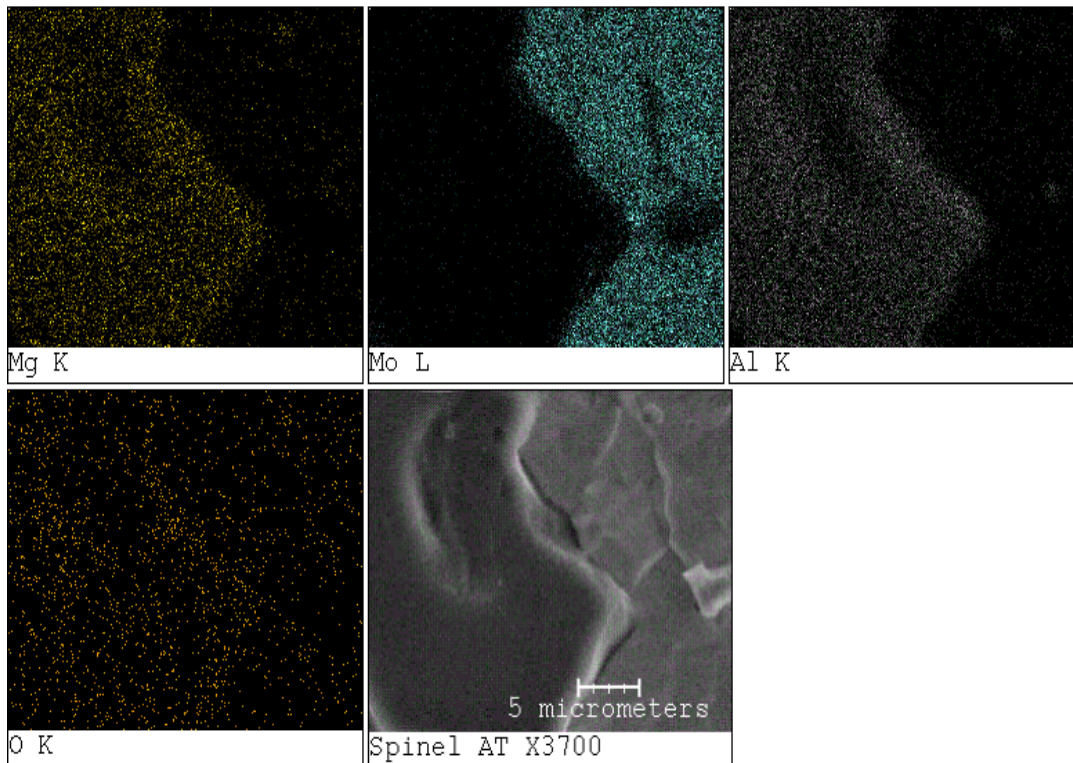


Figure 4.36 The composition of the Mo-MgAl₂O₄ Alloy #678 and the gap formation are clearly visible after 1 cycle of testing in the EDS image

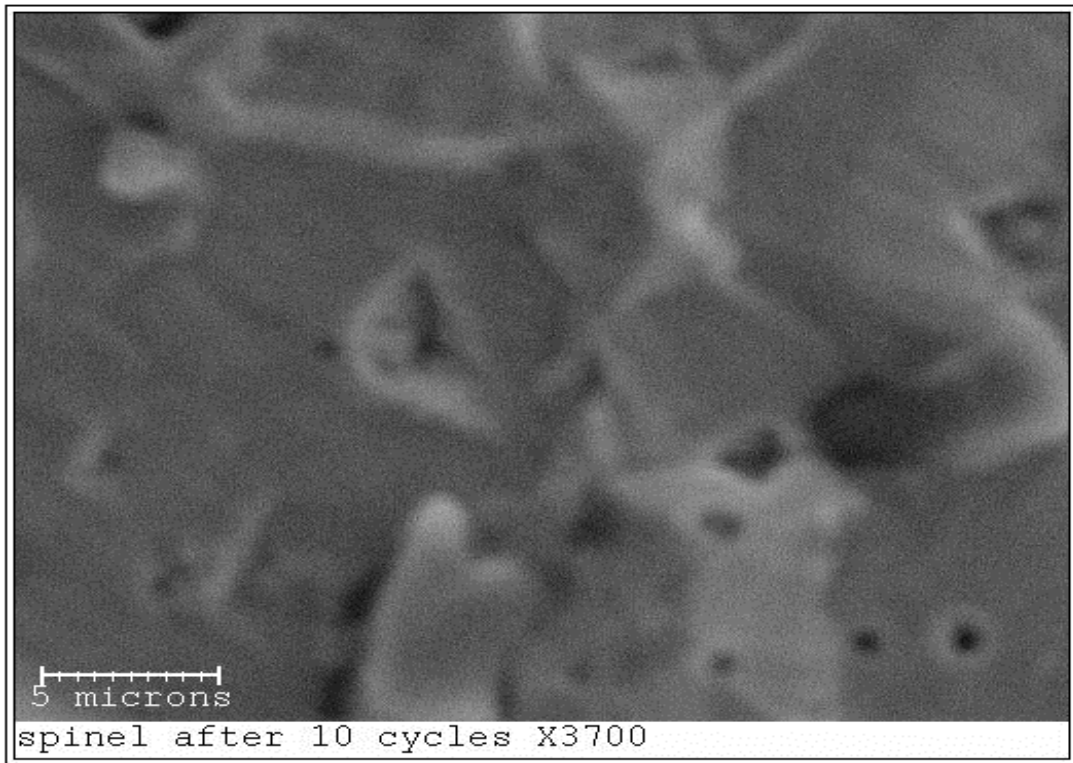


Figure 4.37 The SEM picture showing the crack nucleation point after 10 cycles of thermo-cycling at a magnification of 3700

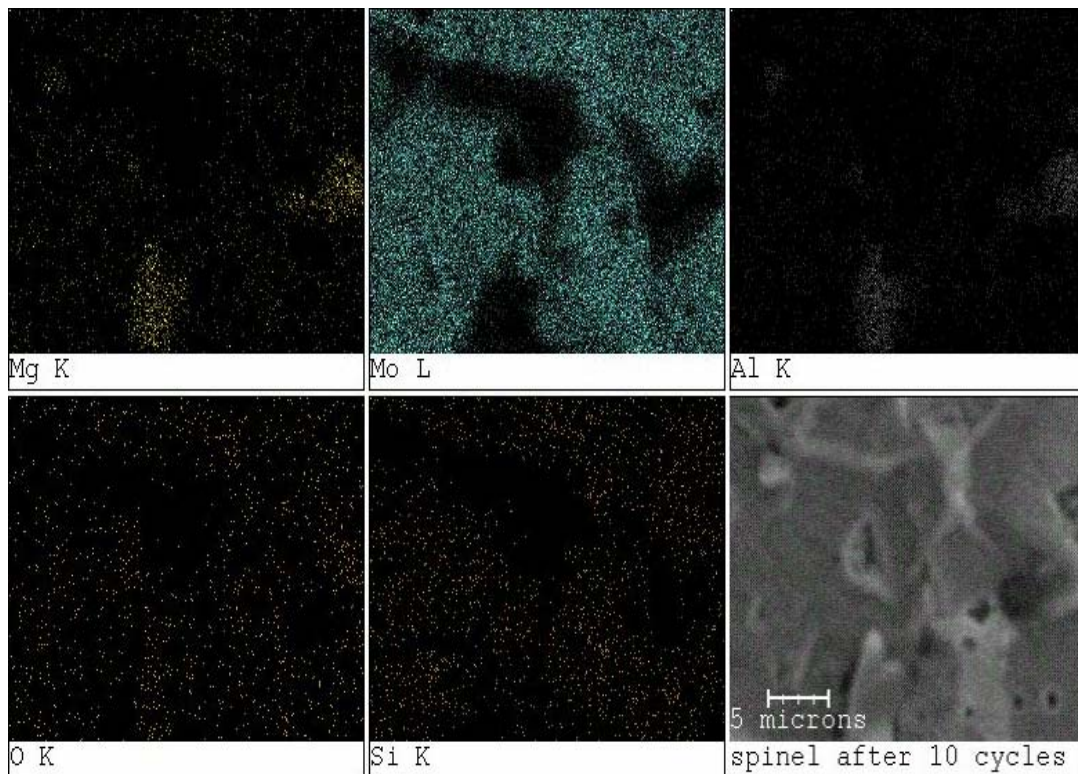


Figure 4.38 The EDS map showing the oxygen content all over the surface of the specimen after 10 cycles proving the formation of oxide after the thermo-cycling

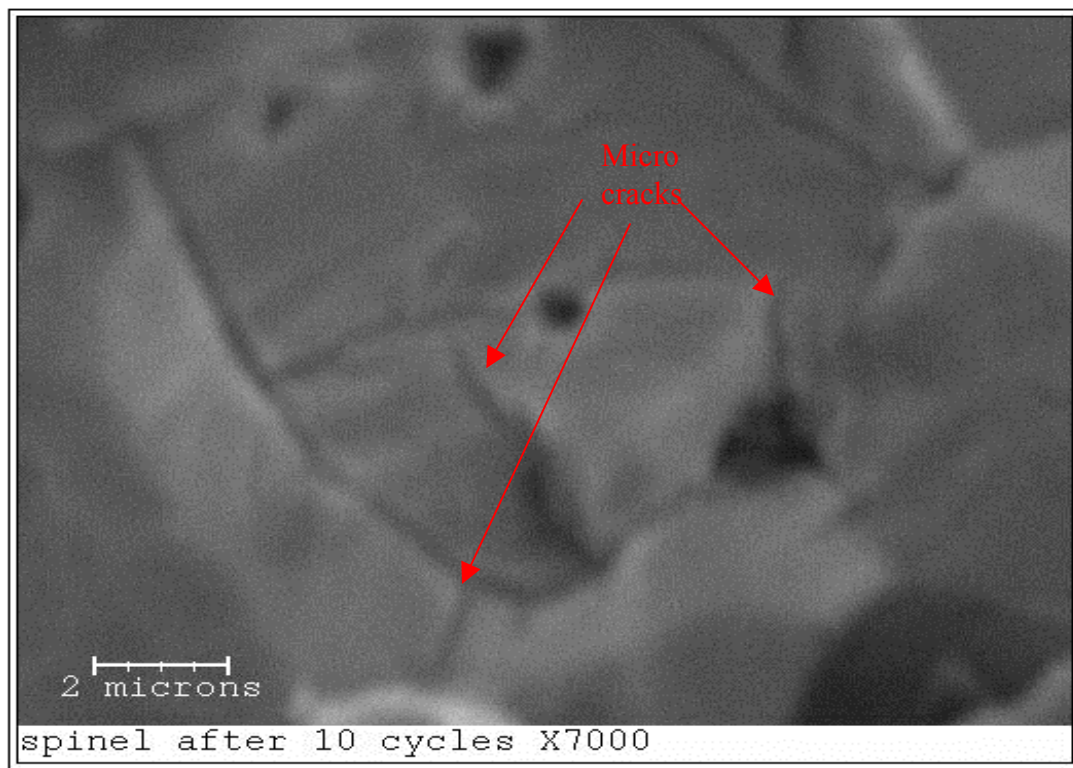


Figure 4.39 The SEM picture clearly showing the cracks propagating from the $MgAl_2O_4$ towards the Mo particle

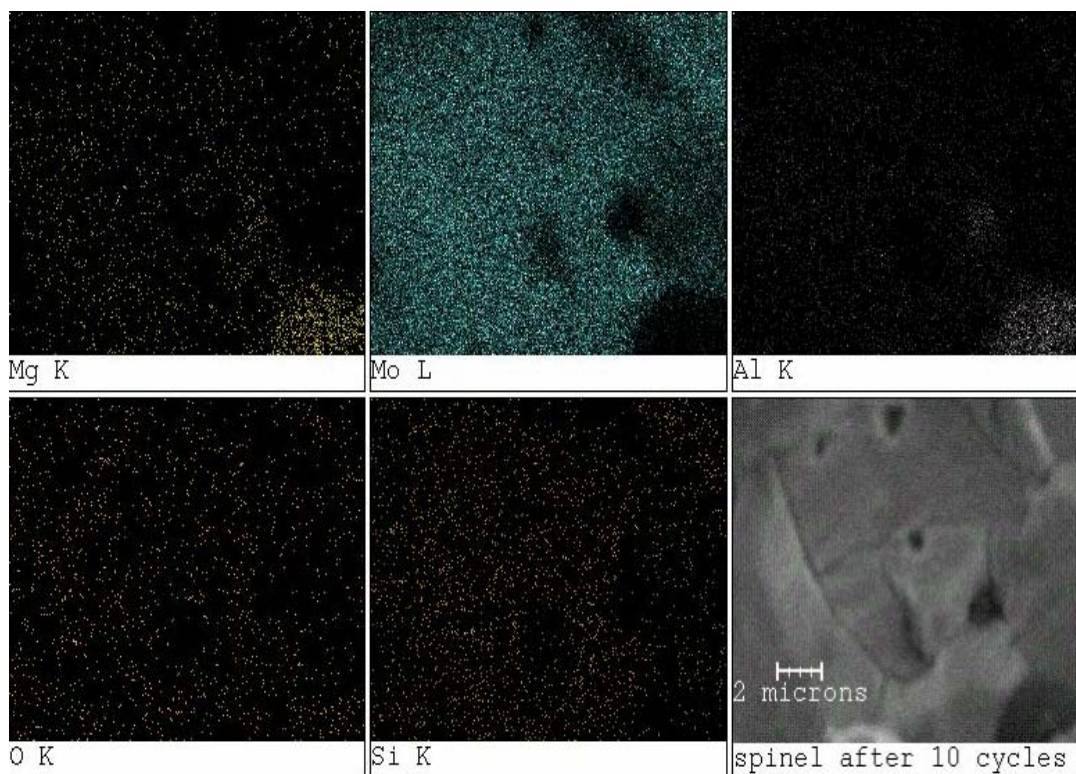


Figure 4.40 The EDS map clearly showing that the cracks start from dark region which are the spinel particle ($MgAl_2O_4$)

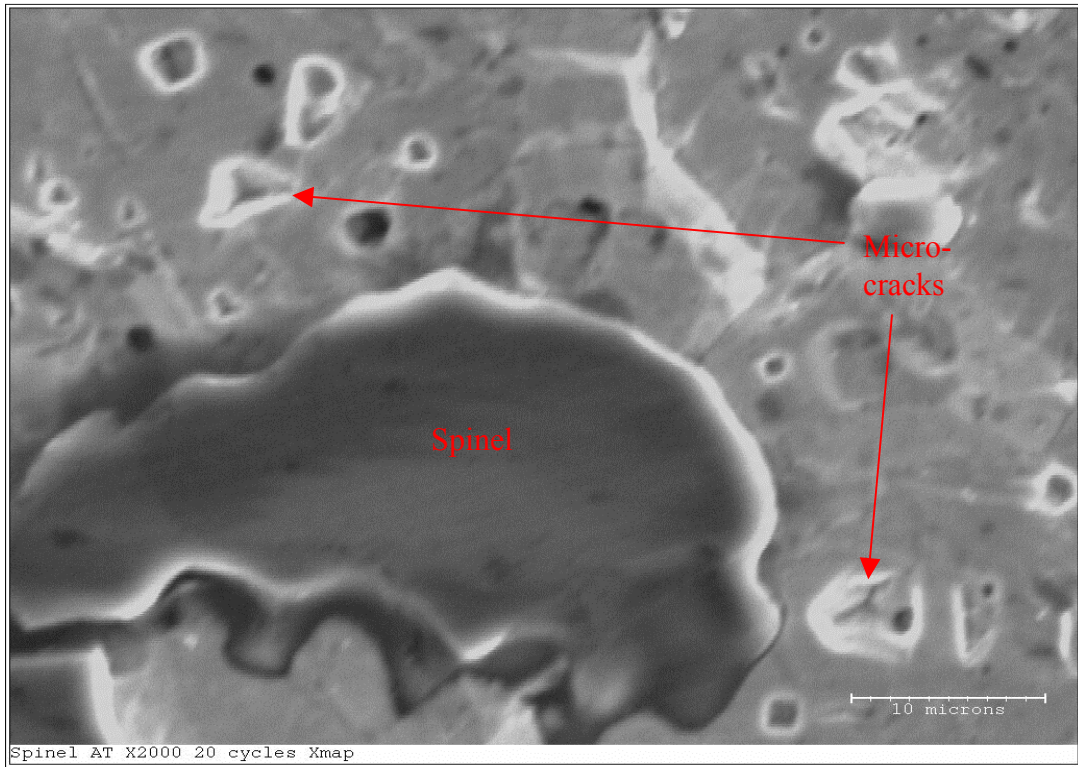


Figure 4.41 In the SEM picture, the big darker spinel particle cause lots of stress concentration points in the Mo matrix which causes more cracks to develop in the nearby matrix, which proves that bigger the spinel particle concentration causes more micro-cracks in the matrix

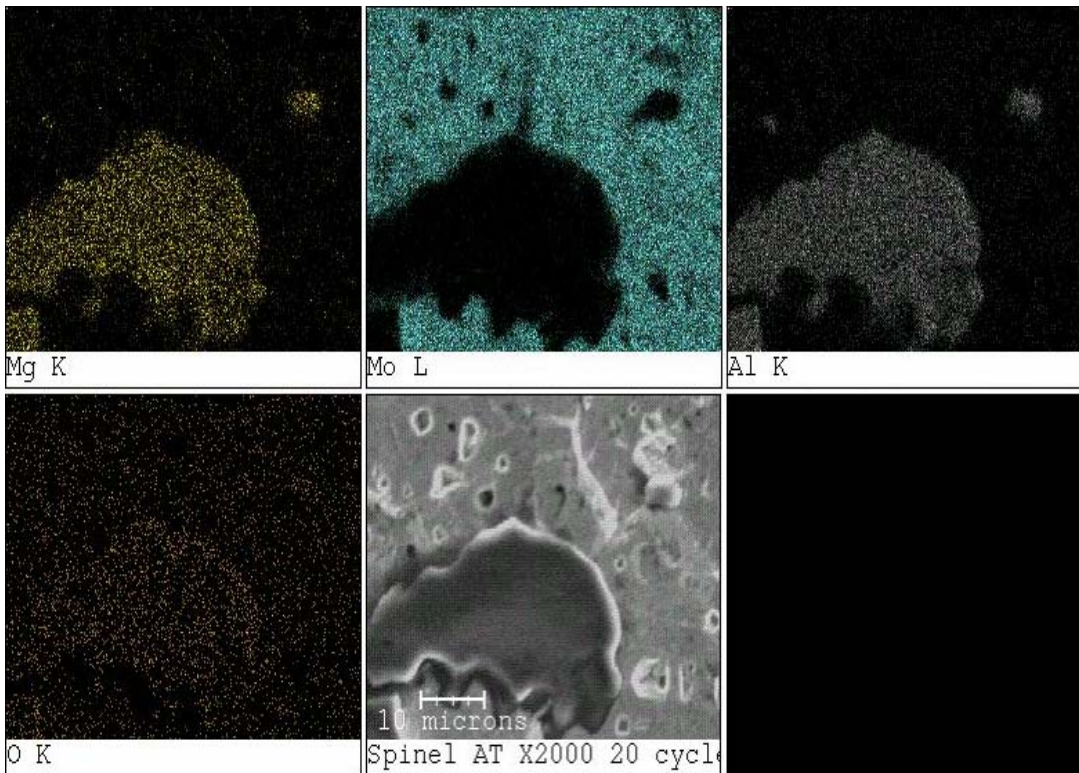


Figure 4.42 The EDS map, which shows the cracks triangular shaped region are cracks which are devoid of any material

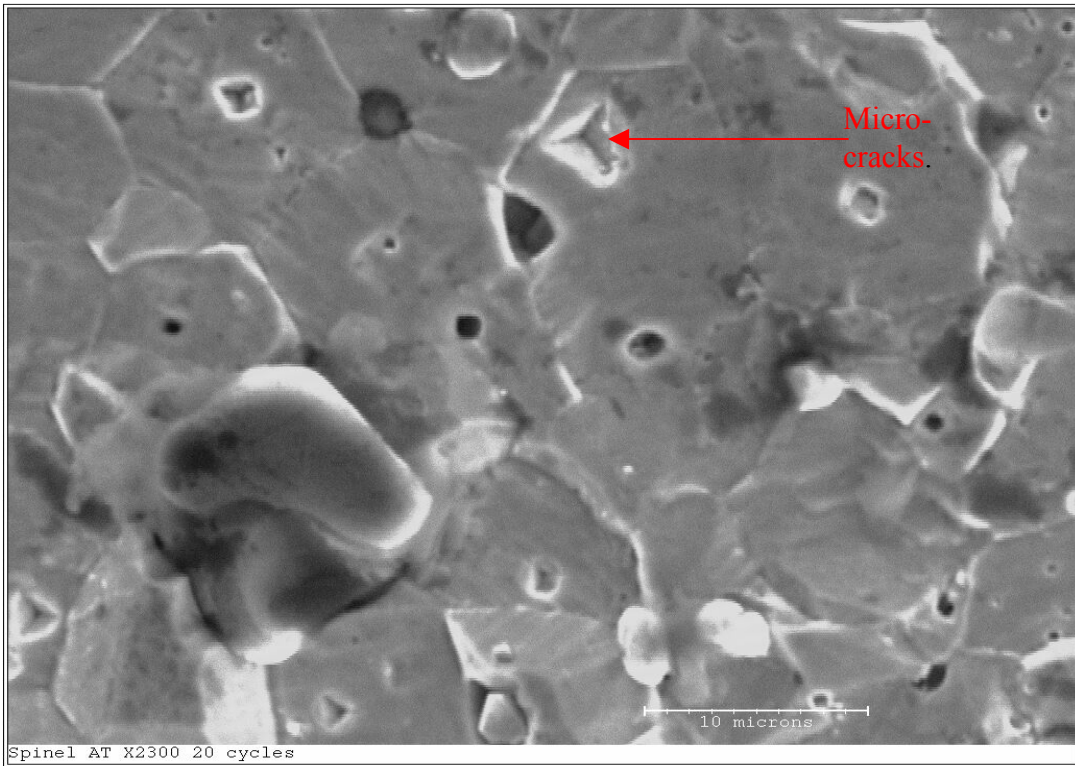


Figure 4.43 Another area of the Spinel #678 clearly shows that the bigger spinel particle causes some micro cracks in the Mo matrix

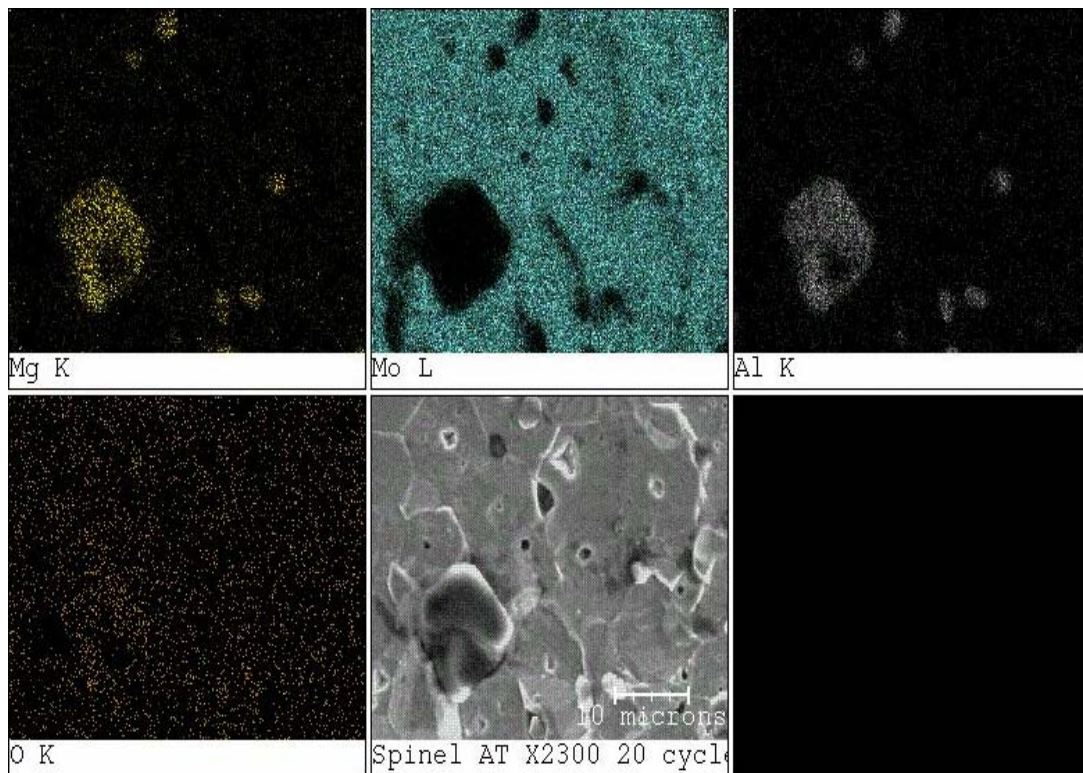


Figure 4.44 The EDS map shows the triangular regions are devoid of any material, which proves that they are cracks in the molybdenum matrix



Figure 4.45 Clear view of the triangular cracks in the molybdenum matrix at a magnification of 2700

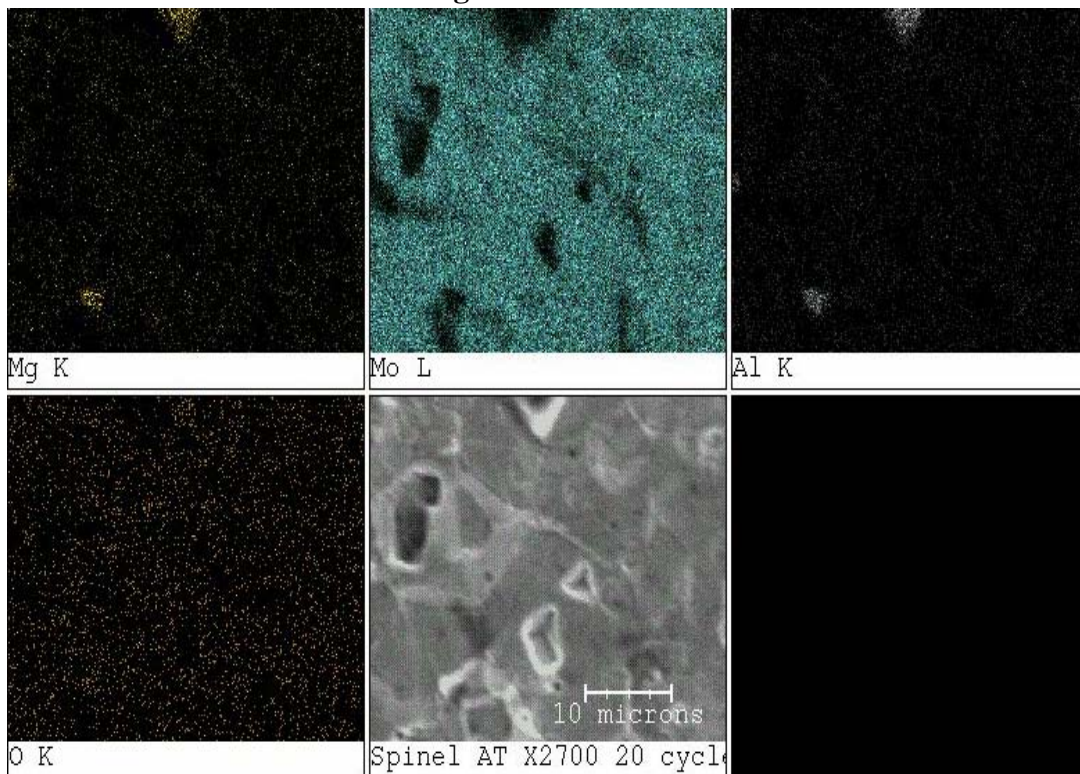


Figure 4.46 The EDS map shows the composition of the alloy #678 with cracks after 20 cycles of thermo-cycling

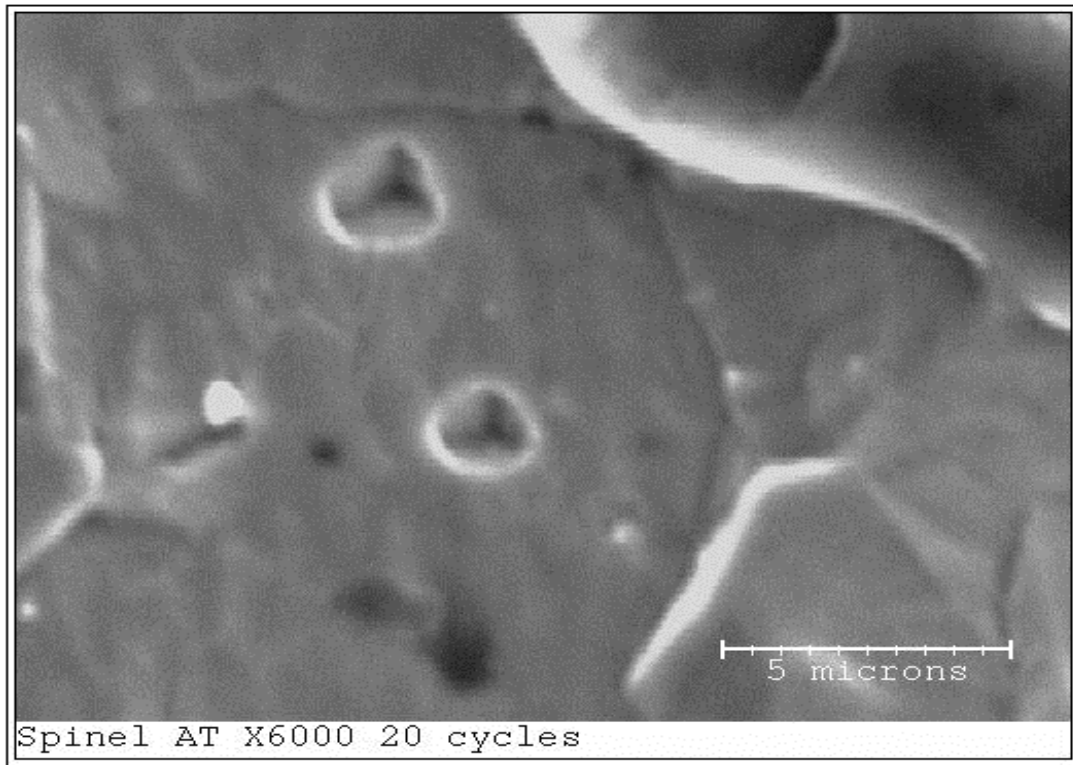


Figure 4.47 At a magnification of 6000, the triangular cracks which are formed in the matrix are clearly visible

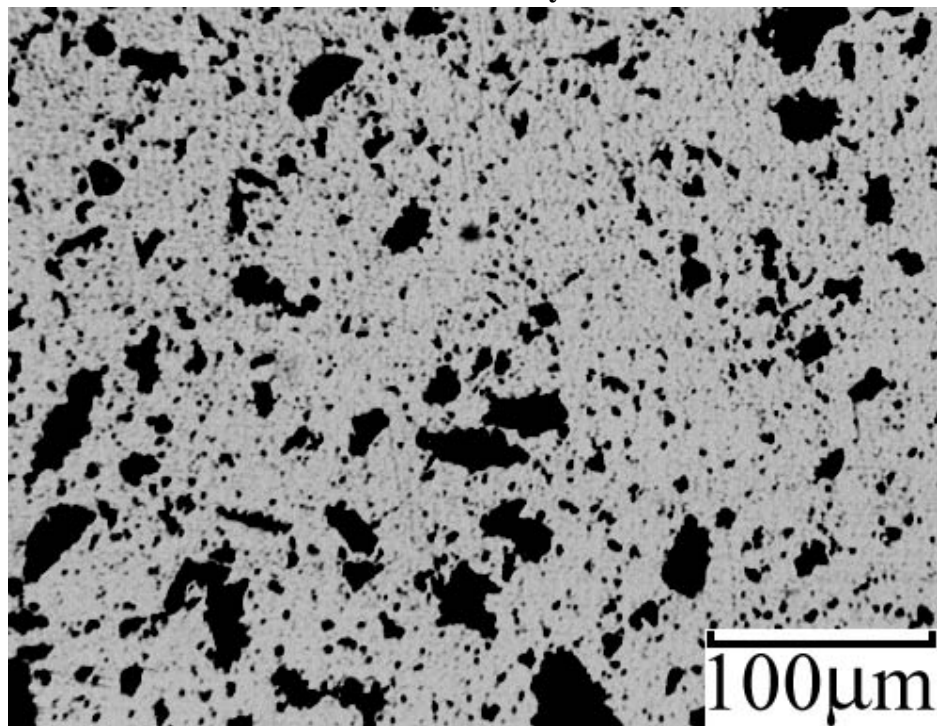


Figure 4.48 The micrograph of #697 before any tests

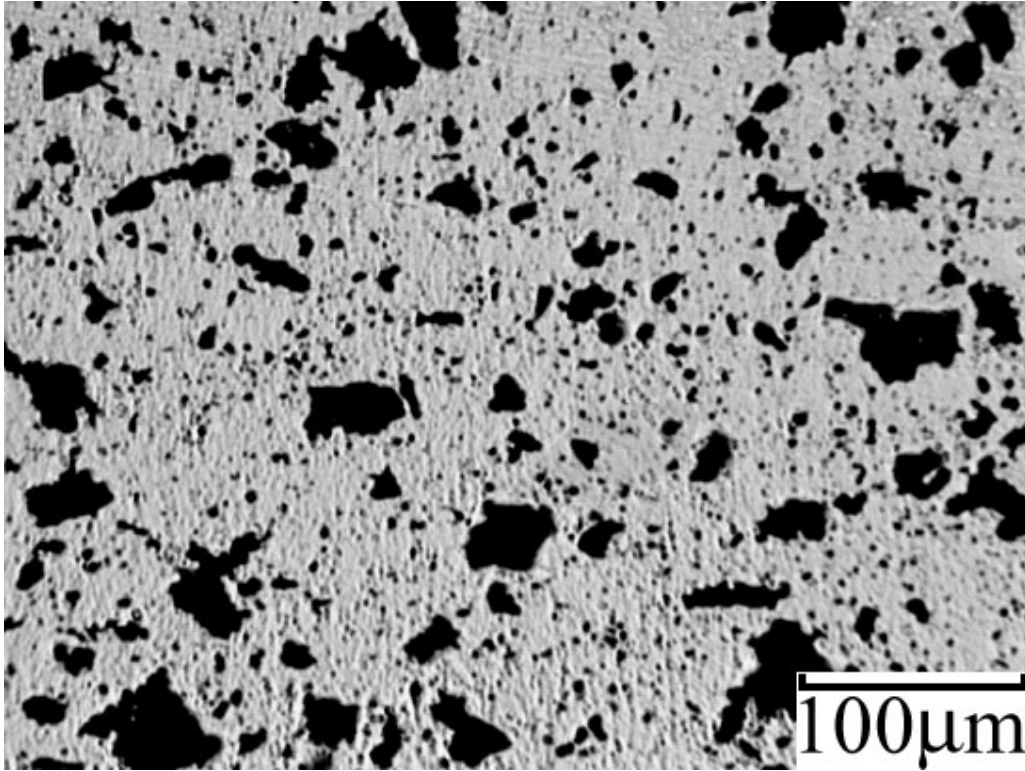


Figure 4.49 Micrograph of #697 after 1 thermo cycling showing no significant change

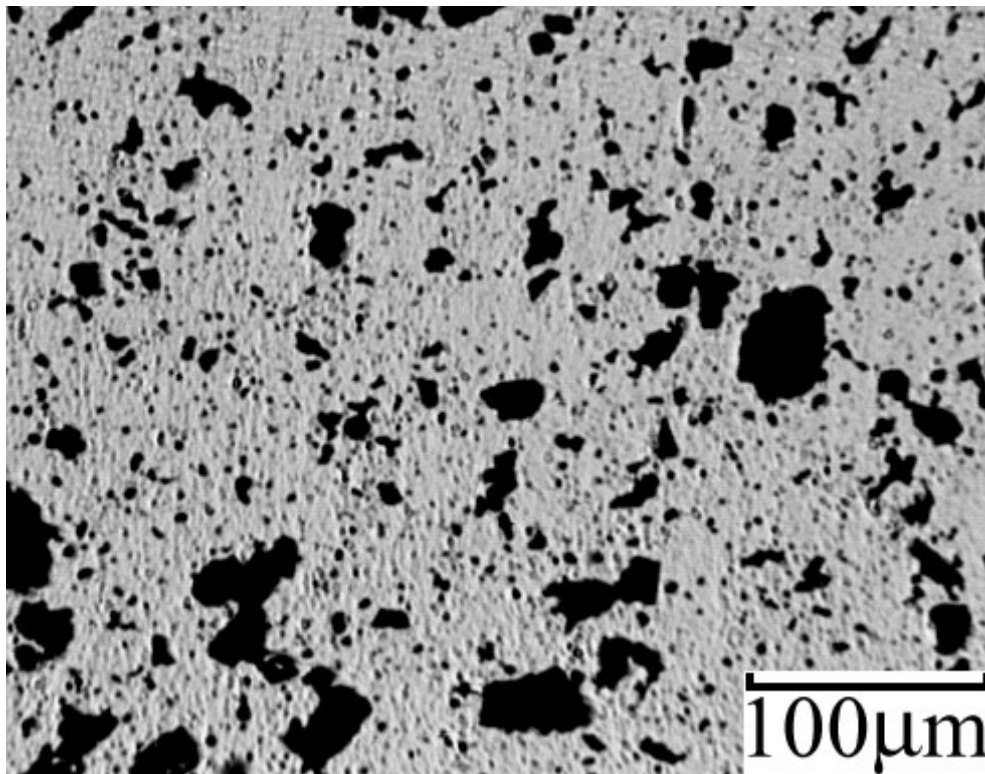


Figure 4.50 Micrograph of #697 after 10 cycles showing no significant changes

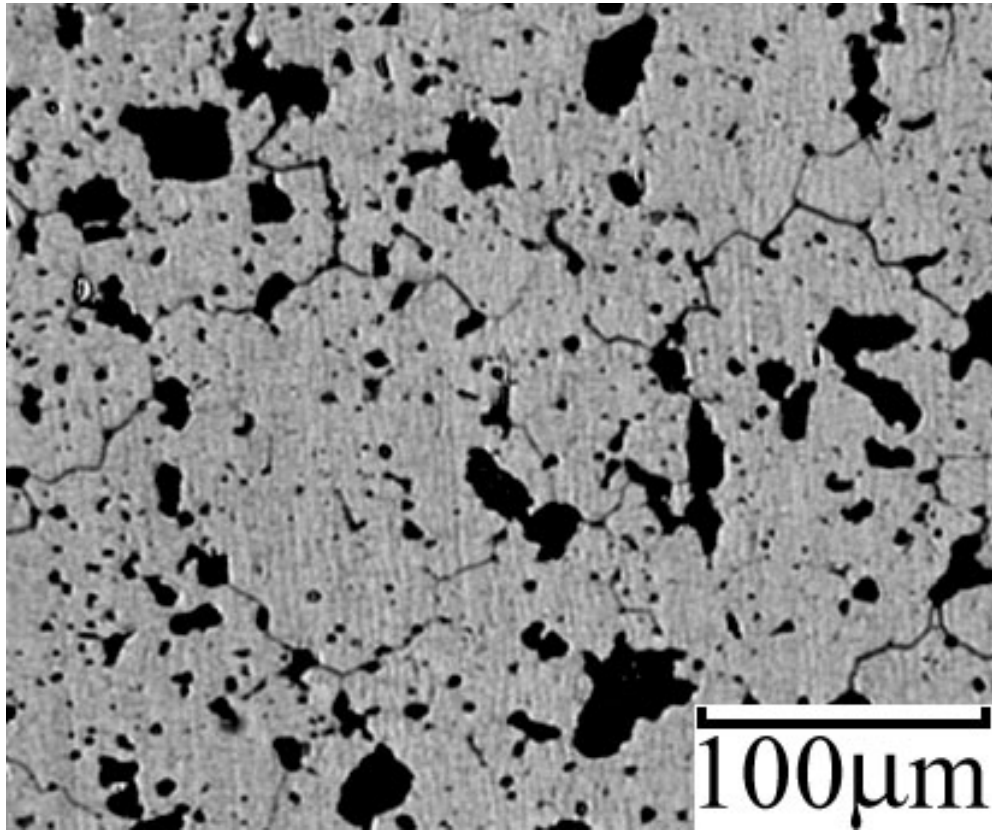


Figure 4.51 Micrograph after 20 cycles in which the cracks can be clearly seen

Chapter 5 CONCLUSIONS AND RECOMMENDATIONS

5.1 Conclusions

The coefficient of thermal expansion and the thermo-cyclic tests were performed on pure molybdenum with two different processing methods, molybdenum with silica, molybdenum with 3.4% or 6% spinel (MgAl_2O_4) particles with different methods of processing.

5.1.1 Coefficient of Thermal Expansion Test

Comparing the tests on molybdenum with different processing methods, it can be concluded that the coefficient of thermal expansion value changes with the method of processing. Similarly by adding 0.745% (wt) of silica to molybdenum, CTE value is less when compared to that of the pure molybdenum. In case of the molybdenum base alloy with spinel (MgAl_2O_4) particles at different percentage, as the percentage of the spinel particle increases, the CTE value decreases, but the optimum percentage of the spinel cannot be decided with only two compositions. The following conclusions were arrived after the series of tests.

1. In material processing methods, the hot pressed material is better when compared to the casting method, as it has the drawbacks of porosity and other defects.
2. Adding silicon decreases the CTE value because of the interaction between molybdenum and silicon compounds at higher temperature.
3. Adding spinel particles decreases the CTE value when compared to pure molybdenum but a exact composition of the spinel particle has to reached by the trying

various composition and at the same time depending upon the method of processing the alloy is also critical.

4. The CTE value of the #697 is less than that of the #678 because of the difference in the percentage of the spinel particle present, even though the processing time is less. The results are well satisfying when compared to the moiré tests as shown in figure B2 & B3.

5.1.2 Thermo-cycling Test.

The thermo-cycling tests revealed that the spinel particle size, distribution and processing time affect the ductility of the molybdenum alloy. From the tests it can be concluded that,

1. Particle size and distribution plays an important role. The bigger the particle of spinel, the micro cracks are seen more than near the smaller spinel particles.

2. Processing time was found to be more critical while preparing the alloy, the big difference between #678 and #697 is the processing time. The #678 has 4 hours processing time at 1800°C, thus making the molybdenum matrix and spinel have more time to form a strong bonding between them and with such a longer processing time at high temperature, the diffusion of spinel particle helps to disperse it evenly. Micro cracks in #697 due to the thermo-cycling, verified that 1 hour processing time may not be long enough to have a very good bonding between the alloying agents in the intermetallic compounds.

3. Microstructure study showed that for, most of the cracks initiate from bigger particles, and ends in the matrix or connected to other bigger particles. This makes it clear that the spinel particle size and distribution are very important factors which influence in the change of thermo mechanical property as seen in the figure B4 [24].

5.2 Recommendations

Based on the tests completed, certain future work may be done to get the optimum alloy composition and processing method.

1. The alloys with spinel differ in both the composition percentage and also with the processing time, thus making it not clear whether the CTE value and the cracks are due to the composition or with that of the processing time.

2. The #678 is more ductile than that of the #698, so various volume fractions of spinel composition with molybdenum have to be studied to get the optimum volume fraction.

3. The study of thermal cracks effect may help in the evaluation of the properties of the molybdenum base alloys.

APPENDIX A

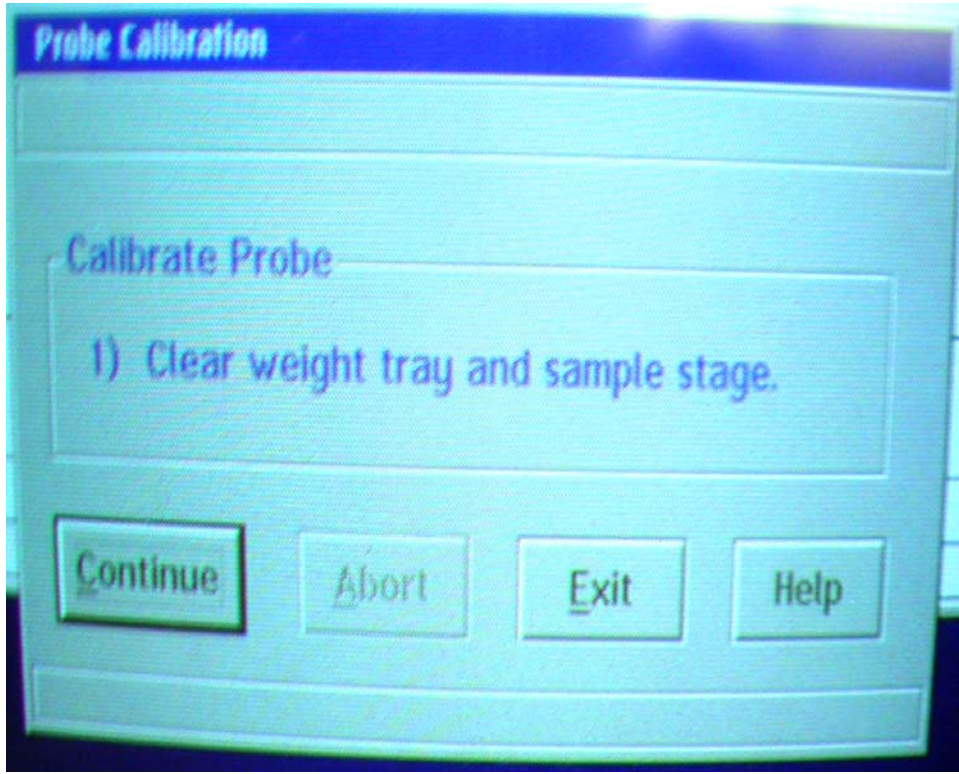


Figure A1 Probe Calibration Step 1

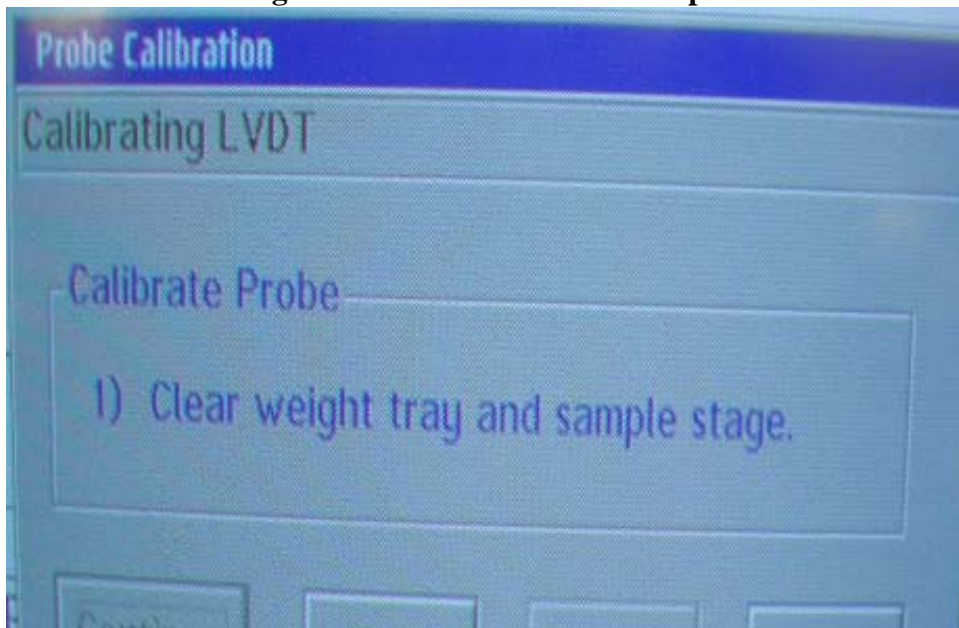


Figure A2 Probe Calibration Step 2

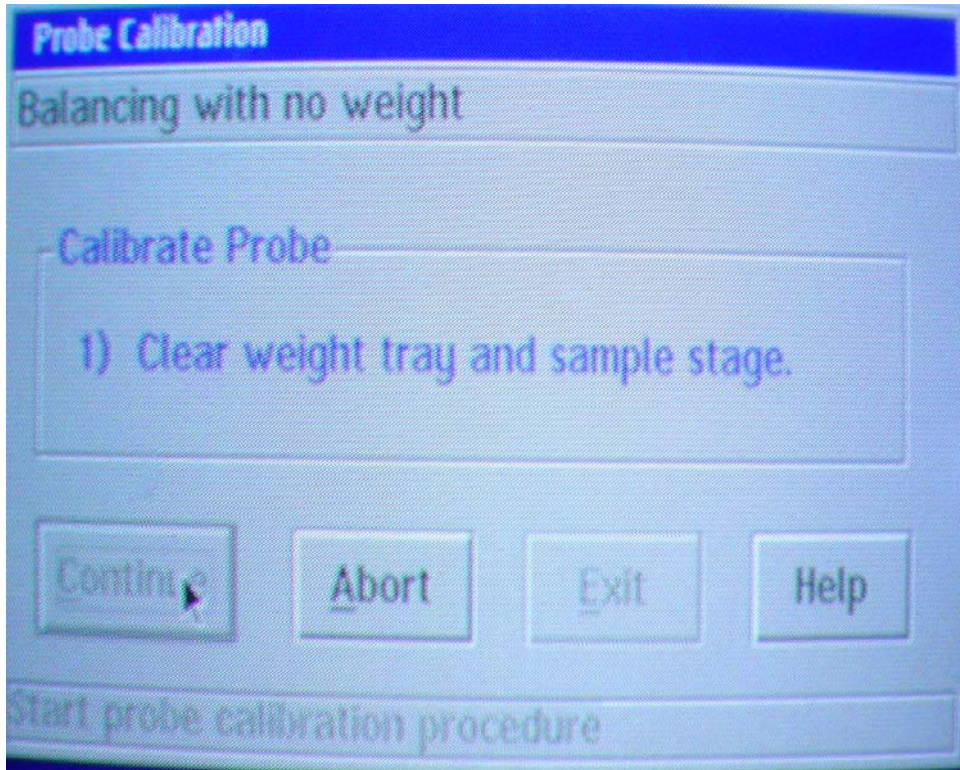


Figure A3 Probe Calibration Step 3

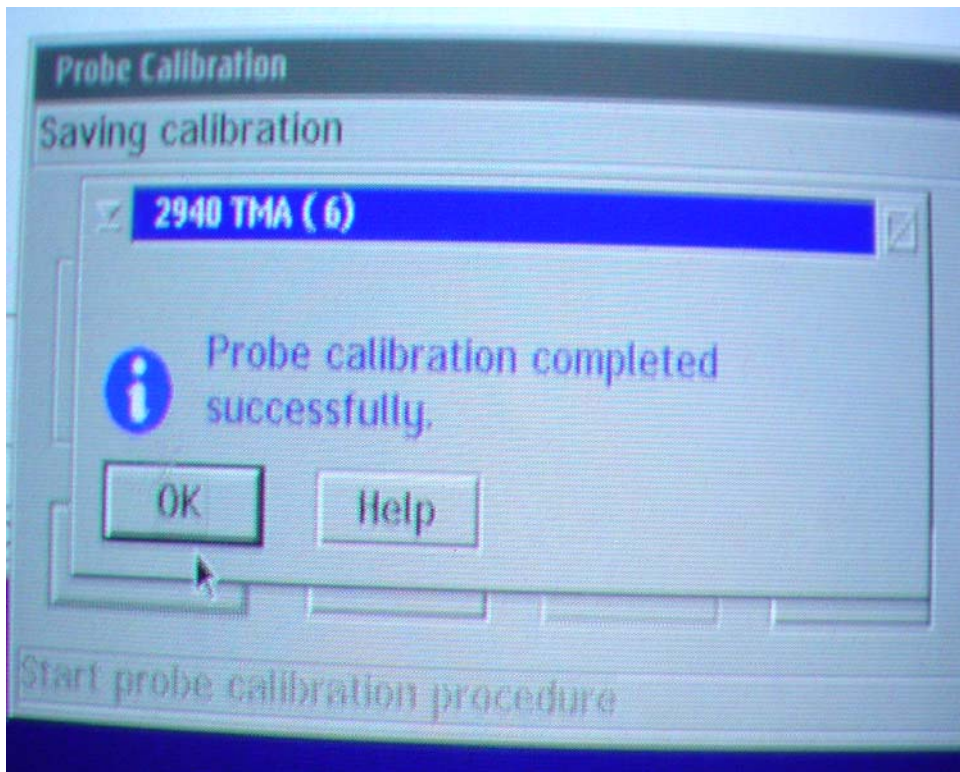


Figure A4 Probe Calibration Step 4

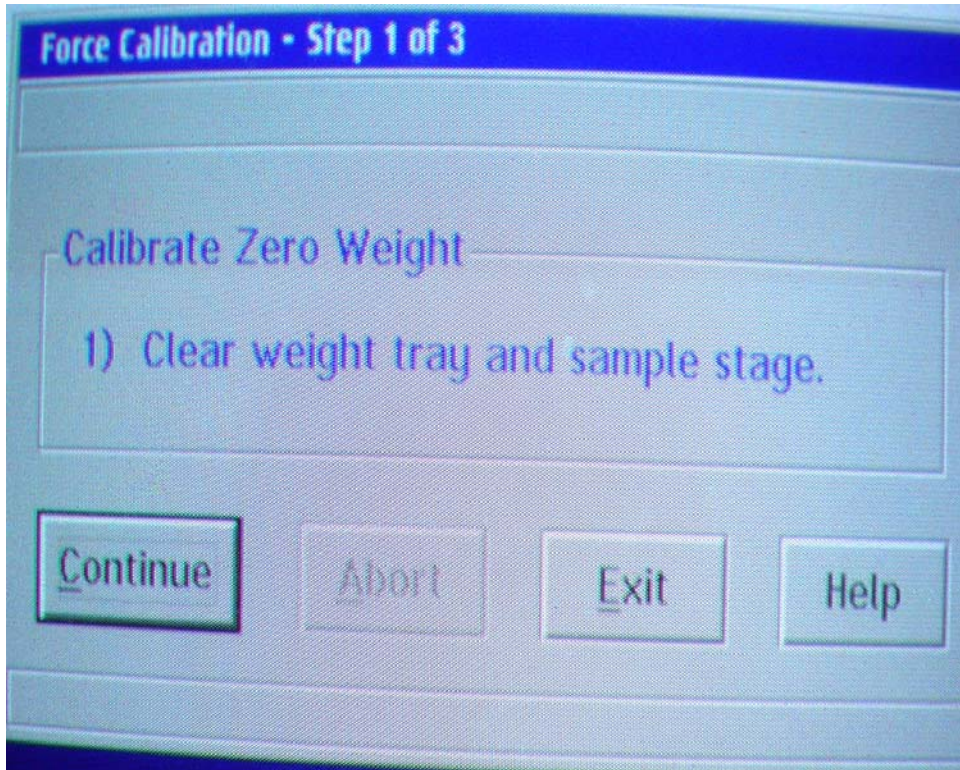


Figure A5 Force Calibration Step 1

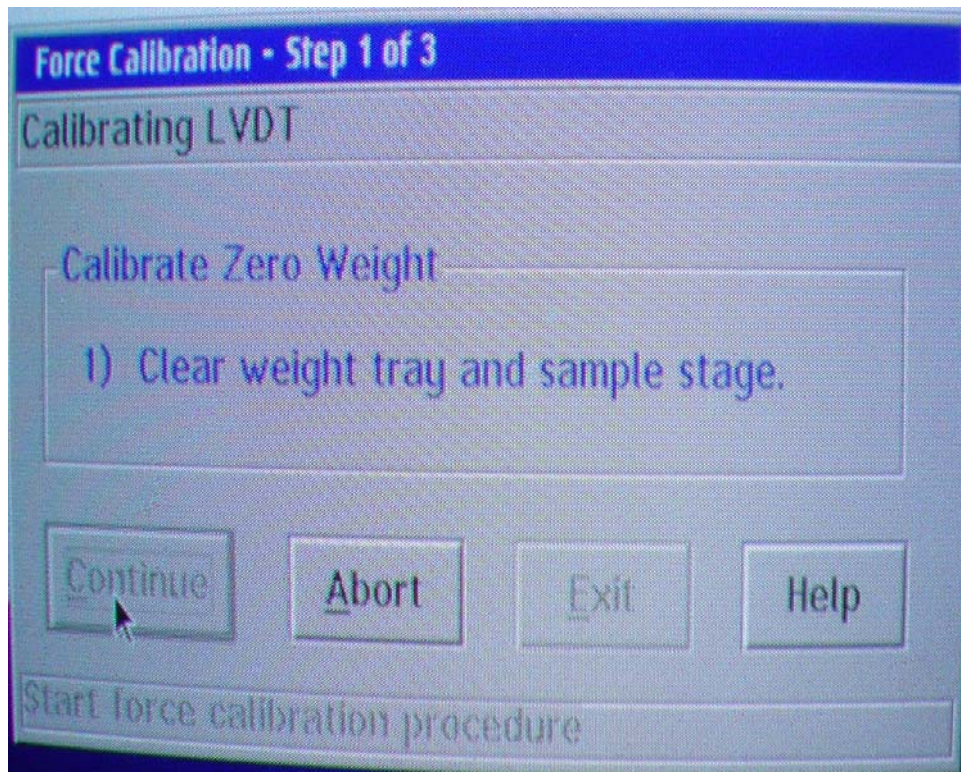


Figure A6 Force Calibration Step 2

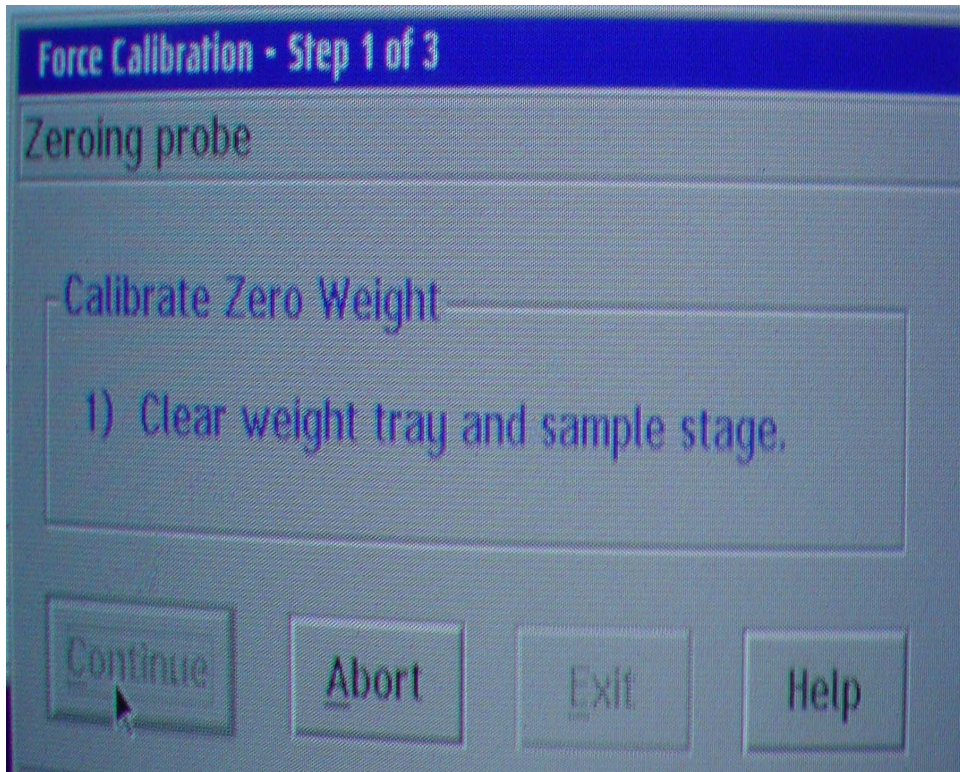


Figure A7 Force Calibration Step 3

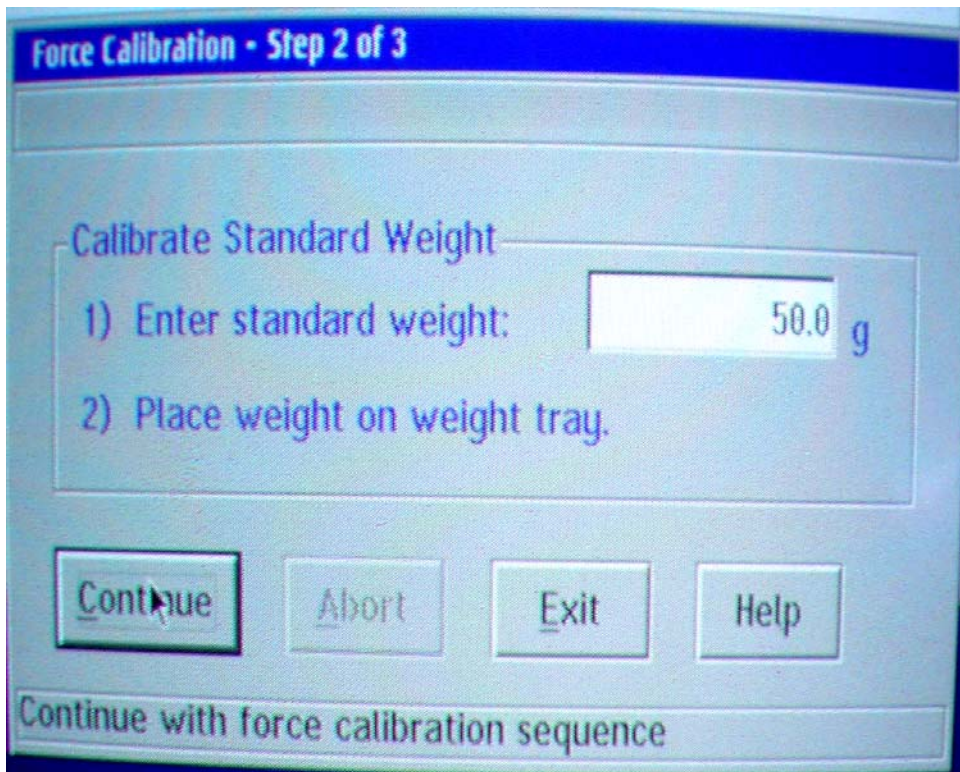


Figure A8 Force Calibration Step 4

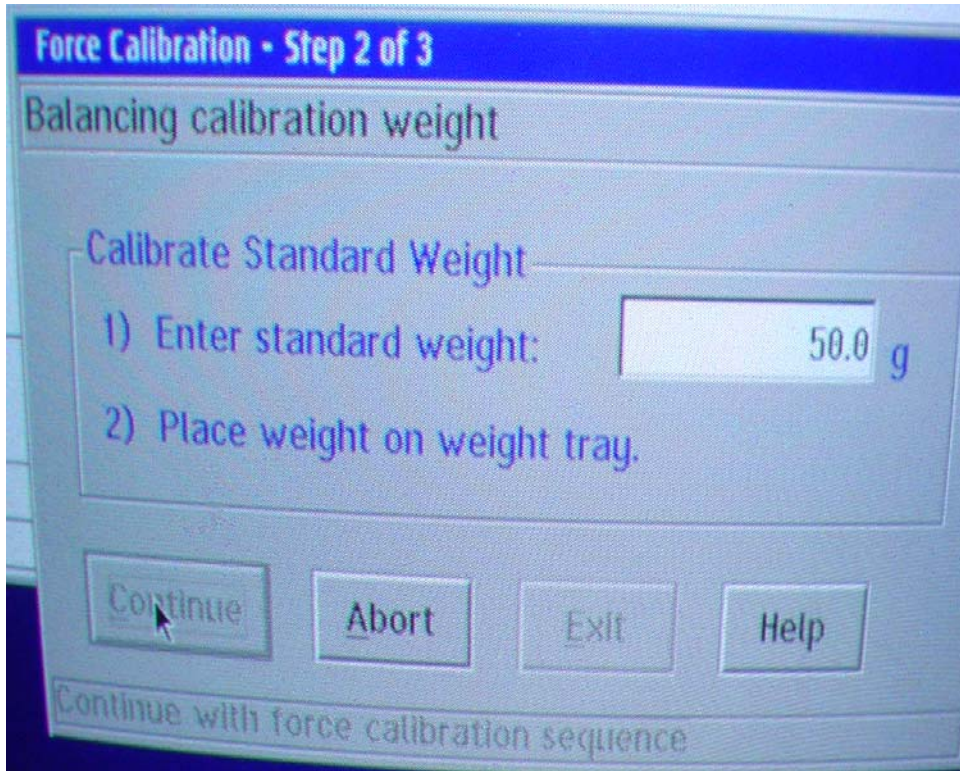


Figure A9 Force Calibration Step 5

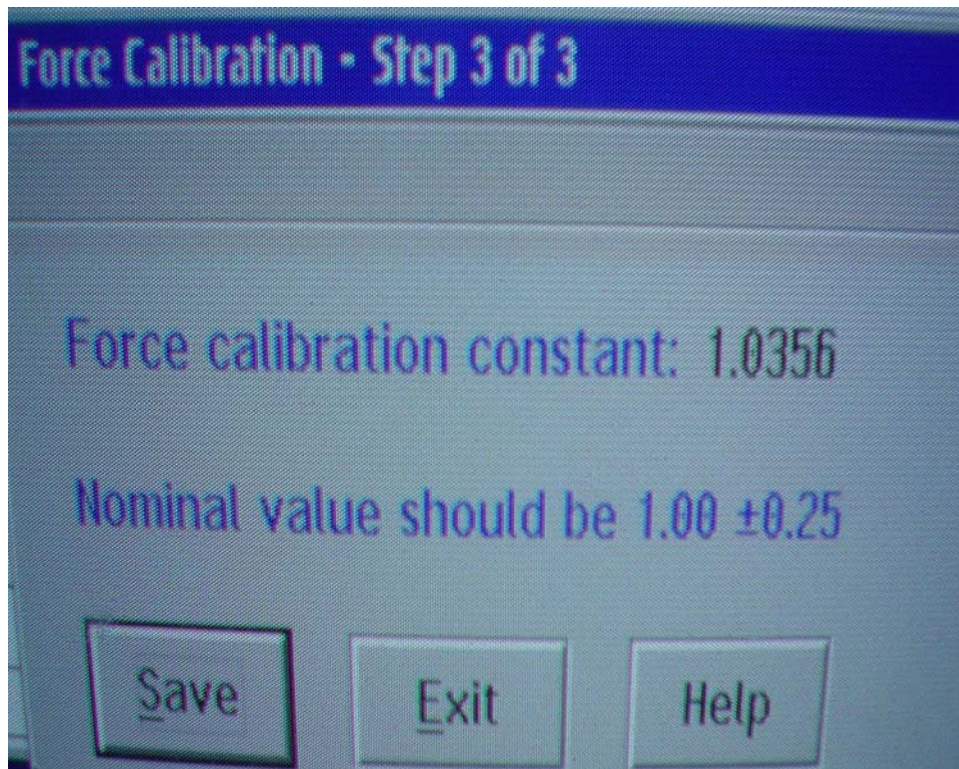


Figure A10 Force Calibration Step 6

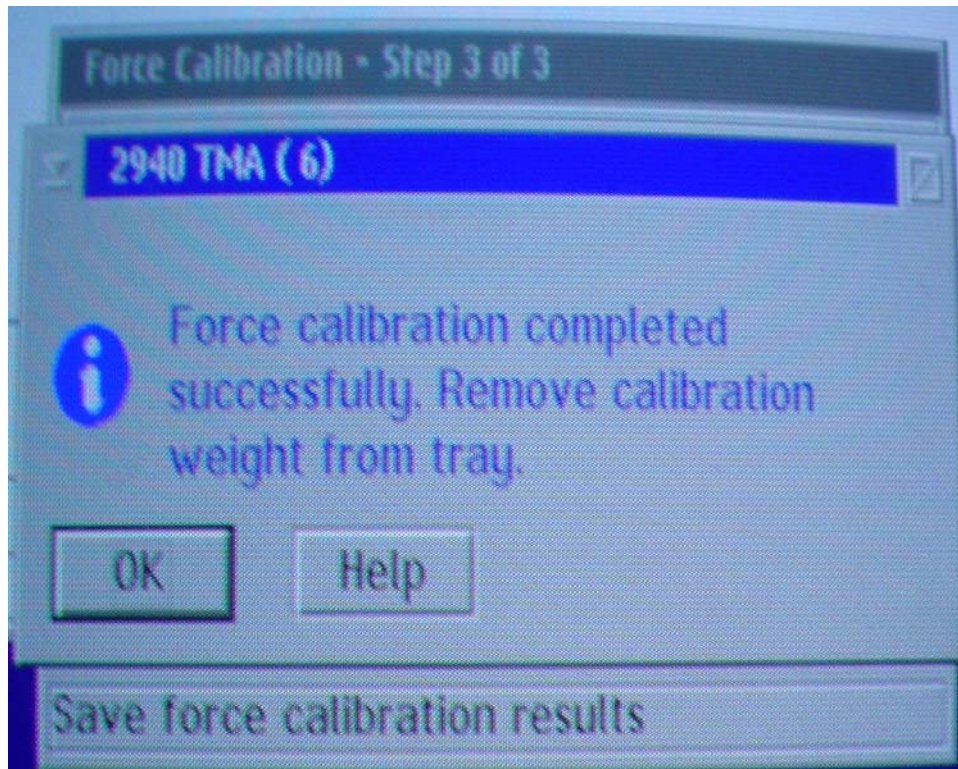


Figure A11 Force Calibration Step 7

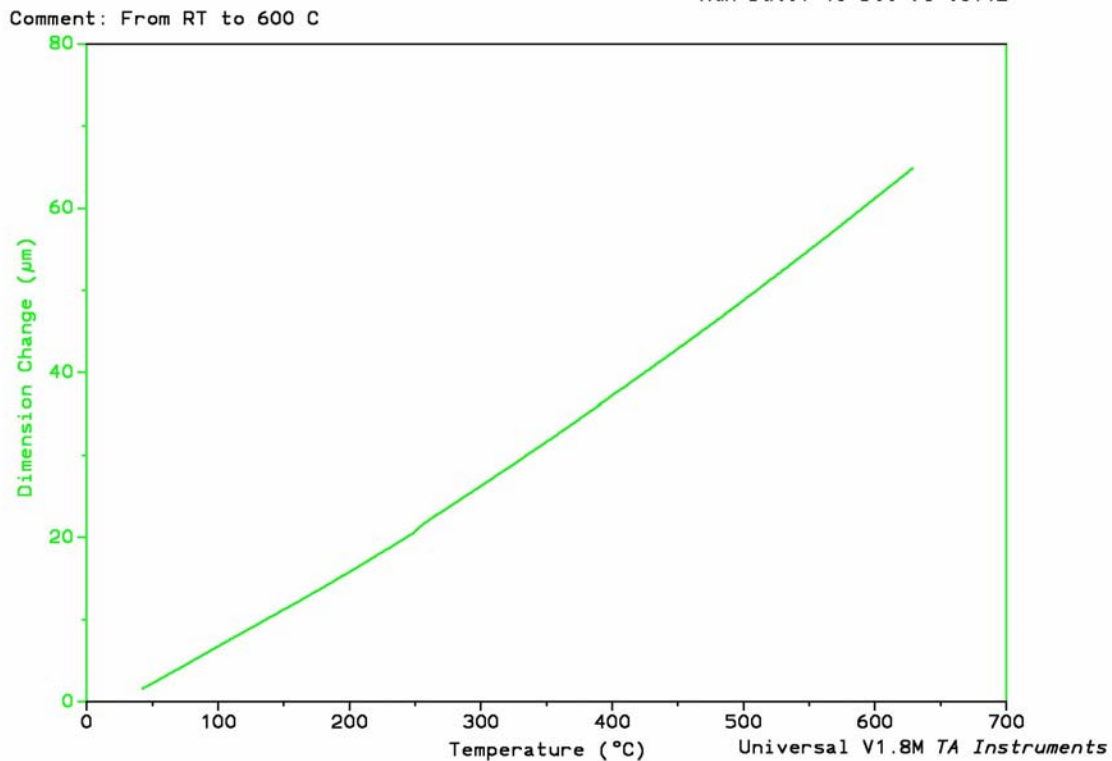


Figure A12 Temperature and Expansion Calibration (Aluminium)

APPENDIX B

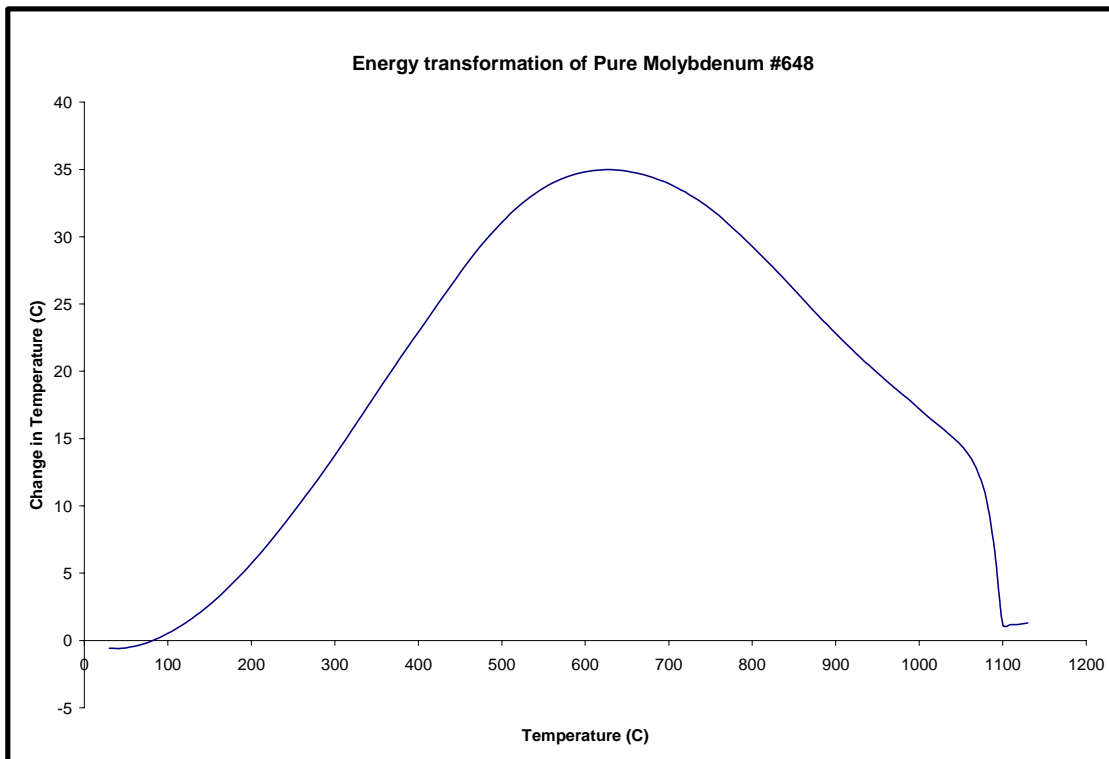


Figure B1 DTA result of pure molybdenum #648

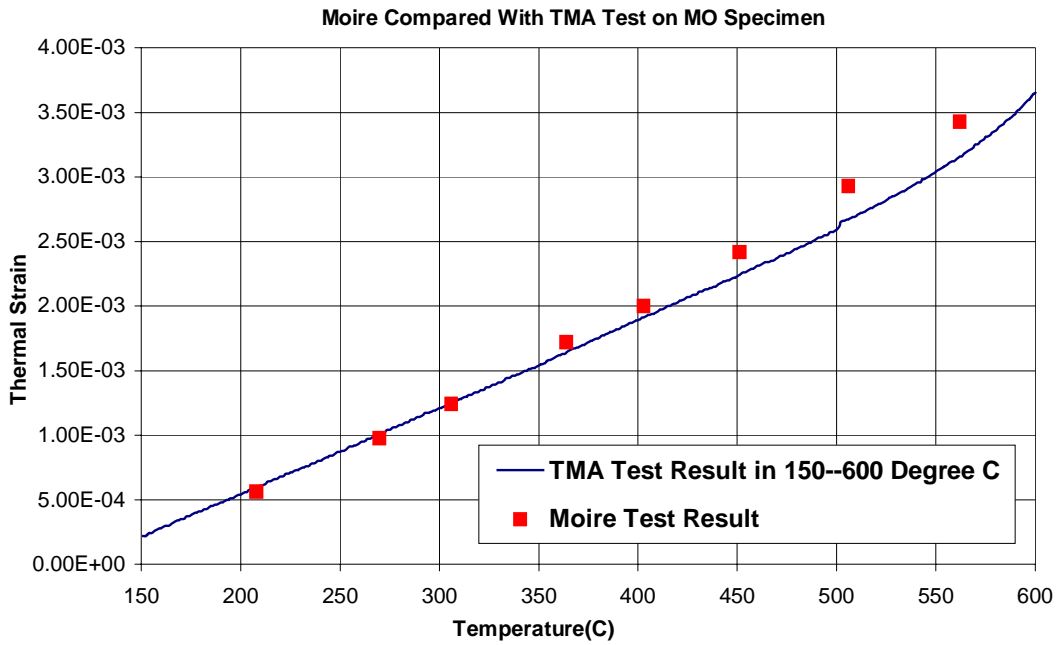


Figure B2 Comparison of CTE values between TMA and Moiré test on #648

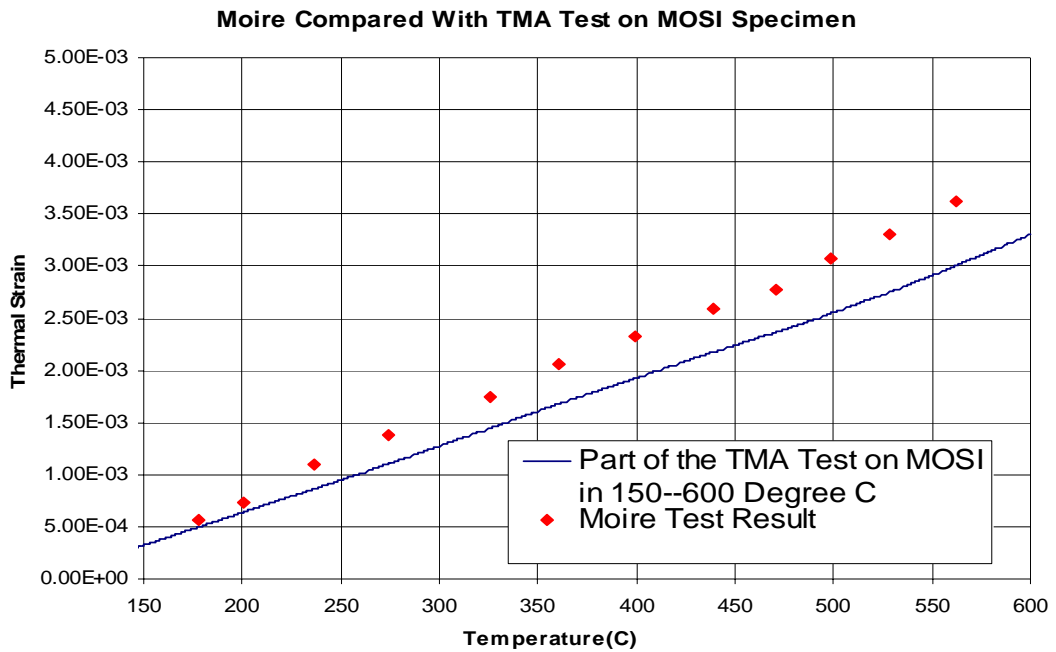
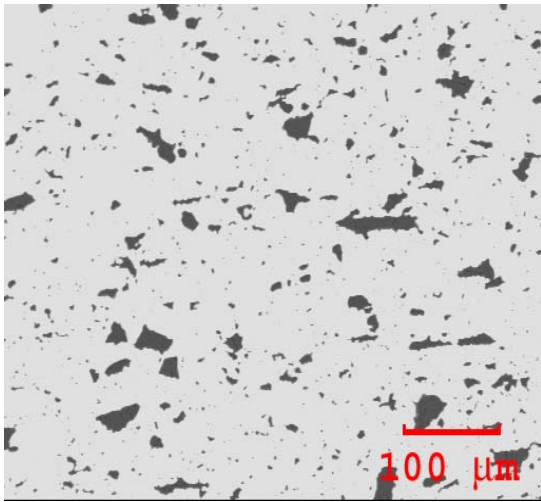
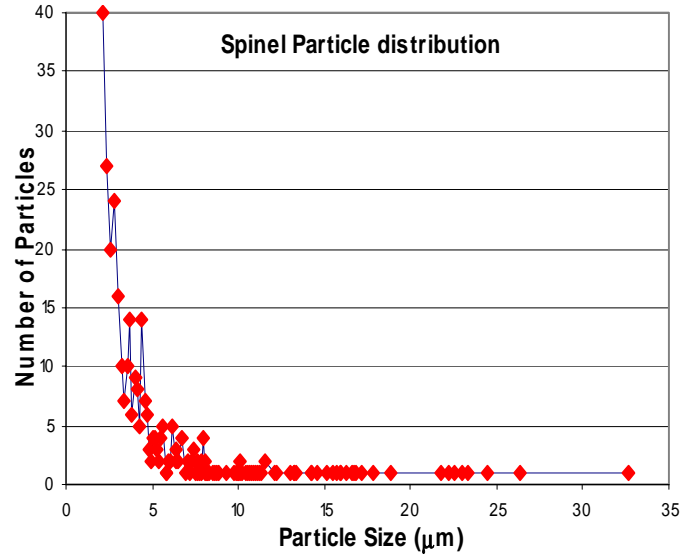


Figure B3 Comparison of CTE values between TMA and Moiré test on #649



(a)



(b)

Figure B4 (a) Microstructure of Mo-MgAl₂O₄. (b) Particle size (μm) and number

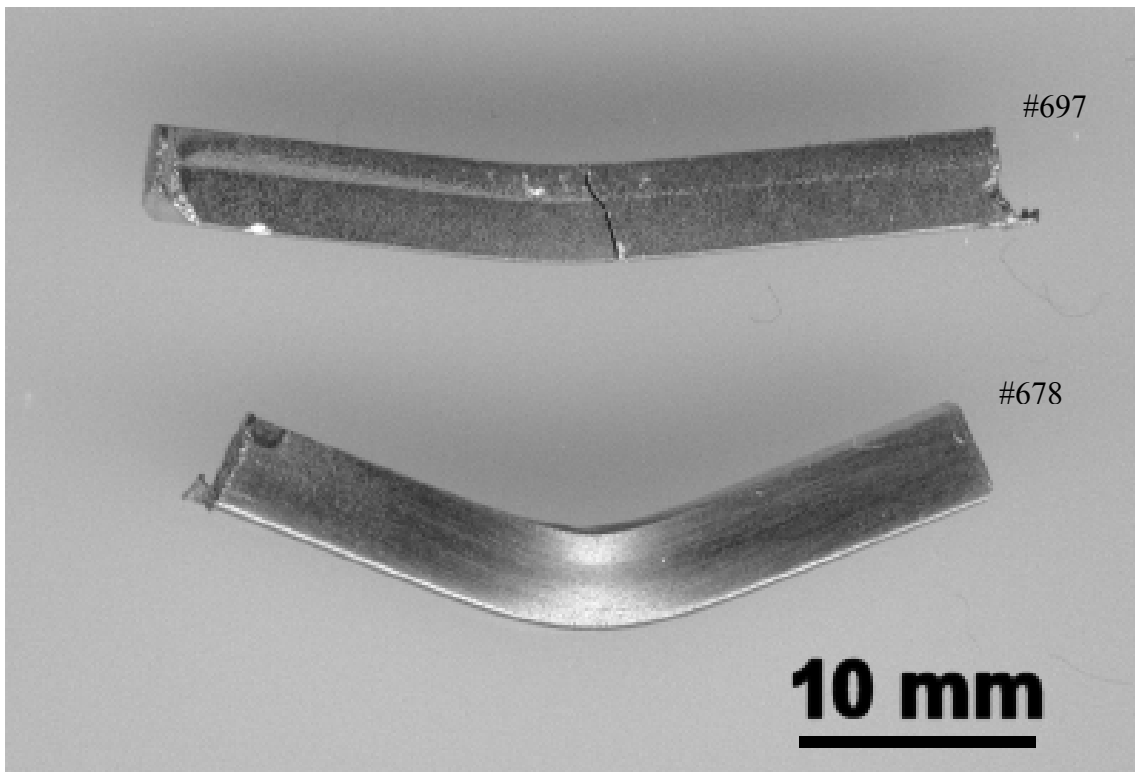


Figure B5 Bending test results show that #678 is more ductile than #697

REFERENCES

1. Donald R. Askeland, "The Science and Engineering of Materials." Pg: 651.
2. www.tms.org Superalloys: A Primer and History.
3. Donald R. Askeland, "The Science and Engineering of Materials." Pg: 240.
4. <http://imoa.org.uk>
5. David Andrew Helmick, PhD Dissertation "High Temperature Oxidation Behavior OF Mo-Si-B Base Alloys" , University of Pittsburgh 2003.
6. Yao, Z., Stiglich, J.; Sudarshan, T.S. , Molybdenum silicide based materials and their properties, Journal of Materials Engineering and Performance, v 8, n 3, 1999, p 291-304.
7. Schneibel, J.H. Easton, D.S.; Choe, H.; Ritchie, R.O. , Fracture toughness, creep strength and oxidation resistance of Mo-Mo₃Si-Mo₅SiB₂ molybdenum silicides, Proceedings of the International Symposium on Structural Intermetallics, 2001, p 801-809
8. H. Choe, D. Chen, J.H. Schneibel and R.O. Rithchie, Fracture and fatigue growth behavior in Mo-12Si-8.5B Intermetallics at ambient and elevated temperature, 2000 TMS proceedings.
9. <http://mineral.galleries.com/minerals/oxides/spinel/spinel.htm>
10. B.S. Kang, C. Feng, J. H. Schneibel, Thermomechanical properties of molybdenum alloys with spinel particles, Twentieth Annual International Pittsburgh Coal Conference proceeding. Sep, 2003

11. C.L.Fu and X.Wang, "Thermal Expansion coefficients of Mo-Si compounds by first-principles calculations" ,Philosophical Magazine Letters 2000, vol 80, No 10 683-690.
12. D. M. Scruggs, "Ductile tungsten composition containing a spinel dispersed uniformly throughout," United States Patent 3,320,037, Patented May 16, 1967.
13. A.K.Vasudevan and J.Petrovic, "A comparative overview of molybdenum silicide composites", Material Science and Engineering. A155(1992)1-17
14. J. H. Schneibel, J. J. Kruzic, R. O. Ritchie, Proceedings of the 17th Annual Conference on Fossil Energy Materials Baltimore, MD, April 22-24, 2003, in print.
15. Vander Voort, Metallography: Principles and Practice. Materials Science and Engineering Series, McGraw-Hill, 1984, 610-655.
16. J. H. Schneibel, Oak Ridge National Laboratory, Jamie J. Kruzic and Robert O. Ritchie, Lawrence Berkeley National Laboratory, "Mo-Si-B Alloy development"
17. M.J. Kramer, M. Akinc, A.J. Thom, J.J. Williams, and H.L. Zhao; J.H. Schneibel, C.J. Rawn, and C.L. Fu, in MRS Symposium Proceedings, 2001
18. Tanaka, R. Past, present, and future of materials for high temperature applications, in Proceeding Symposium of Ultra-high Temperature Materials. 1-10, 1997
19. Joachim H. Schneibel, Claudia J. Rawn, Chong Long Fu., "Tailoring the thermal expansion anisotropy of Mo₅Si₃." Oak Ridge National Laboratory.

20. Bruce S. Kang and B.R.Cooper., “Understanding and improving high temperature structural properties of Metal-Silicide Intermetallics.” Three year research proposal from West Virginia University, Morgantown, USA.
21. C.L. Fu and Xindong Wang., “Thermal expansion coefficients of Mo-Si compounds by first principles calculations.” Oak Ridge National Laboratory.
22. Misra, J.J.Petrovic and T. E. Mitchell., “Microstructures and Mechanical properties of a Mo₃Si- Mo₅Si₃ composite.” Los Alamos National Laboratory.
23. J.H. Schneibel, and C.A.Carmichael., “ Processing and properties of Molybdenum silicide intermetallics containing boron.” Oak Ridge National Laboratory.
24. C.J.Rawn, J.H.Schneibel, C.M. Hoffmann and C.R.Hubbard. “The Crystal Structure and Thermal Expansion of Mo₅SiB₂” Metals and Ceramics Division, Oak Ridge National Laboratory, Oak Ridge, TN 37831.

VITA

Ashok Varadarajan

Date of Birth Sept 24th 1979

Place of Birth Chennai (Madras), INDIA

Education

MS in Mechanical Engineering,
West Virginia University, WV, USA
Date of Graduation: May 2004.

BE in Mechanical Engineering,
Annamalai University, INDIA
Date of Graduation: May 2001.